# AGENTMATH: EMPOWERING MATHEMATICAL REASONING FOR LARGE LANGUAGE MODELS VIA TOOL-AUGMENTED AGENT

**Anonymous authors**
Paper under double-blind review

## ABSTRACT

Large Reasoning Models (LRMs) like o3 and DeepSeek-R1 have achieved remarkable progress in natural language reasoning with long chain-of-thought. However, they remain computationally inefficient and struggle with accuracy when solving problems requiring complex mathematical operations. In this work, we present AgentMath, an agent framework that seamlessly integrates language models' reasoning capabilities with code interpreters' computational precision to efficiently tackle complex mathematical problems. Our approach introduces three key innovations: (1) An automated method that converts natural language chain-of-thought into structured tool-augmented trajectories, generating high-quality supervised fine-tuning (SFT) data to alleviate data scarcity; (2) A novel agentic reinforcement learning (RL) paradigm that dynamically interleaves natural language generation with real-time code execution. This enables models to autonomously learn optimal tool-use strategies through multi-round interactive feedback, while fostering emergent capabilities in code refinement and error correction; (3) An efficient training system incorporating innovative techniques, including request-level asynchronous rollout scheduling, agentic partial rollout, and prefix-aware weighted load balancing, achieving 4-5× speedup and making efficient RL training feasible on ultra-long sequences with scenarios with massive tool calls. Extensive evaluations show that AgentMath achieves state-of-the-art performance on challenging mathematical competition benchmarks including AIME24, AIME25, and HMMT25, substantially outperforming frontier open-source models of comparable size. Specifically, AgentMath-30B-A3B attains 90.6%, 86.4%, and 73.8% accuracy respectively, surpassing OpenAI-o3-mini and Claude-Opus-4.0-Thinking while remaining competitive with OpenAI-o3, Gemini-2.5-Pro, and DeepSeek-R1-671B-0528. These results validate the effectiveness of our approach and pave the way for building more sophisticated and scalable mathematical reasoning agents.

## 1 INTRODUCTION

Large Reasoning Models (LRMs) such as o3 and DeepSeek-R1 have made remarkable progress in natural language reasoning with long chain-of-thought (CoT)(OpenAI et al., 2024; Team et al., 2025; DeepSeek-AI et al., 2025; xAI, 2023; Claude, 2025; Team et al., 2023; Wei et al., 2022). However, when tackling mathematical problems that demand precise computation or intricate symbolic manipulation, including large-number arithmetic, complex equation solving, and geometric reasoning, pure text-based reasoning still has limitations: frequent computational errors necessitate redundant corrections, which in turn leads to inefficiency and erroneous results.

To enhance computational efficiency and accuracy, recent work has explored incorporating external tools (i.e., code interpreters), delegating complex and error-prone computational steps to external environments(Li et al., 2025e; Zhou et al., 2025; Lin & Xu, 2025; Zhang et al., 2025b; Chen et al., 2023; Gao et al., 2023; Gou et al., 2023b). For instance, models like o3 and o4-mini have significantly improved mathematical reasoning accuracy through tool invocation. Nevertheless, existing approaches still face three critical challenges. First, high-quality tool-use data remains extremely scarce. While methods like START(Li et al., 2025b) generate tool-augmented trajectories via prompt engineering, they suffer from delayed code computation and code result distrust; CoRT(Li et al., 2025a) employs manual annotation which is effective but lacks scalability; under supervised learning, models struggle to learn autonomous debugging from code execution failures. Second, the potential for continuous performance improvement and tool-use strategy optimization through agentic RL remains unexplored. Third, competition-level mathematical problems typically involve ultra-long reasoning chains with extensive tool invocations (i.e., 96k tokens, 96 tool calls), making traditional batch-synchronous RL training frameworks inadequate for large-scale agent learning, while the rollout time for ultra-long sequences causes severe long-tail effects.

To address these challenges, we propose AgentMath, a tool-augmented agentic framework that seamlessly integrates model reasoning with code execution for efficient and reliable mathematical problem-solving. AgentMath comprises three core components:

First, we propose an automated tool-augmented trajectory synthesis method that transforms pure-text long chain-of-thought data into structured training samples containing code execution and authentic feedback. Through code injection, execution verification, and multi-dimensional refinement, this effectively alleviates data scarcity.

Second, we design a novel agentic reinforcement learning paradigm that supports dynamic interleaving of natural language generation and code execution during reasoning. Through multi-turn interactive feedback, models autonomously learn optimal tool invocation strategies. Experiments reveal that model accuracy continuously improves with increasing tool invocations, exhibiting emergent code self-correction capabilities.

Third, to support large-scale agentic RL training(Schulman et al., 2017; Li et al., 2025e; Feng et al., 2025a; Mai et al., 2025), we develop an efficient training system incorporating key techniques such as request-level asynchronous rollout scheduling, agentic partial rollout, and prefix-aware weighted load balancing. These innovations improve training efficiency by $4$–$5\times$, effectively supporting reinforcement learning in scenarios with ultra-long sequences and extensive tool invocations.

Experimental results demonstrate that AgentMath achieves state-of-the-art performance on challenging mathematical competition benchmarks including AIME24, AIME25, and HMMT25(Balunović et al., 2025), significantly outperforming frontier open-source tool-augmented models and pure-text reasoning models of comparable scale. Specifically, AgentMath-30B-A3B achieves accuracies of 90.6%, 86.4%, and 73.8% respectively, surpassing OpenAI-o3-mini(OpenAI, 2025) and Claude-Opus-4.0-Thinking(Claude, 2025), while remaining competitive with Gemini-2.5-Pro(Team et al., 2023) and DeepSeek-R1(DeepSeek-AI et al., 2025). These results consistently validate the effectiveness of AgentMath in mathematical reasoning tasks.

Our main contributions include: (1) We propose an efficient automated tool-augmented data synthesis pipeline that effectively alleviates data scarcity issues. (2) We design a novel agentic reinforcement learning paradigm achieving dynamic integration of natural language reasoning and code execution, enabling models to autonomously learn tool-use strategies through multi-turn interactive feedback. (3) We develop an efficient asynchronous training system that provides a scalable solution for ultra-long sequences, multi-turn interaction agent reinforcement learning. (4) We achieve state-of-the-art performance on multiple challenging mathematical competition benchmarks, paving the way for building more complex and scalable mathematical reasoning agents.

Due to space constraints, we will defer the related work to Appendix A.1.

## 2 METHOD

### 2.1 OVERVIEW

This section presents **AgentMath**, a tool-augmented agent framework designed to enhance complex mathematical reasoning by tightly integrating the emergent reasoning capabilities of Large Language Models (LLMs) with the precise arithmetic and symbolic computation facilitated by an external code execution environment. The architecture operates in two stages: (i) supervised fine-tuning (SFT) on curated, synthetic tool-invocation trajectories to establish initial competence in invoking tools appropriately, and (ii) large-scale reinforcement learning (RL) driven by outcome feedback to incentivize exploration and mastery of optimal, self-corrective tool-use strategies.

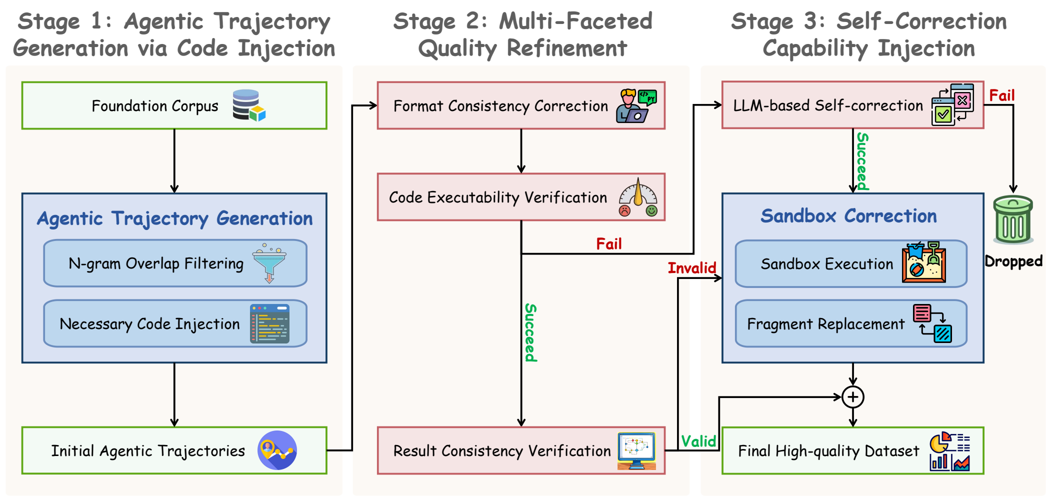
Stage 1: Agentic Trajectory Generation via Code Injection
Stage 2: Multi-Faceted Quality Refinement
Stage 3: Self-Correction Capability Injection
Foundation Corpus
Agentic Trajectory Generation
N-gram Overlap Filtering
Necessary Code Injection
Initial Agentic Trajectories
Format Consistency Correction
Code Executability Verification
Fail
Succeed
Result Consistency Verification
LLM-based Self-correction
Fail
Succeed
Sandbox Correction
Sandbox Execution
Fragment Replacement
Invalid
Valid
Dropped
Final High-quality Dataset

Figure 1: This diagram outlines a three-stage pipeline for creating a high-quality tool-augmented trajectories for training agents, including Agentic Trajectory Generation via Code Injection, Multi-Faceted Quality Refinement and Self-Correction Capability Injection. This automated process transforms pure-text reasoning into verified, executable agentic trajectories.

**Problem Formulation and Interaction Protocol**: We formulate tool-augmented mathematical reasoning as a Markov Decision Process (MDP). The LLM-based policy generates interleaved reasoning segments and executable code blocks through interaction with a sandboxed execution environment. Each trajectory consists of action-observation pairs, where state transitions result from the policy's conditional generation and deterministic code execution. We define a structured markup protocol for agent-environment communication: <think> denotes natural language reasoning, <code> delimits executable code blocks, and <interpreter> encapsulates execution feedback. This bidirectional exchange mechanism incorporates execution results into the generation context, enabling adaptive strategy refinement and planning. See Appendix A.2 for more details.

### 2.2 Tool-Driven Data Synthesis

The scarcity of high-quality training data that captures both complex reasoning patterns and strategic tool utilization remains a fundamental bottleneck in developing code-enabled agents. This work introduces a three-stage automated synthesis-and-refinement pipeline that transforms pure-text long CoT into agent-style demonstrations with executable code invocations and authentic interpreter feedback, yielding a compact and efficient instruction dataset for SFT, as shown in Figure 1.

**Stage 1: Agentic Trajectory Generation via Code Injection.** We assemble a large-scale corpus from public mathematical reasoning sources (i.e., AM-Thinking, Open-Thoughts(Ji et al., 2025; Guha et al., 2025)), which distill responses from DeepSeek-R1-0528. To prevent evaluation contamination, we apply n-gram overlap filtering against benchmark datasets (i.e, AIME24/25, HMMT25), yielding a high-quality pure-text reasoning dataset $\mathcal{D}_{\text{text}}$.

Direct Manual annotation of agent trajectories is both costly and susceptible to noise. To address this, we propose an efficient code-injection strategy that leverages a powerful teacher model (i.e., DeepSeek-V3(DeepSeek-AI et al., 2025)), guided by carefully crafted prompts presented in Appendix A.6.2. Each extensive Chain-of-Thought (CoT) sequence $\tau_{\text{text}} \in \mathcal{D}_{\text{text}}$ is systematically partitioned into multiple segments. Subsequently, each segment undergoes transformation via the injection function $\mathcal{F}_{\text{inject}}$, which substitutes computationally intensive reasoning steps $s_{\text{calc}}$ with executable code blocks and their corresponding execution outputs:

$$\tau'_{\text{agent}} = \mathcal{F}_{\text{inject}}(\tau_{\text{text}}), \quad \text{where } \mathcal{F}_{\text{inject}} : \tau_{\text{text}} \mapsto \big(\tau_{\text{text}} \text{ with } s_{\text{calc}} \Rightarrow (c,\, o_{\text{sim}})\big).$$

where $c$ denotes the injected code segment, $s_{\text{calc}}$ represents the replaced computational step, and $o_{\text{sim}}$ is the teacher-simulated execution result. This injection targets complex operations (exponential computations, matrix manipulations, equation solving) while preserving elementary calculations in textual form to maintain the model's understanding of tool invocation rationale and prevent over-dependence. Code blocks are delimited by <code> </code> tags, with execution results enclosed in <interpreter> </interpreter> tags referring to (Feng et al., 2025a).

**Stage 2: Multi-Faceted Quality Refinement.** Automatically synthesized trajectories can contain formatting issues, code defects, and logical inconsistencies. We apply four complementary procedures to ensure high quality and effectiveness:

***(i) Format consistency correction:*** We employ regular-expression normalization and teacher model regeneration for complex cases to enforce strict adherence to the <code>–<interpreter> structural compliance.

***(ii) Code executability verification:*** Each embedded code snippet is executed within a controlled sandbox environment. For any failures, we initiate a bounded resampling loop to generate equivalent but executable alternatives. If execution remains unsuccessful within a predefined compute budget, the block is reverted to its original textual step $s_{\text{calc}}$ to preserve logical soundness.

***(iii) Environmental feedback alignment:*** Simulated outputs $o_{\text{sim}}$ from the teacher are systematically replaced with ground-truth execution results $o_{\text{real}} = \mathcal{E}(c)$, where $\mathcal{E}$ denotes the interpreter environment. A dedicated verifier model (i.e., Qwen3-32B) is employed to perform this judgment, guided by a specific judge-prompt detailed in Appendix A.6.3, then assesses contextual consistency. Incoherent samples are removed or downgraded to text-only variants to maintain narrative integrity.

***(iv) Tool-usage rationality assessment:*** Heuristic constraints on code complexity metrics (i.e., line count, abstract syntax tree depth) are enforced to eliminate instances of unnecessary code invocation, thereby reinforcing necessity-aware tool utilization patterns.

**Self-Correction Capability Injection.** Beyond correct tool invocation, a robust agent need also recover from erroneous tool feedback. We sample trajectories that were excluded during refinement due to execution failures, and for each failed program $c_{\text{fail}}$ with error output $o_{\text{error}} = \mathcal{E}(c_{\text{fail}})$, we prompt the teacher model to generate a structured self-correction trace (diagnose the error $\rightarrow$ repair the code $\rightarrow$ re-execute $\rightarrow$ continue reasoning). The detailed prompt can be found in Appendix A.6.1. A small fraction of these negative-to-positive corrections is injected to strengthen debugging robustness. The final instruction set $\mathcal{D}_{\text{SFT}}$ combines validated, tool-augmented trajectories with diagnostic correction traces and serves as the foundation for SFT.

### 2.3 Agentic Reinforcement Learning

We present an agentic reinforcement learning (RL) framework that advances code-integrated reasoning capabilities beyond supervised fine-tuning (SFT). This stage pursues two objectives: (i) to quantify the incremental gains of RL over an SFT baseline, and (ii) to elucidate how RL reshapes tool-usage strategies under interleaved natural language generation and program execution. Additionally, the detailed construction of the RL data is described in Appendix A.5.2.

#### 2.3.1 Agent-Specific Reinforcement Learning

Our framework employs Group Relative Policy Optimization (GRPO)(Shao et al., 2024) as the core optimization algorithm, which obviates critic models while enhancing training efficiency through group-wise trajectory sampling and reward normalization described in Appendix A.3. We employed multi-stage RL training, as detailed in Section 3.5. Following DAPO (Yu et al., 2025), we incorporate dynamic sampling, asymmetric gradient clipping, token-level loss computation, and KL divergence removal. We introduce three system innovations tailored for code-integrated agents:

**Agentic trajectories with interleaved code execution.** During rollout, trajectories are constructed through a *generate–pause–execute–resume* loop (See Appendix A.2), yielding hybrid traces composed of chain-of-thought reasoning, inline code snippets, and real-time interpreter feedback. Tool invocations are bounded by a per-instance cap $T$, enabling fine-grained control over agent-environment interactions and promoting sample efficiency.

**Loss Masking for Policy Gradient Updates.** To focus learning on the agent's decision-making process, the advantage signal is applied exclusively to tokens within <think> and <code> segments. Tokens generated by the environment, specifically within <interpreter>, are masked during

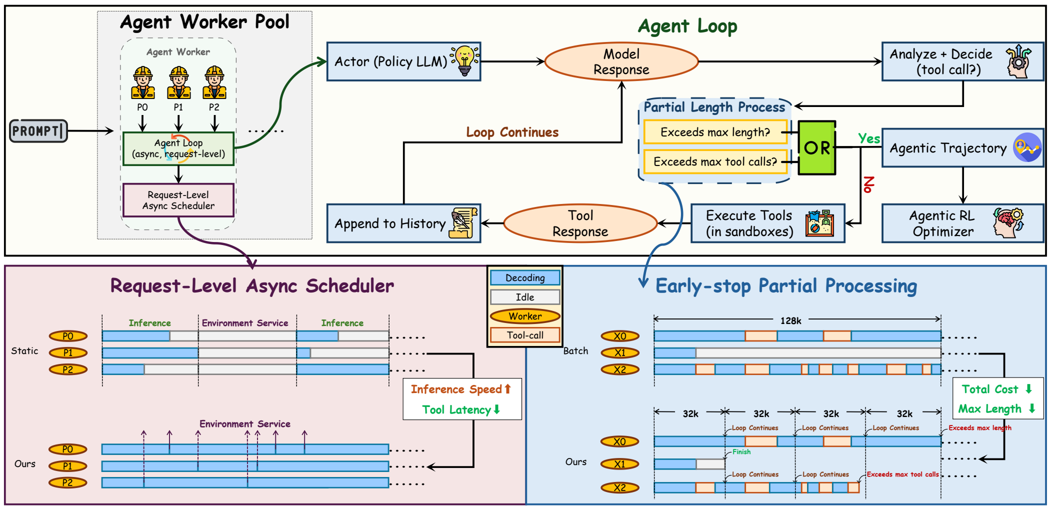

Figure 2: The diagram of agentic reinforcement learning. It depicts the structure and workflow of our agentic reinforcement learning system with core functions including Agent Loop, Asynchronous Scheduler, and Partial Rollout, along with key performance improvement. Based on the Asynchronous Scheduler, the Agent Loop continues running by default. It will stop early only when conditions are met: either the content length exceeds the max length (i.e., 32k) or the number of tool calls exceeds the maximum constraint.

optimization, ensuring that gradient updates are driven by the agent's own actions rather than deterministic environmental responses.

**Adaptive Batch Construction with Filtering and Backfilling.** For each problem instance, we sample $G$ trajectories. Batches are filtered to exclude problems where all trajectories yield either uniformly correct or uniformly incorrect answers, which offer limited learning signal. To maintain consistent batch sizes, we backfill by randomly sampling additional filtered instances from the same pool, thus avoiding inefficient resampling loops while preserving distributional diversity.

### 2.3.2 Reward Design

Our reward function integrates answer correctness with tool-usage efficiency. The accuracy component $R_{\text{acc}}$ provides binary feedback based on mathematical equivalence, validated via the math_verify library:

$$R_{\text{acc}} = \begin{cases} 1, & \text{if is\_equivalent}(\hat{a}, a), \\ 0, & \text{otherwise,} \end{cases}$$

where $\hat{a}$ denotes the predicted answer and $a$ represents ground truth. Conditioned on correctness, the tool-usage reward $R_{\text{tool}}$ incentivizes efficient computational resource utilization:

$$R_{\text{tool}} = \min\big(R_{\max},\, \alpha + \beta \cdot N_{\text{code}}\big) \quad \text{if } N_{\text{code}} > 0,$$

where $\alpha$ represents the base tool-usage reward, $\beta$ scales with invocation count, and $R_{\max}$ caps the maximum tool-usage reward. The composite reward function becomes:

$$R_{\text{total}} = R_{\text{acc}} + \mathbb{I}(R_{\text{acc}} = 1) \cdot R_{\text{tool}}.$$

## 2.4 Scalable Agentic RL Infrastructure

Agentic Reinforcement Learning for complex mathematical reasoning poses significant infrastructural challenges. Empirical analysis reveals that, during RL training with the temperature set to 1.0, complex problems yield trajectories averaging 24k tokens and involve approximately 27 tool invocations. This combination of long-context generation and high-frequency external interactions produces heterogeneous computational workloads. Traditional synchronous batch rollouts exhibit substantial inefficiencies due to synchronization overhead and resource underutilization.

To address these challenges, we design a high-performance, scalable training system tailored to Agentic RL. Through an asynchronous decoupled architecture, an Agentic Partial Rollout algorithm, and prefix-aware load balancing, the system mitigates performance bottlenecks induced by long-tail effects and concurrent tool invocations, achieving $4 \sim 5\times$ improvement in end-to-end training throughput, as shown in Figure 2.

### 2.4.1 Decoupled and Asynchronous System Architecture

The architecture is founded on the principle of decoupling GPU-intensive model inference from CPU/IO-intensive agent logic and environment interactions.

**Distributed code execution sandbox cluster.** We deploy a distributed cluster of isolated worker pods to serve concurrent tool invocations at scale. This design offloads CPU-bound code execution from the training loop while enabling dynamic load distribution. Parallelization reduces tool-call latency from 175 s to 1.2 s and removes inference blocking, substantially improving GPU utilization.

**Request-Level Asynchronous Rollout Scheduling.** Static batch-synchronous processing is replaced with a coroutine-driven, request-level asynchronous scheduler. Each trajectory rollout is treated as an independent long-running request, with the inference engine (server) and agents (clients) fully decoupled via asynchronous communication. When requests suspend for tool invocations, the inference engine immediately processes other ready requests. This fine-grained scheduling eliminates head-of-line blocking and maximizes GPU parallelism across heterogeneous workloads.

### 2.4.2 Agentic Partial Rollout

Agentic RL suffers long-tail latency from both sequence length and tool-invocation counts. We introduce an Agentic Partial Rollout mechanism that decomposes each trajectory $\tau$ into budget-limited segments:

$$\tau = \tau^{(1)} \oplus \tau^{(2)} \oplus \ldots \oplus \tau^{(N)},$$

where $\oplus$ denotes sequence concatenation. Each segment is constrained by a maximum generation length $L_{\text{seg}}$ and a maximum number of tool invocations $T_{\text{seg}}$.

At each training iteration, the scheduler samples from an unfinished pool $\mathcal{U}$ and a set of new tasks $\mathcal{P}$, generating one segment per task. Segment generation terminates when: (i) an EOS token is produced; (ii) segment length reaches $L_{\text{seg}}$; (iii) tool invocations reach $T_{\text{seg}}$; or (iv) cumulative trajectory metrics reach global limits $L_{\text{global}}$ or $T_{\text{global}}$. This segmentation prevents individual trajectories from monopolizing resources and smooths computational load, yielding a 2.2–2.5x speedup. Algorithm 1 outlines the procedure.

### 2.4.3 Prefix-Aware Weighted Load Balancing

Partial rollouts alleviate long-tail latency but introduce requests with long prefixes, increasing KV-cache memory and prefill cost. Therefore, We design a Prefix-Aware Weighted Load Balancing strategy that assigns dynamic weights based on prefix length and routes requests to the least-loaded inference engine.

Each request $R_j$ with prefix length $L_j$ receives a weight

$$w_j = \left\lfloor \frac{L_j}{L_{\text{base}}} \right\rfloor + w_{\text{base}},$$

where $L_{\text{base}}$ (i.e., 16k tokens) normalizes length and $w_{\text{base}}$ quantifies prefill overhead. For $M$ engines $S_1, \ldots, S_M$ with loads $W_k$, a new request $R_j$ is routed to

$$k^* = \arg \min_{k \in \{1,\ldots,M\}} W_k, \quad \text{and} \quad W_{k^*} \leftarrow W_{k^*} + w_j.$$

To maximize KV-cache reuse, we implement sticky sessions via a LRU(Least-Recently-Used) caching, ensuring consecutive segments from the same trajectory preferentially route to the same engine, thereby avoiding redundant context transfer and recomputation. This combination of dynamic weighting and cache-affinity scheduling maintains load balance under heterogeneous traffic patterns while maximizing system throughput.

## 3 Experiments

### 3.1 Supervised Fine-tuning (SFT) Data Construction

**Stage 1: Foundational Data Curation and Filtering.** We aggregate a raw corpus from multiple public math reasoning datasets (i.e., AM-Thinking, OpenThoughts, and AceReason). After problem-level deduplication, we apply N-gram ($N = 4$) and MinHash LSH algorithms to eliminate overlaps with all evaluation sets, including AIME24, AIME25 and HMMT25 with 0.6 similarity threshold. To further prevent data leakage, we compute semantic similarities between training data and evaluation sets using gte-large model(Zhang et al., 2024a) , filtering out the top-5 most similar samples. We then annotate each problem with difficulty scores from 0 to 10 using Qwen3-30B, retaining data with scores above 5, which yields 392k samples. Finally, using DeepSeek-R1-0528 to generate solutions and removing instances with incorrect answers, we obtain 346k data.

**Stage 2: Tool-Augmented Data Synthesis.**We first decompose the problem-solving process into discrete reasoning segments, each with a fixed length of 3k tokens and perform tool-augmented synthesis for each segment using the Prompt presented in Appendix A.6.2 via DeepSeek-V3-0324. During synthesis, we filter out samples with synthesis format error, tool execution failures, or incorrect final answer, yielding 302k high-fidelity, tool-augmented solution trajectories.

**Stage 3: Self-Correction Data Generation.**To incorporate self-correction mechanisms, we sample 30k instances from trajectories with unsuccessful code execution and leverage the Self-correction Prompt presented in Appendix A.6.1 to guide DeepSeek-V3-0324 in generating correction processes, producing 14k valid self-correction trajectories.

Through this comprehensive pipeline, we construct a 316k tool-augmented synthetic training set with an average of 8.3 tool calls and an average sequence length of 16.9K tokens per sample.

### 3.2 Reinforcement Learning (RL) Data Construction

For RL, we collect problems from multiple public high-quality RL datasets (i.e., DeepScaler, Skywork-OR1, Retool, POLARIS). We apply the same deduplication strategy as for SFT data, ensuring no overlap with evaluation sets through N-gram (N=4), MinHash LSH, and semantic similarity computation with 0.6 similarity threshold. To identify challenging problems, we use AgentMath-8B-SFT to perform 8 inference attempts on all data, filtering out problems that are solved correctly 8 times, culminating in a final set of 42k high-difficulty RL training data. This focuses training on hard instances that push the model's strategic capabilities and maximize potential gains from RL.

### 3.3 Training Settings

**Base Models.**Our experiments utilize four base models from the Qwen3 series: Qwen3-1.7B-Base and Qwen3-8B-Base are pre-trained models without post-training; Qwen3-30B-A3B-Instruct-2507 (Non-Thinking mode, 30B total parameters, 3B activated) and Qwen3-235B-A22B-Instruct-2507 (Non-Thinking mode, 235B total parameters, 22B activated) are instruction-tuned Mixture-of-Experts (MoE) models without long chain-of-thought training.

**SFT Training.**We employ the Llama-Factory framework, training for 6 epochs with learning rates of $6 \times 10^{-5}$ (1.7B, 8B, A3B models) and $2 \times 10^{-5}$ (A22B model), using cosine decay with 10% warmup, batch size of 512, and maximum sequence length of 32k tokens.

**RL Training.**Our RL training is built on the verl 0.5.0.dev0 framework(Sheng et al., 2024), initializing from the best SFT checkpoint and using VLLM(Kwon et al., 2023) as the inference engine, with a 128-node Sandbox cluster for large-scale code execution. We use a constant learning rate of $1 \times 10^{-6}$, a batch size of 64, and a temperature of 1.0, performing 8 rollouts per problem. Training progresses through three stages, dynamically adjusted to maintain length truncation and tool-call excess rates below 10%: maximum response length increases from 48k to 72k to 96k tokens, with corresponding tool invocation limits of 48, 72, and 96 calls, and partial rollout counts of 2, 3, and 4, ensuring each segment rollout remains within 24k tokens and 24 tool invocations. Due to computational constraints, AgentMath-235B-A22B is trained solely via supervised fine-tuning (SFT). More details for data synthesis, SFT, RL, and evaluation are provided in Appendix A.5

## 3.4 Main Results

In this section, we comprehensively evaluate AgentMath by comparing it against the advanced reasoning models on three challenging math competition benchmarks: AIME24, AIME25, and HMMT25. Results are presented in Table 1 with more extensive model comparisons available in Appendix Table 4. To ensure robust evaluation, we perform 32 independent inference runs per test sample, using avg@32 as the pass@1 metric. We use a consistent configuration: 96K maximum sequence length, 96 maximum tool calls, and code interpreter output is limited 1024 tokens, and we set 0.6 temperature, and 0.95 top-p.

Table 1: Performance of AgentMath on AIME24/25, and HMMT25. Our model (highlighted in blue) is compared against other leading models, with accuracy (avg@32) as the evaluation metric. Due to space limitations, we use DS, QW2.5, and QM2.5 to denote DeepSeek-R1, Qwen2.5, and Qwen-2.5-Math, respectively. For a more detailed and comprehensive performance table, refer to Table 4 in the Appendix.

| Models | Base Model | Tool Use | AIME24 | AIME25 | HMMT25 |
|---|---|---|---|---|---|
| | | Proprietary models | | | |
| OpenAI-o4-mini-w/tools | - | ✓ | 98.7 | 99.5 | - |
| OpenAI-o3-w/tools | - | ✓ | 95.2 | 98.4 | - |
| OpenAI-o4-mini | - | ✗ | 93.4 | 92.7 | 83.0 |
| Gemini-2.5-Pro | - | ✗ | 92.0 | 88.0 | 82.5 |
| OpenAI-o3 | - | ✗ | 91.6 | 88.9 | 77.5 |
| OpenAI-o3-mini | - | ✗ | 87.3 | 86.3 | 53.0 |
| Claude-Opus-4.0-Thinking | - | ✗ | 83.0 | 72.0 | 58.3 |
| | | Frontier Models (1B $\sim$ 2B) | | | |
| ToRL-1.5B | QM2.5-1.5B-Base | ✓ | 26.7 | 26.7 | - |
| DS-Distill-Qwen-1.5B | QM2.5-1.5B-Base | ✗ | 28.8 | 21.8 | 15.3 |
| CoRT-1.5B | DS-Distill-Qwen-1.5B | ✓ | 43.1 | 30.2 | 20.1 |
| Qwen3-1.7B Thinking | Qwen3-1.7B-Base | ✗ | 52.0 | 35.3 | 23.3 |
| OpenThinker3-1.5B | QW2.5-1.5B-Instruct | ✗ | 52.0 | 41.7 | 27.3 |
| OpenReasoning-1.5B | QW2.5-1.5B-Instruct | ✗ | 55.5 | 45.6 | 31.5 |
| AgentMath-1.7B | Qwen3-1.7B-Base | ✓ | 59.6 | 48.1 | 40.2 |
| | | Frontier Models (7B $\sim$ 8B) | | | |
| ToRL-7B | QM2.5-7B-Base | ✓ | 43.3 | 30.0 | - |
| ZeroTIR-7B | QW2.5-7B-Base | ✓ | 46.7 | 30.0 | 22.5 |
| SimpleTIR-7B | QW2.5-7B-Base | ✓ | 50.5 | 30.9 | 29.7 |
| AFM-7B | QW2.5-7B-Instruct | ✓ | 51.9 | 37.8 | - |
| rStar-Math-Qwen-7B | QM2.5-7B-Base | ✓ | 53.3 | - | - |
| DS-Distill-Qwen-7B | QM2.5-7B-Base | ✗ | 55.0 | 39.7 | - |
| CIR-Qwen3-NT8-8B | Qwen3-8B | ✓ | 61.5 | 46.3 | - |
| AReal-boba-7B | DS-Distill-Qwen-7B | ✗ | 61.9 | 48.3 | 29.4 |
| Skywork-OR1-7B | DS-Distill-Qwen-7B | ✗ | 70.2 | 54.6 | 35.7 |
| POLARIS-7B-Preview | DS-Distill-Qwen-7B | ✗ | 72.6 | 52.6 | - |
| Qwen3-8B-Thinking | Qwen3-8B-Base | ✗ | 76.0 | 67.3 | 44.7 |
| OpenReasoning-7B | QW2.5-7B-Instruct | ✗ | 84.7 | 78.2 | 63.5 |
| DS-0528-Qwen3-8B | Qwen3-8B-Base | ✗ | 86.0 | 76.3 | 61.5 |
| AgentMath-8B | Qwen3-8B-Base | ✓ | 89.8 | 84.7 | 71.3 |
| | | Frontier Models (30B $\sim$ 32B) | | | |
| ZeroTIR-32B | Q2.5-32B-Base | ✓ | 56.7 | 33.3 | 20.0 |
| START-32B | QwQ-32B | ✓ | 66.7 | 47.1 | - |
| AFM-32B | QW2.5-32B-Instruct | ✓ | 66.7 | 59.8 | - |
| ReTool-32B | QW2.5-32B-Instruct | ✓ | 67.0 | 49.3 | |
| rStar2-Agent-32B | QW2.5-32B-instruct | ✓ | 69.4 | 57.3 | - |
| ReTool-R1-32B-distill | DS-Distill-Qwen-32B | ✓ | 72.5 | 54.3 | - |
| DS-Distill-Qwen-32B | QW2.5-32B-Base | ✗ | 72.9 | 59.0 | 33.0 |
| Qwen3-30B-A3B-Instruct-2507 | Qwen3-30B-A3B-Base | ✗ | 72.9 | 61.3 | 43.0 |
| CoRT-32B | DS-Distill-Qwen-32B | ✓ | 76.7 | 67.1 | - |
| QwQ-32B | - | ✗ | 79.5 | 65.3 | 48.0 |
| STILL-3-TOOL-32B | DS-Distill-Qwen-32B | ✓ | 81.7 | 64.2 | 45.4 |
| Skywork-OR1-32B | DS-Distill-Qwen-32B | ✗ | 82.2 | 73.3 | - |
| AM-Thinking-v1-32B | Qwen 2.5-32B-Base | ✗ | 85.3 | 74.4 | - |
| Qwen3-30B-A3B-Thinking-2507 | Qwen3-30B-A3B-Base | ✗ | 87.7 | 85.0 | 71.4 |
| AgentMath-30B-A3B | Qwen3-30B-A3B-Instruct-2507 | ✓ | 90.6 | 86.4 | 73.8 |
| | | Frontier Models (>32B) | | | |
| Qwen3-235B-A22B-Instruct-2507 | Qwen3-235B-A22B-Base | ✗ | 79.2 | 70.3 | 55.4 |
| DS-671B | DeepSeek-V3-Base | ✗ | 79.8 | 70.0 | 44.4 |
| Qwen3-235B-A22B-Thinking | Qwen3-235B-A22B-Base | ✗ | 85.7 | 81.5 | 62.5 |
| DS-671B-0528 | DeepSeek-V3-Base | ✗ | 91.4 | 87.5 | 77.0 |
| Qwen3-235B-A22B-Thinking-2507 | Qwen3-235B-A22B-Base | ✗ | 94.2 | 92.3 | 83.9 |
| AgentMath-235B-A22B-SFT | Qwen3-235B-A22B-Instruct-2507 | ✓ | 93.4 | 90.8 | 81.7 |

The results show that AgentMath significantly outperforms existing tool-augmented and text-only frontier reasoning models across all three benchmarks at comparable parameter scales. Among small-scale models (1B $\sim$ 2B), AgentMath-1.7B attains 59.6%, 48.1%, and 40.2% accuracy on AIME24, AIME25, and HMMT25 respectively, substantially surpassing both the tool-augmented CoRT-1.5B (43.1%, 30.2%, 20.1%) and the text-only OpenReasoning-1.5B (55.5%, 45.6%, 31.5%). At the medium scale (7B $\sim$ 8B), AgentMath-8B achieves 89.8%, 84.7%, and 71.3%, significantly outperforming the tool-augmented CIR-Qwen3-NT8-8B and text-only DS-0528-Qwen3-8B (86.0%, 76.3%, 61.5%). For larger-scale models (30B $\sim$ 32B), AgentMath-30B-A3B reaches 90.6%, 86.4%, and 73.8%, exceeding the tool-augmented STILL-3-TOOL-32B (81.7%, 64.2%, 45.4%) and text-only Qwen3-30B-A3B-Thinking-2507 (87.7%, 85.0%, 74.3%).

Notably, the Mixture-of-Experts model AgentMath-30B-A3B with 3B active parameters and 30B total parameters outperforms most dense 30B models on AIME24 and AIME25, approaching the performance of DS-671B-0528. This demonstrates that our approach achieves competitive performance with substantially larger models while maintaining computational efficiency.

At ultra-large scale (>32B), AgentMath-235B-A22B-SFT achieves 93.4%, 90.8%, and 81.7% across the three benchmarks, surpassing DS-671B-0528 (91.4%, 87.5%, 77.0%) and achieving performance on par with Qwen3-235B-A22B-Thinking-2507. Compared to proprietary models, AgentMath-30B-A3B outperforms OpenAI-o3-mini and Claude-Opus-4.0-Thinking on three benchmarks and is competitive with OpenAI-o3 and Gemini-2.5-Pro. Furthermore, AgentMath-235B-A22B-SFT exceeds OpenAI-o3, approaching OpenAI-o4-mini and Gemini-2.5-Pro. Notably, due to computational constraints, AgentMath-235B-A22B is trained solely via SFT.

These results validate the effectiveness of our tool-augmented data synthesis method and large-scale reinforcement learning training strategy, yielding consistent improvements in math reasoning capabilities across diverse model scales. We provide the case study of AgentMath in Appendix A.8.

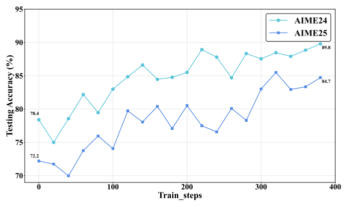

(a) Acc on AIME24 and AIME25

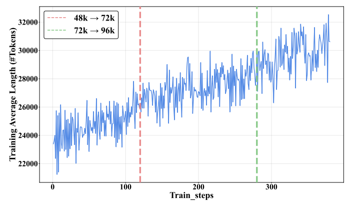

(b) Training response length

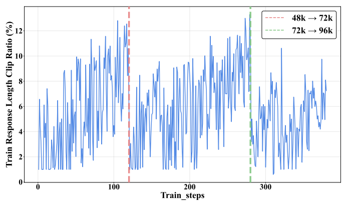

(c) Training length clip ratio

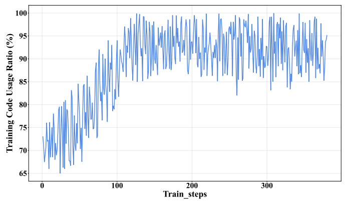

(d) Code ratio

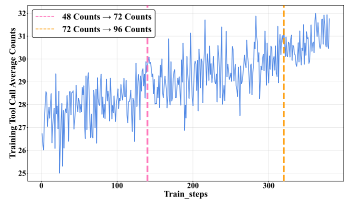

(e) Tool call counts.

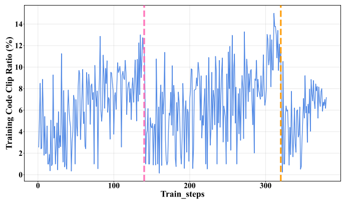

(f) Code clip ratio

Figure 3: Evolution of key metrics during multi-stage RL training: (a-c) accuracy on AIME24 and AIME25, response length, length clip ratio; (d-f) code ratio, tool call counts, code clip ratio.

## 3.5 Cognition Analysis

Table 2: Performance comparison between AgentMath and Text-Based Model in SFT and RL stages.

| **Models** | **AIME24** | **AIME25** |
|---|---|---|
| Text-Based-SFT-20k | 57.1% | 49.2% |
| AgentMath-SFT-20k | 60.5% | 53.3% |
| Text-Based-RL | 68.7% | 57.5% |
| AgentMath-RL | 76.2% | 67.5% |

**Tool-Augmented Synthetic Data vs. Text-Based Data.** To assess the effectiveness of tool-augmented synthetic data method, we conduct experiments addressing two core questions: the comparative advantage of tool-augmented synthetic data over text-based data in SFT, and the impact of tool augmentation on performance and efficiency during RL. We employ Qwen3-8B-Base as the backbone model and an identical 20k data. As shown in Table 2, in SFT stage, AgentMath-SFT achieves accuracies of 60.5% on AIME24 and 53.3% on AIME25, surpassing the text-based baseline by 3.4% and 4.1%, validating our method of converting computation-intensive steps into executable code. The benefits are further amplified in RL: as detailed in Figure 4 and Table 2, AgentMath-RL requires only $\sim$400 steps to reach 76.2% (AIME24) and 67.5% (AIME25), a 4.0$\times$ efficiency improvement over the $\sim$1600 steps needed by the Text-Based-SFT model to achieve inferior results (68.7% and 57.5%). Notably, it matches the Text-Based model's final performance in just 100–200 steps. Additionally, inference efficiency improves substantially, as indicated in Figure 5, with sequence lengths reduced by $\sim$4k tokens ($\sim$14%) and slower length growth, attributable to precise code execution replacing verbose manual calculations. Collectively, AgentMath demonstrates superior accuracy, training efficiency, and inference scalability, confirming the power of interleaving natural language reasoning with computational tools. See Appendix A.7.1 for more details.

**Multi Stage RL Training.** Following the supervised fine-tuning phase, we observed that the model frequently generated responses exceeding 32k tokens for complex mathematical problems, with the most challenging instances surpassing 64k tokens. To effectively balance training efficiency with model capacity, we developed an adaptive, multi-stage RL strategy that progressively unlocks the model's potential by dynamically expanding the sequence length and tool-call budget. This process is triggered automatically when truncation rates for either response length or tool usage exceed 10%, incrementally increasing the context length from 48k to 72k (at step 120) and finally to 96k (at step 280), while the tool-call limit expands from 48 to 72 (step 140) and then to 96 (step 320), as illustrated in Figure 3c and 3f. The training progression, detailed in Figure 3, reveals significant trends: generated trajectory average lengths increased from 24k to 30k (Figure 3b), tool average invocation frequency rose from 27 to 31 calls per problem (Figure 3e), and code utilization improved markedly from 70% to 95% (Figure 3d), indicating enhanced proficiency in multi-step reasoning. Consequently, accuracy on the AIME24 benchmark rose from 78.4% to 89.8% (+11.4%) and on AIME25 from 72.2% to 84.7% (+12.5%) (Figure 3a), with consistent improvements following each capac-

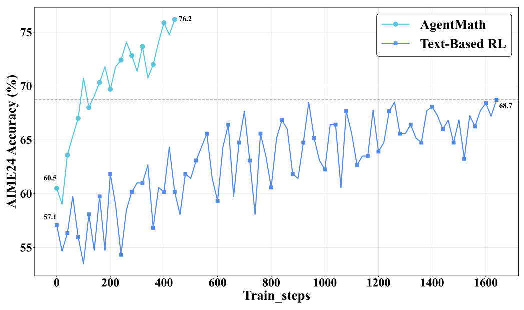

(a) AIME24 Accuracy

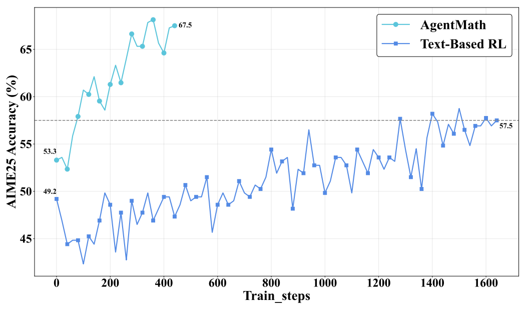

(b) AIME25 Accuracy

Figure 4: Performance Comparison of AgentMath vs. Text-Based Model in the RL phase on AIME24/25. Both models were initialized from their best SFT checkpoint trained on 20k data.

ity expansion. Notably, the model exhibited emergent code self-correction capabilities as shown in Appendix A.8.2 Figure 9. These results, along with the performance of AgentMath with different backbones detailed in Table 5, confirm the efficacy of our strategy. The experiments establish three key insights: (1) expanded capacity is crucial for facilitating deeper reasoning chains; (2) The composite reward effectively guides the model's tool-call decisions; and (3) the stable training under extreme configurations (96k tokens, 96 tool calls) underscores the robustness of the AgentMath framework and its asynchronous training infrastructure. See Appendix A.7.2 for more details.

Table 3: Performance improvements on AIME24/25 through progressive refinement steps.

| Models / Refinement Steps | AIME24 | AIME25 |
|---|---|---|
| Initial Unrefined CI-Synthetic Data (20k) | 35.3% | 25.7% |
| + Format consistency correction | 47.4% | 40.1% |
| + Code executability verification | 52.8% | 44.8% |
| + Environmental feedback alignment | 56.3% | 48.3% |
| + Self-correction capability injection | 58.6% | 50.8% |
| + SFT with selective feedback masking | 60.5% | 53.3% |

**Synthetic Data Refinement and Scaling Law.** As detailed in Table 3, we conduct a systematic evaluation of AgentMath's data synthesis pipeline, revealing that progressive multi-dimensional refinement is critical for performance. The initial unrefined synthetic data yielded suboptimal results (AIME24: 35.3%; AIME25: 25.7%), primarily due to formatting inconsistencies and non-executable code. By systematically applying refinements,including format consistency, code executability verification, and environment feedback alignment, performance substantially improved to 58.6% on AIME24 and 50.8% on AIME25. The subsequent integration of a self-correction mechanism, combined with supervised fine-tuning using selective feedback masking guided by code execution results, culminated in final accuracies of 60.5% on AIME24 and 53.3% on AIME25, underscoring the necessity of each refinement stage. Furthermore, scaling the tool-augmented dataset from 2k to 300k (Figure 7) yielded significant performance gains, improving accuracy from 27.2% to 78.4% on AIME24 and from 21.1% to 72.2% on AIME25. This combination of rigorous quality control and effective data scaling effectively mitigates data scarcity in tool-augmented mathematical reasoning, establishing a robust foundation for high-performance reasoning agents. Further details are provided in Appendix A.7.3.

Owing to space constraints, a comprehensive analysis of the AgentMath framework's training efficiency and the impact of the partial rollout segment count is deferred to Appendix A.7.4.

## 4 CONCLUSION

This paper introduces AgentMath, a tool-augmented agent framework that seamlessly integrates language model reasoning with the precision of code interpreters to tackle complex mathematical problems. Extensive evaluations show that AgentMath achieves state-of-the-art performance on challenging mathematical competition benchmarks, including AIME24, AIME25, and HMMT25. Remarkably, AgentMath-30B-A3B with only 3B active parameters achieves 90.6%, 86.4%, and 78.9% accuracy, outperforming OpenAI-o3-mini and Claude-Opus-4.0-Thinking while remaining competitive with OpenAI-o3, Gemini-2.5-Pro, and DeepSeek-R1-671B. Furthermore, our work highlights the essential role of automated tool-augmented data synthesis and a scalable asynchronous training infrastructure in enabling effective and efficient agentic learning for mathematical reasoning.

## Reproducibility Statement

To ensure the reproducibility of AgentMath, we provide comprehensive details on algorithms, data synthesis procedures, Agent RL training, and experimental configurations throughout the main paper and appendices. The data synthesis pipeline, multi-dimensional quality refinement mechanisms, and the design of synthesis and judge prompts are detailed in Sections 2.1 and 2.2, and Appendices A.2 and A.6. The RL training framework and implementation details are presented in Section 2.3 and Appendix A.3. Optimization strategies for RL training efficiency and the design of Algorithm 1 are described in Section 2.4 and Appendix A.4. We systematically evaluate the individual contributions of tool-augmented data synthesis, multi-stage RL training, scaling laws of synthetic data, and multi-dimensional quality refinement through ablation experiments in Section 3.5 and Appendix A.7. Case analyses are provided in Appendix A.8. Detailed experimental settings, including SFT and RL training data, training strategies, evaluation settings and main results, are documented in Sections 3.1 , 3.2, 3.3, 3.4 and Appendix A.5. To further facilitate community reproducibility and future research, we have made available our anonymous source code, data synthesis pipeline, and training/eval scripts in the supplementary materials. We believe these materials will help researchers better understand and reproduce our work.

## References

a-m team. Am-deepseek-r1-0528-distilled, June 2025. URL `https://github.com/a-m-team/a-m-models`.

Mayank Agarwal, Ibrahim Abdelaziz, Kinjal Basu, Merve Unuvar, Luis A Lastras, Yara Rizk, and Pavan Kapanipathi. Toolrm: Outcome reward models for tool-calling large language models. *arXiv preprint arXiv:2509.11963*, 2025.

Wasi Uddin Ahmad, Somshubra Majumdar, Aleksander Ficek, Sean Narenthiran, Mehrzad Samadi, Jocelyn Huang, Siddhartha Jain, Vahid Noroozi, and Boris Ginsburg. OpenCodeReasoning-II: A Simple Test Time Scaling Approach via Self-Critique, 2025. URL `https://arxiv.org/abs/2507.09075`.

Chenxin An, Zhihui Xie, Xiaonan Li, Lei Li, Jun Zhang, Shansan Gong, Ming Zhong, Jingjing Xu, Xipeng Qiu, Mingxuan Wang, and Lingpeng Kong. Polaris: A post-training recipe for scaling reinforcement learning on advanced reasoning models. URL `https://hkunlp.github.io/blog/2025/Polaris`.

Zhangir Azerbayev, Hailey Schoelkopf, Keiran Paster, Marco Dos Santos, Stephen McAleer, Albert Q Jiang, Jia Deng, Stella Biderman, and Sean Welleck. Llemma: An open language model for mathematics. *arXiv preprint arXiv:2310.10631*, 2023.

Fei Bai, Yingqian Min, Beichen Zhang, Zhipeng Chen, Wayne Xin Zhao, Lei Fang, Zheng Liu, Zhongyuan Wang, and Ji-Rong Wen. Towards effective code-integrated reasoning, 2025. URL `https://arxiv.org/abs/2505.24480`.

Mislav Balunović, Jasper Dekoninck, Ivo Petrov, Nikola Jovanović, and Martin Vechev. Matharena: Evaluating llms on uncontaminated math competitions, February 2025. URL `https://matharena.ai/`.

Qikai Chang, Zhenrong Zhang, Pengfei Hu, Jiefeng Ma, Yicheng Pan, Jianshu Zhang, Jun Du, Quan Liu, and Jianqing Gao. Thor: Tool-integrated hierarchical optimization via rl for mathematical reasoning. *arXiv preprint arXiv:2509.13761*, 2025.

Wenhu Chen, Xueguang Ma, Xinyi Wang, and William W. Cohen. Program of thoughts prompting: Disentangling computation from reasoning for numerical reasoning tasks, 2023. URL `https://arxiv.org/abs/2211.12588`.

Yang Chen, Zhuolin Yang, Zihan Liu, Chankyu Lee, Peng Xu, Mohammad Shoeybi, Bryan Catanzaro, and Wei Ping. Acereason-nemotron: Advancing math and code reasoning through reinforcement learning. *arXiv preprint arXiv:2505.16400*, 2025a.

Zhipeng Chen, Yingqian Min, Beichen Zhang, Jie Chen, Jinhao Jiang, Daixuan Cheng, Wayne Xin Zhao, Zheng Liu, Xu Miao, Yang Lu, Lei Fang, Zhongyuan Wang, and Ji-Rong Wen. An empirical study on eliciting and improving r1-like reasoning models. *arXiv preprint arXiv:2503.04548*, 2025b.

Zhipeng Chen, Yingqian Min, Beichen Zhang, Jie Chen, Jinhao Jiang, Daixuan Cheng, Wayne Xin Zhao, Zheng Liu, Xu Miao, Yang Lu, et al. An empirical study on eliciting and improving r1-like reasoning models. *arXiv preprint arXiv:2503.04548*, 2025c.

Claude. Claude 3.7 sonnet. 2025. URL `https://www.anthropic.com/news/claude-3-7-sonnet`.

Karl Cobbe, Vineet Kosaraju, Mohammad Bavarian, Mark Chen, Heewoo Jun, Lukasz Kaiser, Matthias Plappert, Jerry Tworek, Jacob Hilton, Reiichiro Nakano, et al. Training verifiers to solve math word problems. *arXiv preprint arXiv:2110.14168*, 2021.

Ganqu Cui, Lifan Yuan, Zefan Wang, Hanbin Wang, Wendi Li, Bingxiang He, Yuchen Fan, Tianyu Yu, Qixin Xu, Weize Chen, et al. Process reinforcement through implicit rewards. *arXiv preprint arXiv:2502.01456*, 2025.

DeepSeek-AI, Daya Guo, Dejian Yang, Haowei Zhang, Junxiao Song, Ruoyu Zhang, Runxin Xu, Qihao Zhu, Shirong Ma, Peiyi Wang, Xiao Bi, Xiaokang Zhang, Xingkai Yu, Yu Wu, Z. F. Wu, Zhibin Gou, Zhihong Shao, Zhuoshu Li, Ziyi Gao, Aixin Liu, Bing Xue, Bingxuan Wang, Bochao Wu, Bei Feng, Chengda Lu, Chenggang Zhao, Chengqi Deng, Chenyu Zhang, Chong Ruan, Damai Dai, Deli Chen, Dongjie Ji, Erhang Li, Fangyun Lin, Fucong Dai, Fuli Luo, Guangbo Hao, Guanting Chen, Guowei Li, H. Zhang, Han Bao, Hanwei Xu, Haocheng Wang, Honghui Ding, Huajian Xin, Huazuo Gao, Hui Qu, Hui Li, Jianzhong Guo, Jiashi Li, Jiawei Wang, Jingchang Chen, Jingyang Yuan, Junjie Qiu, Junlong Li, J. L. Cai, Jiaqi Ni, Jian Liang, Jin Chen, Kai Dong, Kai Hu, Kaige Gao, Kang Guan, Kexin Huang, Kuai Yu, Lean Wang, Lecong Zhang, Liang Zhao, Litong Wang, Liyue Zhang, Lei Xu, Leyi Xia, Mingchuan Zhang, Minghua Zhang, Minghui Tang, Meng Li, Miaojun Wang, Mingming Li, Ning Tian, Panpan Huang, Peng Zhang, Qiancheng Wang, Qinyu Chen, Qiushi Du, Ruiqi Ge, Ruisong Zhang, Ruizhe Pan, Runji Wang, R. J. Chen, R. L. Jin, Ruyi Chen, Shanghao Lu, Shangyan Zhou, Shanhuang Chen, Shengfeng Ye, Shiyu Wang, Shuiping Yu, Shunfeng Zhou, Shuting Pan, S. S. Li, Shuang Zhou, Shaoqing Wu, Shengfeng Ye, Tao Yun, Tian Pei, Tianyu Sun, T. Wang, Wangding Zeng, Wanjia Zhao, Wen Liu, Wenfeng Liang, Wenjun Gao, Wenqin Yu, Wentao Zhang, W. L. Xiao, Wei An, Xiaodong Liu, Xiaohan Wang, Xiaokang Chen, Xiaotao Nie, Xin Cheng, Xin Liu, Xin Xie, Xingchao Liu, Xinyu Yang, Xinyuan Li, Xuecheng Su, Xuheng Lin, X. Q. Li, Xiangyue Jin, Xiaojin Shen, Xiaosha Chen, Xiaowen Sun, Xiaoxiang Wang, Xinnan Song, Xinyi Zhou, Xianzu Wang, Xinxia Shan, Y. K. Li, Y. Q. Wang, Y. X. Wei, Yang Zhang, Yanhong Xu, Yao Li, Yao Zhao, Yaofeng Sun, Yaohui Wang, Yi Yu, Yichao Zhang, Yifan Shi, Yiliang Xiong, Ying He, Yishi Piao, Yisong Wang, Yixuan Tan, Yiyang Ma, Yiyuan Liu, Yongqiang Guo, Yuan Ou, Yuduan Wang, Yue Gong, Yuheng Zou, Yujia He, Yunfan Xiong, Yuxiang Luo, Yuxiang You, Yuxuan Liu, Yuyang Zhou, Y. X. Zhu, Yanhong Xu, Yanping Huang, Yaohui Li, Yi Zheng, Yuchen Zhu, Yunxian Ma, Ying Tang, Yukun Zha, Yuting Yan, Z. Z. Ren, Zehui Ren, Zhangli Sha, Zhe Fu, Zhean Xu, Zhenda Xie, Zhengyan Zhang, Zhewen Hao, Zhicheng Ma, Zhigang Yan, Zhiyu Wu, Zihui Gu, Zijia Zhu, Zijun Liu, Zilin Li, Ziwei Xie, Ziyang Song, Zizheng Pan, Zhen Huang, Zhipeng Xu, Zhongyu Zhang, and Zhen Zhang. Deepseek-r1: Incentivizing reasoning capability in llms via reinforcement learning, 2025. URL `https://arxiv.org/abs/2501.12948`.

Guanting Dong, Hangyu Mao, Kai Ma, Licheng Bao, Yifei Chen, Zhongyuan Wang, Zhongxia Chen, Jiazhen Du, Huiyang Wang, Fuzheng Zhang, et al. Agentic reinforced policy optimization. *arXiv preprint arXiv:2507.19849*, 2025.

Dong Du, Shulin Liu, Tao Yang, Shaohua Chen, and Yang Li. Ulorl: An ultra-long output reinforcement learning approach for advancing large language models' reasoning abilities. *arXiv preprint arXiv:2507.19766*, 2025a.

Weihua Du, Pranjal Aggarwal, Sean Welleck, and Yiming Yang. Agentic-r1: Distilled dual-strategy reasoning. *arXiv preprint arXiv:2507.05707*, 2025b.

Hugging Face. Open r1: A fully open reproduction of deepseek-r1, January 2025. URL https://github.com/huggingface/open-r1.

Tiantian Fan, Lingjun Liu, Yu Yue, Jiaze Chen, Chengyi Wang, Qiying Yu, Chi Zhang, Zhiqi Lin, Ruofei Zhu, Yufeng Yuan, Xiaochen Zuo, Bole Ma, Mofan Zhang, Gaohong Liu, Ru Zhang, Haotian Zhou, Cong Xie, Ruidong Zhu, Zhi Zhang, Xin Liu, Mingxuan Wang, Lin Yan, and Yonghui Wu. Truncated proximal policy optimization, 2025. URL https://arxiv.org/abs/2506.15050.

Jinyuan Fang, Yanwen Peng, Xi Zhang, Yingxu Wang, Xinhao Yi, Guibin Zhang, Yi Xu, Bin Wu, Siwei Liu, Zihao Li, et al. A comprehensive survey of self-evolving ai agents: A new paradigm bridging foundation models and lifelong agentic systems. *arXiv preprint arXiv:2508.07407*, 2025.

Jiazhan Feng, Shijue Huang, Xingwei Qu, Ge Zhang, Yujia Qin, Baoquan Zhong, Chengquan Jiang, Jinxin Chi, and Wanjun Zhong. Retool: Reinforcement learning for strategic tool use in llms, 2025a. URL https://arxiv.org/abs/2504.11536.

Zihao Feng, Xiaoxue Wang, Bowen Wu, Hailong Cao, Tiejun Zhao, Qun Yu, and Baoxun Wang. Toolsample: Dual dynamic sampling methods with curriculum learning for rl-based tool learning. *arXiv preprint arXiv:2509.14718*, 2025b.

Wei Fu, Jiaxuan Gao, Xujie Shen, Chen Zhu, Zhiyu Mei, Chuyi He, Shusheng Xu, Guo Wei, Jun Mei, Jiashu Wang, Tongkai Yang, Binhang Yuan, and Yi Wu. Areal: A large-scale asynchronous reinforcement learning system for language reasoning, 2025. URL https://arxiv.org/abs/2505.24298.

Jiaxuan Gao, Wei Fu, Minyang Xie, Shusheng Xu, Chuyi He, Zhiyu Mei, Banghua Zhu, and Yi Wu. Beyond ten turns: Unlocking long-horizon agentic search with large-scale asynchronous rl, 2025a. URL https://arxiv.org/abs/2508.07976.

Luyu Gao, Aman Madaan, Shuyan Zhou, Uri Alon, Pengfei Liu, Yiming Yang, Jamie Callan, and Graham Neubig. Pal: Program-aided language models, 2023. URL https://arxiv.org/abs/2211.10435.

Wei Gao, Yuheng Zhao, Dakai An, Tianyuan Wu, Lunxi Cao, Shaopan Xiong, Ju Huang, Weixun Wang, Siran Yang, Wenbo Su, Jiamang Wang, Lin Qu, Bo Zheng, and Wei Wang. Roll-packer: Mitigating long-tail rollouts for fast, synchronous rl post-training, 2025b. URL https://arxiv.org/abs/2509.21009.

Zhibin Gou, Zhihong Shao, Yeyun Gong, Yelong Shen, Yujiu Yang, Nan Duan, and Weizhu Chen. Critic: Large language models can self-correct with tool-interactive critiquing. *arXiv preprint arXiv:2305.11738*, 2023a.

Zhibin Gou, Zhihong Shao, Yeyun Gong, Yelong Shen, Yujiu Yang, Minlie Huang, Nan Duan, and Weizhu Chen. Tora: A tool-integrated reasoning agent for mathematical problem solving. *arXiv preprint arXiv:2309.17452*, 2023b.

Etash Guha, Ryan Marten, Sedrick Keh, Negin Raoof, Georgios Smyrnis, Hritik Bansal, Marianna Nezhurina, Jean Mercat, Trung Vu, Zayne Sprague, Ashima Suvarna, Benjamin Feuer, Liangyu Chen, Zaid Khan, Eric Frankel, Sachin Grover, Caroline Choi, Niklas Muennighoff, Shiye Su, Wanjia Zhao, John Yang, Shreyas Pimpalgaonkar, Kartik Sharma, Charlie Cheng-Jie Ji, Yichuan Deng, Sarah Pratt, Vivek Ramanujan, Jon Saad-Falcon, Jeffrey Li, Achal Dave, Alon Albalak, Kushal Arora, Blake Wulfe, Chinmay Hegde, Greg Durrett, Sewoong Oh, Mohit Bansal, Saadia Gabriel, Aditya Grover, Kai-Wei Chang, Vaishaal Shankar, Aaron Gokaslan, Mike A. Merrill, Tatsunori Hashimoto, Yejin Choi, Jenia Jitsev, Reinhard Heckel, Maheswaran Sathiamoorthy, Alexandros G. Dimakis, and Ludwig Schmidt. Openthoughts: Data recipes for reasoning models, 2025. URL https://arxiv.org/abs/2506.04178.

Chuzhan Hao, Wenfeng Feng, Yuewei Zhang, and Hao Wang. Dynasearcher: Dynamic knowledge graph augmented search agent via multi-reward reinforcement learning. *arXiv preprint arXiv:2507.17365*, 2025.

Jujie He, Jiacai Liu, Chris Yuhao Liu, Rui Yan, Chaojie Wang, Peng Cheng, Xiaoyu Zhang, Fuxiang Zhang, Jiacheng Xu, Wei Shen, Siyuan Li, Liang Zeng, Tianwen Wei, Cheng Cheng, Bo An, Yang Liu, and Yahui Zhou. Skywork open reasoner 1 technical report. *arXiv preprint arXiv:2505.22312*, 2025a.

Tao He, Hao Li, Jingchang Chen, Runxuan Liu, Yixin Cao, Lizi Liao, Zihao Zheng, Zheng Chu, Jiafeng Liang, Ming Liu, et al. Breaking the reasoning barrier a survey on llm complex reasoning through the lens of self-evolution. In *Findings of the Association for Computational Linguistics: ACL 2025*, pp. 7377–7417, 2025b.

Dan Hendrycks, Collin Burns, Saurav Kadavath, Akul Arora, Steven Basart, Eric Tang, Dawn Song, and Jacob Steinhardt. Measuring mathematical problem solving with the math dataset. *arXiv preprint arXiv:2103.03874*, 2021.

Jian Hu, Xibin Wu, Zilin Zhu, Xianyu, Weixun Wang, Dehao Zhang, and Yu Cao. Openrlhf: An easy-to-use, scalable and high-performance rlhf framework. *arXiv preprint arXiv:2405.11143*, 2024.

Jingcheng Hu, Yinmin Zhang, Qi Han, Daxin Jiang, Xiangyu Zhang, and Heung-Yeung Shum. Open-reasoner-zero: An open source approach to scaling up reinforcement learning on the base model, 2025. URL `https://arxiv.org/abs/2503.24290`.

Yunjie Ji, Xiaoyu Tian, Sitong Zhao, Haotian Wang, Shuaiting Chen, Yiping Peng, Han Zhao, and Xiangang Li. AM-Thinking-v1: Advancing the frontier of reasoning at 32B scale. `https://arxiv.org/abs/2505.08311`, 2025. arXiv:2505.08311 [cs.CL].

Bowen Jin, Hansi Zeng, Zhenrui Yue, Jinsung Yoon, Sercan Arik, Dong Wang, Hamed Zamani, and Jiawei Han. Search-r1: Training llms to reason and leverage search engines with reinforcement learning, 2025a. URL `https://arxiv.org/abs/2503.09516`.

Yiyang Jin, Kunzhao Xu, Hang Li, Xueting Han, Yanmin Zhou, Cheng Li, and Jing Bai. Reveal: Self-evolving code agents via iterative generation-verification. *arXiv preprint arXiv:2506.11442*, 2025b.

Woosuk Kwon, Zhuohan Li, Siyuan Zhuang, Ying Sheng, Lianmin Zheng, Cody Hao Yu, Joseph E. Gonzalez, Hao Zhang, and Ion Stoica. Efficient memory management for large language model serving with pagedattention. In *Proceedings of the ACM SIGOPS 29th Symposium on Operating Systems Principles*, 2023.

Xin Lai, Zhuotao Tian, Yukang Chen, Senqiao Yang, Xiangru Peng, and Jiaya Jia. Step-dpo: Step-wise preference optimization for long-chain reasoning of llms, 2024. URL `https://arxiv.org/abs/2406.18629`.

Chengpeng Li, Zhengyang Tang, Ziniu Li, Mingfeng Xue, Keqin Bao, Tian Ding, Ruoyu Sun, Benyou Wang, Xiang Wang, Junyang Lin, et al. Cort: Code-integrated reasoning within thinking. *arXiv preprint arXiv:2506.09820*, 2025a.

Chengpeng Li, Mingfeng Xue, Zhenru Zhang, Jiaxi Yang, Beichen Zhang, Xiang Wang, Bowen Yu, Binyuan Hui, Junyang Lin, and Dayiheng Liu. Start: Self-taught reasoner with tools. *arXiv preprint arXiv:2503.04625*, 2025b.

Weizhen Li, Jianbo Lin, Zhuosong Jiang, Jingyi Cao, Xinpeng Liu, Jiayu Zhang, Zhenqiang Huang, Qianben Chen, Weichen Sun, Qiexiang Wang, Hongxuan Lu, Tianrui Qin, Chenghao Zhu, Yi Yao, Shuying Fan, Xiaowan Li, Tiannan Wang, Pai Liu, King Zhu, He Zhu, Dingfeng Shi, Piaohong Wang, Yeyi Guan, Xiangru Tang, Minghao Liu, Yuchen Eleanor Jiang, Jian Yang, Jiaheng Liu, Ge Zhang, and Wangchunshu Zhou. Chain-of-agents: End-to-end agent foundation models via multi-agent distillation and agentic rl, 2025c. URL `https://arxiv.org/abs/2508.13167`.

Xiaoxi Li, Guanting Dong, Jiajie Jin, Yuyao Zhang, Yujia Zhou, Yutao Zhu, Peitian Zhang, and Zhicheng Dou. Search-o1: Agentic search-enhanced large reasoning models, 2025d. URL `https://arxiv.org/abs/2501.05366`.

Xuefeng Li, Haoyang Zou, and Pengfei Liu. Torl: Scaling tool-integrated rl, 2025e. URL `https://arxiv.org/abs/2503.23383`.

Yang Li, Zhichen Dong, Yuhan Sun, Weixun Wang, Shaopan Xiong, Yijia Luo, Jiashun Liu, Han Lu, Jiamang Wang, Wenbo Su, Bo Zheng, and Junchi Yan. Attention illuminates llm reasoning: The preplan-and-anchor rhythm enables fine-grained policy optimization, 2025f. URL `https://arxiv.org/abs/2510.13554`.

Ziniu Li, Tian Xu, Yushun Zhang, Zhihang Lin, Yang Yu, Ruoyu Sun, and Zhi-Quan Luo. Remax: A simple, effective, and efficient reinforcement learning method for aligning large language models. In *Forty-first International Conference on Machine Learning*, 2024.

Hunter Lightman, Vineet Kosaraju, Yuri Burda, Harrison Edwards, Bowen Baker, Teddy Lee, Jan Leike, John Schulman, Ilya Sutskever, and Karl Cobbe. Let's verify step by step. In *The Twelfth International Conference on Learning Representations*, 2023.

Heng Lin and Zhongwen Xu. Understanding tool-integrated reasoning. *arXiv preprint arXiv:2508.19201*, 2025.

Jiashun Liu, Johan Obando-Ceron, Han Lu, Yancheng He, Weixun Wang, Wenbo Su, Bo Zheng, Pablo Samuel Castro, Aaron Courville, and Ling Pan. Asymmetric proximal policy optimization: mini-critics boost llm reasoning, 2025a. URL `https://arxiv.org/abs/2510.01656`.

Licheng Liu, Zihan Wang, Linjie Li, Chenwei Xu, Yiping Lu, Han Liu, Avirup Sil, and Manling Li. Let's try again: Eliciting multi-turn reasoning in language models via simplistic feedback. In *2nd AI for Math Workshop@ ICML 2025*, 2025b.

Mingjie Liu, Shizhe Diao, Ximing Lu, Jian Hu, Xin Dong, Yejin Choi, Jan Kautz, and Yi Dong. ProRL: Prolonged reinforcement learning expands reasoning boundaries in large language models. *arXiv*, 2025c. URL `https://arxiv.org/abs/2505.24864`.

Wei Liu, Siya Qi, Xinyu Wang, Chen Qian, Yali Du, and Yulan He. Nover: Incentive training for language models via verifier-free reinforcement learning. *arXiv preprint arXiv:2505.16022*, 2025d.

Zihe Liu, Jiashun Liu, Yancheng He, Weixun Wang, Jiaheng Liu, Ling Pan, Xinyu Hu, Shaopan Xiong, Ju Huang, Jian Hu, Shengyi Huang, Johan Obando-Ceron, Siran Yang, Jiamang Wang, Wenbo Su, and Bo Zheng. Part i: Tricks or traps? a deep dive into rl for llm reasoning, 2025e. URL `https://arxiv.org/abs/2508.08221`.

Zuxin Liu, Thai Hoang, Jianguo Zhang, Ming Zhu, Tian Lan, Juntao Tan, Weiran Yao, Zhiwei Liu, Yihao Feng, Rithesh RN, et al. Apigen: Automated pipeline for generating verifiable and diverse function-calling datasets. *Advances in Neural Information Processing Systems*, 37:54463–54482, 2024.

Han Lu, Zichen Liu, Shaopan Xiong, Yancheng He, Wei Gao, Yanan Wu, Weixun Wang, Jiashun Liu, Yang Li, Haizhou Zhao, Ju Huang, Siran Yang, Xiaoyang Li, Yijia Luo, Zihe Liu, Ling Pan, Junchi Yan, Wei Wang, Wenbo Su, Jiamang Wang, Lin Qu, and Bo Zheng. Part ii: Roll flash – accelerating rlvr and agentic training with asynchrony, 2025a. URL `https://arxiv.org/abs/2510.11345`.

Keer Lu, Chong Chen, Bin Cui, Huang Leng, and Wentao Zhang. Pilotrl: Training language model agents via global planning-guided progressive reinforcement learning. *arXiv preprint arXiv:2508.00344*, 2025b.

Haipeng Luo, Qingfeng Sun, Can Xu, Pu Zhao, Jianguang Lou, Chongyang Tao, Xiubo Geng, Qingwei Lin, Shifeng Chen, and Dongmei Zhang. Wizardmath: Empowering mathematical reasoning for large language models via reinforced evol-instruct. *arXiv preprint arXiv:2308.09583*, 2023.

Michael Luo, Sijun Tan, Justin Wong, Xiaoxiang Shi, William Y. Tang, Manan Roongta, Colin Cai, Jeffrey Luo, Li Erran Li, Raluca Ada Popa, and Ion Stoica. DeepScaleR: Surpassing O1-Preview with a 1.5b model by scaling RL. `https://pretty-radio-b75.notion.site/DeepScaleR-Surpassing-O1-Preview-with-a-1-5B-Model-Scaling-RL`, 2025a. Notion blog; accessed 2025-09-24.

Xufang Luo, Yuge Zhang, Zhiyuan He, Zilong Wang, Siyun Zhao, Dongsheng Li, Luna K Qiu, and Yuqing Yang. Agent lightning: Train any ai agents with reinforcement learning. *arXiv preprint arXiv:2508.03680*, 2025b.

Trung Quoc Luong, Xinbo Zhang, Zhanming Jie, Peng Sun, Xiaoran Jin, and Hang Li. Reft: Reasoning with reinforced fine-tuning, 2024. URL `https://arxiv.org/abs/2401.08967`.

Xinji Mai, Haotian Xu, Zhong-Zhi Li, Xing W, Weinong Wang, Jian Hu, Yingying Zhang, and Wenqiang Zhang. Agent rl scaling law: Agent rl with spontaneous code execution for mathematical problem solving, 2025. URL `https://arxiv.org/abs/2505.07773`.

Zhiyu Mei, Wei Fu, Kaiwei Li, Guangju Wang, Huanchen Zhang, and Yi Wu. Realhf: Optimized rlhf training for large language models through parameter reallocation. *arXiv preprint arXiv:2406.14088*, 2024.

Zhiyu Mei, Wei Fu, Kaiwei Li, Guangju Wang, Huanchen Zhang, and Yi Wu. Real: Efficient rlhf training of large language models with parameter reallocation. In *Proceedings of the Eighth Conference on Machine Learning and Systems, MLSys 2025, Santa Clara, CA, USA, May 12-15, 2025*. mlsys.org, 2025.

Ivan Moshkov, Darragh Hanley, Ivan Sorokin, Shubham Toshniwal, Christof Henkel, Benedikt Schifferer, Wei Du, and Igor Gitman. Aimo-2 winning solution: Building state-of-the-art mathematical reasoning models with openmathreasoning dataset. *arXiv preprint arXiv:2504.16891*, 2025.

Niklas Muennighoff, Zitong Yang, Weijia Shi, Xiang Lisa Li, Li Fei-Fei, Hannaneh Hajishirzi, Luke Zettlemoyer, Percy Liang, Emmanuel Candès, and Tatsunori Hashimoto. s1: Simple test-time scaling, 2025. URL `https://arxiv.org/abs/2501.19393`.

Reiichiro Nakano, Jacob Hilton, Suchir Balaji, Jeff Wu, Long Ouyang, Christina Kim, Christopher Hesse, Shantanu Jain, William Saunders, and John *et al.* Schulman. WebGPT: Browser-assisted Question-Answering with Human Feedback. *arXiv preprint arXiv:2112.09332*, 2022.

Xuan-Phi Nguyen, Shrey Pandit, Revanth Gangi Reddy, Austin Xu, Silvio Savarese, Caiming Xiong, and Shafiq Joty. Sfr-deepresearch: Towards effective reinforcement learning for autonomously reasoning single agents. *arXiv preprint arXiv:2509.06283*, 2025.

OpenAI. Learning to reason with llms. *https://openai.com/index/learnin g-to-reason-with-llms/*, 2024.

OpenAI. Introducing openai o3 and o4-mini, 2025. URL `https://openai.com/index/introducing-o3-and-o4-mini/`.

OpenAI, :, Aaron Jaech, Adam Kalai, Adam Lerer, Adam Richardson, Ahmed El-Kishky, Aiden Low, Alec Helyar, Aleksander Madry, Alex Beutel, Alex Carney, Alex Iftimie, Alex Karpenko, Alex Tachard Passos, Alexander Neitz, Alexander Prokofiev, Alexander Wei, Allison Tam, Ally Bennett, Ananya Kumar, Andre Saraiva, Andrea Vallone, Andrew Duberstein, Andrew Kondrich, Andrey Mishchenko, Andy Applebaum, Angela Jiang, Ashvin Nair, Barret Zoph, Behrooz Ghorbani, Ben Rossen, Benjamin Sokolowsky, Boaz Barak, Bob McGrew, Borys Minaiev, Botao Hao, Bowen Baker, Brandon Houghton, Brandon McKinzie, Brydon Eastman, Camillo Lugaresi, Cary Bassin, Cary Hudson, Chak Ming Li, Charles de Bourcy, Chelsea Voss, Chen Shen, Chong Zhang, Chris Koch, Chris Orsinger, Christopher Hesse, Claudia Fischer, Clive Chan, Dan Roberts, Daniel Kappler, Daniel Levy, Daniel Selsam, David Dohan, David Farhi, David Mely, David Robinson, Dimitris Tsipras, Doug Li, Dragos Oprica, Eben Freeman, Eddie Zhang, Edmund Wong, Elizabeth Proehl, Enoch Cheung, Eric Mitchell, Eric Wallace, Erik Ritter, Evan Mays, Fan Wang, Felipe Petroski Such, Filippo Raso, Florencia Leoni, Foivos Tsimpourlas, Francis Song, Fred von Lohmann, Freddie Sulit, Geoff Salmon, Giambattista Parascandolo, Gildas Chabot, Grace Zhao, Greg Brockman, Guillaume Leclerc, Hadi Salman, Haiming Bao, Hao Sheng, Hart Andrin, Hessam Bagherinezhad, Hongyu Ren, Hunter Lightman, Hyung Won Chung, Ian Kivlichan, Ian O'Connell, Ian Osband, Ignasi Clavera Gilaberte, Ilge Akkaya, Ilya Kostrikov, Ilya Sutskever, Irina Kofman, Jakub Pachocki, James Lennon, Jason Wei, Jean Harb, Jerry Twore, Jiacheng Feng, Jiahui Yu, Jiayi Weng, Jie Tang, Jieqi Yu, Joaquin Quiñonero Candela, Joe Palermo, Joel Parish, Johannes Heidecke, John Hallman, John Rizzo, Jonathan Gordon, Jonathan Uesato, Jonathan Ward, Joost Huizinga, Julie Wang, Kai Chen, Kai Xiao, Karan Singhal, Karina Nguyen, Karl Cobbe, Katy Shi, Kayla Wood, Kendra Rimbach, Keren Gu-Lemberg, Kevin Liu, Kevin Lu, Kevin Stone, Kevin Yu, Lama Ahmad, Lauren Yang, Leo Liu, Leon Maksin, Leyton Ho, Liam Fedus, Lilian Weng, Linden Li, Lindsay McCallum, Lindsey Held, Lorenz Kuhn, Lukas Kondraciuk, Lukasz Kaiser, Luke Metz, Madelaine Boyd, Maja Trebacz, Manas Joglekar, Mark Chen, Marko Tintor, Mason Meyer, Matt Jones, Matt Kaufer, Max Schwarzer, Meghan Shah, Mehmet Yatbaz, Melody Y. Guan, Mengyuan Xu, Mengyuan Yan, Mia Glaese, Mianna Chen, Michael Lampe, Michael Malek, Michele Wang, Michelle Fradin, Mike McClay, Mikhail Pavlov, Miles Wang, Mingxuan Wang, Mira Murati, Mo Bavarian, Mostafa Rohaninejad, Nat McAleese, Neil Chowdhury, Neil Chowdhury, Nick Ryder, Nikolas Tezak, Noam Brown, Ofir Nachum, Oleg Boiko, Oleg Murk, Olivia Watkins, Patrick Chao, Paul Ashbourne, Pavel Izmailov, Peter Zhokhov, Rachel Dias, Rahul Arora, Randall Lin, Rapha Gontijo Lopes, Raz Gaon, Reah Miyara, Reimar Leike, Renny Hwang, Rhythm Garg, Robin Brown, Roshan James, Rui Shu, Ryan Cheu, Ryan Greene, Saachi Jain, Sam Altman, Sam Toizer, Sam Toyer, Samuel Miserendino, Sandhini Agarwal, Santiago Hernandez, Sasha Baker, Scott McKinney, Scottie Yan, Shengjia Zhao, Shengli Hu, Shibani Santurkar, Shraman Ray Chaudhuri, Shuyuan Zhang, Siyuan Fu, Spencer Papay, Steph Lin, Suchir Balaji, Suvansh Sanjeev, Szymon Sidor, Tal Broda, Aidan Clark, Tao Wang, Taylor Gordon, Ted Sanders, Tejal Patwardhan, Thibault Sottiaux, Thomas Degry, Thomas Dimson, Tianhao Zheng, Timur Garipov, Tom Stasi, Trapit Bansal, Trevor Creech, Troy Peterson, Tyna Eloundou, Valerie Qi, Vineet Kosaraju, Vinnie Monaco, Vitchyr Pong, Vlad Fomenko, Weiyi Zheng, Wenda Zhou, Wes McCabe, Wojciech Zaremba, Yann Dubois, Yinghai Lu, Yining Chen, Young Cha, Yu Bai, Yuchen He, Yuchen Zhang, Yunyun Wang, Zheng Shao, and Zhuohan Li. Openai o1 system card, 2024. URL `https://arxiv.org/abs/2412.16720`.

Richard Yuanzhe Pang, Weizhe Yuan, He He, Kyunghyun Cho, Sainbayar Sukhbaatar, and Jason Weston. Iterative reasoning preference optimization. *Advances in Neural Information Processing Systems*, 37:116617–116637, 2024.

Changle Qu, Sunhao Dai, Xiaochi Wei, Hengyi Cai, Shuaiqiang Wang, Dawei Yin, Jun Xu, and Ji-Rong Wen. Tool learning with large language models: A survey. *Frontiers of Computer Science*, 19(8):198343, 2025.

Rafael Rafailov, Archit Sharma, Eric Mitchell, Christopher D Manning, Stefano Ermon, and Chelsea Finn. Direct preference optimization: Your language model is secretly a reward model. *Advances in neural information processing systems*, 36:53728–53741, 2023.

Timo Schick, Jane Dwivedi-Yu, Roberto Dessì, Roberta Raileanu, Maria Lomeli, Luke Zettlemoyer, Nicola Cancedda, and Thomas Scialom. Toolformer: Language models can teach themselves to use tools, 2023. URL `https://arxiv.org/abs/2302.04761`.

John Schulman, Filip Wolski, Prafulla Dhariwal, Alec Radford, and Oleg Klimov. Proximal policy optimization algorithms. *arXiv preprint arXiv:1707.06347*, 2017.

ByteDance Seed, :, Jiaze Chen, Tiantian Fan, Xin Liu, Lingjun Liu, Zhiqi Lin, Mingxuan Wang, Chengyi Wang, Xiangpeng Wei, Wenyuan Xu, Yufeng Yuan, Yu Yue, Lin Yan, Qiying Yu, Xiaochen Zuo, Chi Zhang, Ruofei Zhu, Zhecheng An, Zhihao Bai, Yu Bao, Xingyan Bin, Jiangjie Chen, Feng Chen, Hongmin Chen, Riwei Chen, Liangqiang Chen, Zixin Chen, Jinsong Chen, Siyan Chen, Kaiyuan Chen, Zhi Chen, Jin Chen, Jiecao Chen, Jinxin Chi, Weinan Dai, Ning Dai, Jiahui Dai, Shihan Dou, Yantao Du, Zhengyin Du, Jianhui Duan, Chen Dun, Ting-Han Fan, Jiazhan Feng, Junda Feng, Ziyuan Feng, Yuwei Fu, Wenqi Fu, Hanjie Fu, Hao Ge, Hongyi Guo, Mingji Han, Li Han, Wenhao Hao, Xintong Hao, Qianyu He, Jerry He, Feng He, Wen Heng, Zehua Hong, Qi Hou, Liang Hu, Shengding Hu, Nan Hu, Kai Hua, Qi Huang, Ziyue Huang, Hongzhi Huang, Zihao Huang, Ting Huang, Wenhao Huang, Wei Jia, Bin Jia, Xiaoying Jia, Yuhua Jiang, Haobin Jiang, Ziheng Jiang, Kaihua Jiang, Chengquan Jiang, Jianpeng Jiao, Xiaoran Jin, Xing Jin, Xunhao Lai, Zheng Li, Xiang Li, Liyi Li, Hongkai Li, Zheng Li, Shengxian Wan, Ya Wang, Yunshui Li, Chenggang Li, Niuniu Li, Siyu Li, Xi Li, Xiao Li, Aoyan Li, Yuntao Li, Nianning Liang, Xinnian Liang, Haibin Lin, Weijian Lin, Ye Lin, Zhicheng Liu, Guanlin Liu, Guanlin Liu, Chenxiao Liu, Yan Liu, Gaohong Liu, Juncai Liu, Chundian Liu, Deyi Liu, Kaibo Liu, Siyao Liu, Qi Liu, Yongfei Liu, Kang Liu, Gan Liu, Boyi Liu, Rui Long, Weiqiang Lou, Chenwei Lou, Xiang Luo, Yao Luo, Caiping Lv, Heyang Lv, Bole Ma, Qianli Ma, Hongzhi Ma, Yiyuan Ma, Jin Ma, Wenchang Ma, Tingting Ma, Chen Mao, Qiyang Min, Zhe Nan, Guanghan Ning, Jinxiang Ou, Haojie Pan, Renming Pang, Yanghua Peng, Tao Peng, Lihua Qian, Lihua Qian, Mu Qiao, Meng Qu, Cheng Ren, Hongbin Ren, Yong Shan, Wei Shen, Ke Shen, Kai Shen, Guangming Sheng, Jinlong Shi, Wenlei Shi, Guang Shi, Shuai Shuai Cao, Yuxin Song, Zuquan Song, Jing Su, Yifan Sun, Tao Sun, Zewei Sun, Borui Wan, Zihan Wang, Xiaohui Wang, Xi Wang, Shuguang Wang, Jun Wang, Qinlong Wang, Chenyuan Wang, Shuai Wang, Zihan Wang, Changbao Wang, Jiaqiang Wang, Shihang Wang, Xuwu Wang, Zaiyuan Wang, Yuxuan Wang, Wenqi Wang, Taiqing Wang, Chengzhi Wei, Houmin Wei, Ziyun Wei, Shufa Wei, Zheng Wu, Yonghui Wu, Yangjun Wu, Bohong Wu, Shuang Wu, Jingqiao Wu, Ning Wu, Shuangzhi Wu, Jianmin Wu, Chenguang Xi, Fan Xia, Yuqiao Xian, Liang Xiang, Boren Xiang, Bowen Xiao, Zhen Xiao, Xia Xiao, Yongsheng Xiao, Chao Xin, Shulin Xin, Yuwen Xiong, Jingjing Xu, Ziwen Xu, Chenyin Xu, Jiayi Xu, Yifan Xu, Wei Xu, Yufei Xu, Shikun Xu, Shipeng Yan, Shen Yan, Qingping Yang, Xi Yang, Tianhao Yang, Yuehang Yang, Yuan Yang, Ximing Yang, Zeyu Yang, Guang Yang, Yifan Yang, Xuesong Yao, Bairen Yi, Fan Yin, Jianian Yin, Ziqiang Ying, Xiangyu Yu, Hongli Yu, Song Yu, Menghan Yu, Huan Yu, Siyu Yuan, Jun Yuan, Yutao Zeng, Tianyang Zhan, Zheng Zhang, Yun Zhang, Mofan Zhang, Wang Zhang, Ru Zhang, Zhi Zhang, Tianqi Zhang, Xinyi Zhang, Zhexi Zhang, Sijun Zhang, Wenqiang Zhang, Xiangxiang Zhang, Yongtao Zhang, Yuyu Zhang, Ge Zhang, He Zhang, Yue Zhang, Renjie Zheng, Ningxin Zheng, Zhuolin Zheng, Yaowei Zheng, Chen Zheng, Xiaoyun Zhi, Wanjun Zhong, Cheng Zhong, Zheng Zhong, Baoquan Zhong, Xun Zhou, Na Zhou, Huan Zhou, Hang Zhu, Defa Zhu, Wenjia Zhu, and Lei Zuo. Seed1.5-thinking: Advancing superb reasoning models with reinforcement learning, 2025. URL `https://arxiv.org/abs/2504.13914`.

Ning Shang, Yifei Liu, Yi Zhu, Li Lyna Zhang, Weijiang Xu, Xinyu Guan, Buze Zhang, Bingcheng Dong, Xudong Zhou, Bowen Zhang, et al. rstar2-agent: Agentic reasoning technical report. *arXiv preprint arXiv:2508.20722*, 2025.

Zhihong Shao, Peiyi Wang, Qihao Zhu, Runxin Xu, Junxiao Song, Xiao Bi, Haowei Zhang, Mingchuan Zhang, YK Li, Y Wu, et al. Deepseekmath: Pushing the limits of mathematical reasoning in open language models. *arXiv preprint arXiv:2402.03300*, 2024.

Gerald Shen, Zhilin Wang, Olivier Delalleau, Jiaqi Zeng, Yi Dong, Daniel Egert, Shengyang Sun, Jimmy Zhang, Sahil Jain, Ali Taghibakhshi, Markel Sanz Ausin, Ashwath Aithal, and Oleksii Kuchaiev. Nemo-aligner: Scalable toolkit for efficient model alignment, 2024.

Guangming Sheng, Chi Zhang, Zilingfeng Ye, Xibin Wu, Wang Zhang, Ru Zhang, Yanghua Peng, Haibin Lin, and Chuan Wu. Hybridflow: A flexible and efficient rlhf framework. *arXiv preprint arXiv: 2409.19256*, 2024.

Joykirat Singh, Raghav Magazine, Yash Pandya, and Akshay Nambi. Agentic reasoning and tool integration for llms via reinforcement learning. *arXiv preprint arXiv:2505.01441*, 2025.

Charlie Snell, Jaehoon Lee, Kelvin Xu, and Aviral Kumar. Scaling llm test-time compute optimally can be more effective than scaling model parameters, 2024. URL `https://arxiv.org/abs/2408.03314`.

Huatong Song, Jinhao Jiang, Yingqian Min, Jie Chen, Zhipeng Chen, Wayne Xin Zhao, Lei Fang, and Ji-Rong Wen. R1-searcher: Incentivizing the search capability in llms via reinforcement learning, 2025. URL `https://arxiv.org/abs/2503.05592`.

ByteDance Seed Team. Seed-oss open-source models. `https://github.com/ByteDance-Seed/seed-oss`, 2025a.

Gemini Team, Rohan Anil, Sebastian Borgeaud, Jean-Baptiste Alayrac, Jiahui Yu, Radu Soricut, Johan Schalkwyk, Andrew M Dai, Anja Hauth, Katie Millican, et al. Gemini: a family of highly capable multimodal models. *arXiv preprint arXiv:2312.11805*, 2023.

Kimi Team, Angang Du, Bofei Gao, Bowei Xing, Changjiu Jiang, Cheng Chen, Cheng Li, Chenjun Xiao, Chenzhuang Du, Chonghua Liao, Chuning Tang, Congcong Wang, Dehao Zhang, Enming Yuan, Enzhe Lu, Fengxiang Tang, Flood Sung, Guangda Wei, Guokun Lai, Haiqing Guo, Han Zhu, Hao Ding, Hao Hu, Hao Yang, Hao Zhang, Haotian Yao, Haotian Zhao, Haoyu Lu, Haoze Li, Haozhen Yu, Hongcheng Gao, Huabin Zheng, Huan Yuan, Jia Chen, Jianhang Guo, Jianlin Su, Jianzhou Wang, Jie Zhao, Jin Zhang, Jingyuan Liu, Junjie Yan, Junyan Wu, Lidong Shi, Ling Ye, Longhui Yu, Mengnan Dong, Neo Zhang, Ningchen Ma, Qiwei Pan, Qucheng Gong, Shaowei Liu, Shengling Ma, Shupeng Wei, Sihan Cao, Siying Huang, Tao Jiang, Weihao Gao, Weimin Xiong, Weiran He, Weixiao Huang, Wenhao Wu, Wenyang He, Xianghui Wei, Xianqing Jia, Xingzhe Wu, Xinran Xu, Xinxing Zu, Xinyu Zhou, Xuehai Pan, Y. Charles, Yang Li, Yangyang Hu, Yangyang Liu, Yanru Chen, Yejie Wang, Yibo Liu, Yidao Qin, Yifeng Liu, Ying Yang, Yiping Bao, Yulun Du, Yuxin Wu, Yuzhi Wang, Zaida Zhou, Zhaoji Wang, Zhaowei Li, Zhen Zhu, Zheng Zhang, Zhexu Wang, Zhilin Yang, Zhiqi Huang, Zihao Huang, Ziyao Xu, and Zonghan Yang. Kimi k1.5: Scaling reinforcement learning with llms, 2025. URL https://arxiv.org/abs/2501.12599.

NovaSky Team. Sky-t1: Fully open-source reasoning model with o1-preview performance in $450 budget. https://novasky-ai.github.io/posts/sky-t1, 2025b. Accessed: 2025-01-09.

Qwen Team. Qwen3 technical report, 2025c. URL https://arxiv.org/abs/2505.09388.

Qwen Team. Qwq-32b: Embracing the power of reinforcement learning, March 2025d. URL https://qwenlm.github.io/blog/qwq-32b/.

TinyR1 Team. Superdistillation achieves near-r1 performance with just 5 URL https://huggingface.co/qihoo360/TinyR1-32B-Preview.

Haozhe Wang, Long Li, Chao Qu, Fengming Zhu, Weidi Xu, Wei Chu, and Fangzhen Lin. Learning autonomous code integration for math language models, 2025a. URL https://arxiv.org/abs/2502.00691.

Hongru Wang, Yujia Qin, Yankai Lin, Jeff Z. Pan, and Kam-Fai Wong. Empowering large language models: Tool learning for real-world interaction. In *Proceedings of the 47th International ACM SIGIR Conference on Research and Development in Information Retrieval*, SIGIR '24, pp. 2983–2986, New York, NY, USA, 2024. Association for Computing Machinery. ISBN 9798400704314. doi: 10.1145/3626772.3661381. URL https://doi.org/10.1145/3626772.3661381.

Hongru Wang, Cheng Qian, Wanjun Zhong, Xiusi Chen, Jiahao Qiu, Shijue Huang, Bowen Jin, Mengdi Wang, Kam-Fai Wong, and Heng Ji. Otc: Optimal tool calls via reinforcement learning. *arXiv preprint arXiv:2504.14870*, 2025b.

Ke Wang, Houxing Ren, Aojun Zhou, Zimu Lu, Sichun Luo, Weikang Shi, Renrui Zhang, Linqi Song, Mingjie Zhan, and Hongsheng Li. Mathcoder: Seamless code integration in llms for enhanced mathematical reasoning, 2023a. URL https://arxiv.org/abs/2310.03731.

Peiyi Wang, Lei Li, Zhihong Shao, RX Xu, Damai Dai, Yifei Li, Deli Chen, Yu Wu, and Zhifang Sui. Math-shepherd: Verify and reinforce llms step-by-step without human annotations. *arXiv preprint arXiv:2312.08935*, 2023b.

Weixun Wang, Shaopan Xiong, Gengru Chen, Wei Gao, Sheng Guo, Yancheng He, Ju Huang, Jiaheng Liu, Zhendong Li, Xiaoyang Li, et al. Reinforcement learning optimization for large-scale learning: An efficient and user-friendly scaling library. *arXiv preprint arXiv:2506.06122*, 2025c.

Zihan Wang, Kangrui Wang, Qineng Wang, Pingyue Zhang, Linjie Li, Zhengyuan Yang, Xing Jin, Kefan Yu, Minh Nhat Nguyen, Licheng Liu, Eli Gottlieb, Yiping Lu, Kyunghyun Cho, Jiajun Wu, Li Fei-Fei, Lijuan Wang, Yejin Choi, and Manling Li. Ragen: Understanding self-evolution in llm agents via multi-turn reinforcement learning, 2025d. URL https://arxiv.org/abs/2504.20073.

Jason Wei, Xuezhi Wang, Dale Schuurmans, Maarten Bosma, brian ichter, Fei Xia, Ed Chi, Quoc V Le, and Denny Zhou. Chain-of-thought prompting elicits reasoning in large language models. In S. Koyejo, S. Mohamed, A. Agarwal, D. Belgrave, K. Cho, and A. Oh (eds.), *Advances in Neural Information Processing Systems*, volume 35, pp. 24824–24837. Curran Associates, Inc., 2022. URL https://proceedings.neurips.cc/paper_files/paper/2022/file/9d5609613524ecf4f15af0f7b31abca4-Paper-Conference.pdf.

Yifan Wei, Xiaoyan Yu, Yixuan Weng, Tengfei Pan, Angsheng Li, and Li Du. Autotir: Autonomous tools integrated reasoning via reinforcement learning. *arXiv preprint arXiv:2507.21836*, 2025.

Liang Wen, Yunke Cai, Fenrui Xiao, Xin He, Qi An, Zhenyu Duan, Yimin Du, Junchen Liu, Lifu Tang, Xiaowei Lv, Haosheng Zou, Yongchao Deng, Shousheng Jia, and Xiangzheng Zhang. Light-R1: Curriculum sft, dpo and rl for long cot from scratch and beyond, 2025. URL `https://github.com/Qihoo360/Light-R1`. GitHub repository.

Xiaobao Wu. Sailing by the stars: A survey on reward models and learning strategies for learning from rewards. *arXiv preprint arXiv:2505.02686*, 2025a.

Xiaobao Wu. Sailing ai by the stars: A survey of learning from rewards in post-training and test-time scaling of large language models. *arXiv preprint arXiv:2505.02686*, 2025b.

xAI. Grok. `https://x.ai/`, 2023. URL `https://x.ai/`. Large language model.

LLM-Core-Team Xiaomi. Mimo: Unlocking the reasoning potential of language model – from pretraining to posttraining, 2025. URL `https://arxiv.org/abs/2505.07608`.

Yuxi Xie, Anirudh Goyal, Wenyue Zheng, Min-Yen Kan, Timothy P. Lillicrap, Kenji Kawaguchi, and Michael Shieh. Monte carlo tree search boosts reasoning via iterative preference learning, 2024. URL `https://arxiv.org/abs/2405.00451`.

Zhenghai Xue, Longtao Zheng, Qian Liu, Yingru Li, Xiaosen Zheng, Zejun Ma, and Bo An. Simpletir: End-to-end reinforcement learning for multi-turn tool-integrated reasoning. *arXiv preprint arXiv:2509.02479*, 2025.

An Yang, Baosong Yang, Beichen Zhang, Binyuan Hui, Bo Zheng, Bowen Yu, Chengyuan Li, Dayiheng Liu, Fei Huang, Haoran Wei, Huan Lin, Jian Yang, Jianhong Tu, Jianwei Zhang, Jianxin Yang, Jiaxi Yang, Jingren Zhou, Junyang Lin, Kai Dang, Keming Lu, Keqin Bao, Kexin Yang, Le Yu, Mei Li, Mingfeng Xue, Pei Zhang, Qin Zhu, Rui Men, Runji Lin, Tianhao Li, Tianyi Tang, Tingyu Xia, Xingzhang Ren, Xuancheng Ren, Yang Fan, Yang Su, Yichang Zhang, Yu Wan, Yuqiong Liu, Zeyu Cui, Zhenru Zhang, and Zihan Qiu. Qwen2.5 technical report. *arXiv preprint arXiv:2412.15115*, 2024a.

An Yang, Beichen Zhang, Binyuan Hui, Bofei Gao, Bowen Yu, Chengpeng Li, Dayiheng Liu, Jianhong Tu, Jingren Zhou, Junyang Lin, Keming Lu, Mingfeng Xue, Runji Lin, Tianyu Liu, Xingzhang Ren, and Zhenru Zhang. Qwen2.5-math technical report: Toward mathematical expert model via self-improvement, 2024b. URL `https://arxiv.org/abs/2409.12122`.

Shunyu Yao, Dian Yu, Jeffrey Zhao, Izhak Shafran, Thomas L. Griffiths, Yuan Cao, and Karthik Narasimhan. Tree of thoughts: deliberate problem solving with large language models. In *Proceedings of the 37th International Conference on Neural Information Processing Systems*, NIPS '23, Red Hook, NY, USA, 2023. Curran Associates Inc.

Longhui Yu, Weisen Jiang, Han Shi, Jincheng Yu, Zhengying Liu, Yu Zhang, James T. Kwok, Zhenguo Li, Adrian Weller, and Weiyang Liu. Metamath: Bootstrap your own mathematical questions for large language models, 2023.

Qiying Yu, Zheng Zhang, Ruofei Zhu, Yufeng Yuan, Xiaochen Zuo, Yu Yue, Tiantian Fan, Gaohong Liu, Lingjun Liu, Xin Liu, Haibin Lin, Zhiqi Lin, Bole Ma, Guangming Sheng, Yuxuan Tong, Chi Zhang, Mofan Zhang, Wang Zhang, Hang Zhu, Jinhua Zhu, Jiaze Chen, Jiangjie Chen, Chengyi Wang, Hongli Yu, Weinan Dai, Yuxuan Song, Xiangpeng Wei, Hao Zhou, Jingjing Liu, Wei-Ying Ma, Ya-Qin Zhang, Lin Yan, Mu Qiao, Yonghui Wu, and Mingxuan Wang. Dapo: An open-source llm reinforcement learning system at scale, 2025. URL `https://arxiv.org/abs/2503.14476`.

Xiang Yue, Xingwei Qu, Ge Zhang, Yao Fu, Wenhao Huang, Huan Sun, Yu Su, and Wenhu Chen. Mammoth: Building math generalist models through hybrid instruction tuning, 2023. URL `https://arxiv.org/abs/2309.05653`.

Siliang Zeng, Quan Wei, William Brown, Oana Frunza, Yuriy Nevmyvaka, and Mingyi Hong. Reinforcing multi-turn reasoning in llm agents via turn-level credit assignment. *arXiv preprint arXiv:2505.11821*, 2025a.

Weihao Zeng, Yuzhen Huang, Qian Liu, Wei Liu, Keqing He, Zejun Ma, and Junxian He. Simplerl-zoo: Investigating and taming zero reinforcement learning for open base models in the wild. *arXiv preprint arXiv:2503.18892*, 2025b.

Guibin Zhang, Hejia Geng, Xiaohang Yu, Zhenfei Yin, Zaibin Zhang, Zelin Tan, Heng Zhou, Zhongzhi Li, Xiangyuan Xue, Yijiang Li, et al. The landscape of agentic reinforcement learning for llms: A survey. *arXiv preprint arXiv:2509.02547*, 2025a.

Kechi Zhang, Ge Li, Jia Li, Huangzhao Zhang, Jingjing Xu, Hao Zhu, Lecheng Wang, Yihong Dong, Jing Mai, Bin Gu, et al. Computational thinking reasoning in large language models. *arXiv preprint arXiv:2506.02658*, 2025b.

Shaokun Zhang, Yi Dong, Jieyu Zhang, Jan Kautz, Bryan Catanzaro, Andrew Tao, Qingyun Wu, Zhiding Yu, and Guilin Liu. Nemotron-research-tool-n1: Tool-using language models with reinforced reasoning. *arXiv preprint arXiv:2505.00024*, 2025c.

Xin Zhang, Yanzhao Zhang, Dingkun Long, Wen Xie, Ziqi Dai, Jialong Tang, Huan Lin, Baosong Yang, Pengjun Xie, Fei Huang, et al. mgte: Generalized long-context text representation and reranking models for multilingual text retrieval. *arXiv preprint arXiv:2407.19669*, 2024a.

Yao Zhang, Hongxiao Zhang, Jiacheng Zhang, Jingcheng Zhao, Rui Yan, Xiaoqing Liu, Jiahuan Wang, Min Zhang, Houfeng Wang, and Zhengguang Guo. rStar-Math: Small LLMs can master math reasoning with self-evolved deep thinking. *arXiv preprint arXiv:2403.01707*, 2024b.

Yusen Zhang, Ruoxi Sun, Yanfei Chen, Tomas Pfister, Rui Zhang, and Sercan Arik. Chain of agents: Large language models collaborating on long-context tasks. *Advances in Neural Information Processing Systems*, 37:132208–132237, 2024c.

Huichi Zhou, Yihang Chen, Siyuan Guo, Xue Yan, Kin Hei Lee, Zihan Wang, Ka Yiu Lee, Guchun Zhang, Kun Shao, Linyi Yang, et al. Memento: Fine-tuning llm agents without fine-tuning llms. *Preprint*, 2025.

Zilin Zhu, Chengxing Xie, Xin Lv, and slime Contributors. slime: An llm post-training framework for rl scaling. `https://github.com/THUDM/slime`, 2025. GitHub repository. Corresponding author: Xin Lv.

## A Appendix

### A.1 Related work

**Mathematical Reasoning in LLMs.** Large Language Models (LLMs) have made remarkable progress in mathematical reasoning(Wei et al., 2022; Yao et al., 2023; Luong et al., 2024; OpenAI et al., 2024; Team et al., 2025; DeepSeek-AI et al., 2025; xAI, 2023; Claude, 2025; Team et al., 2023; Yang et al., 2024a;b; He et al., 2025b; Fang et al., 2025; Zhang et al., 2025a; Wu, 2025b;a). The introduction of Chain-of-Thought (CoT)(Wei et al., 2022; Yao et al., 2023) prompting enabled models to decompose complex problems into intermediate reasoning steps, substantially enhancing their problem-solving capabilities. Subsequently, research has shifted from a singular focus on model scaling towards optimizing the reasoning process itself(Snell et al., 2024). This paradigm shift has spurred the development of Large Reasoning Models (LRMs) trained with advanced methods like Reinforcement Learning(Schulman et al., 2017; Li et al., 2024; Shao et al., 2024), Direct Preference Optimization(Rafailov et al., 2023; Lai et al., 2024; Pang et al., 2024), and Monte Carlo Tree Search(Xie et al., 2024; Wang et al., 2023b). State-of-the-art models such as OpenAI's o1 and DeepSeek-R1(OpenAI et al., 2024; DeepSeek-AI et al., 2025; Team, 2025d; Team et al., 2023; 2025) exhibit human-like cognitive planning on long-chain reasoning tasks, pushing the frontiers of mathematical performance. Despite these advances, reasoning purely within natural language is constrained by inherent limitations: complex arithmetic and symbolic manipulations are prone to error, and self-correction is often inefficient. These shortcomings fundamentally limit their accuracy and efficiency on competition-level mathematical problems.

**Tool-Augmented LLM Reasoning.** Tool-augmented reasoning has emerged as a promising solution to the limitations of text-based approaches(Li et al., 2025e; Zhou et al., 2025; Lin & Xu, 2025; Zhang et al., 2025b; Jin et al., 2025b; Liu et al., 2025b; Luo et al., 2023; Azerbayev et al., 2023; Yu et al., 2023). Program-of-Thought (PoT)Chen et al. (2023); Gao et al. (2023); Yue et al. (2023); Jin et al. (2025a); Wang et al. (2024; 2023a); Cobbe et al. (2021); Hendrycks et al. (2021); Lightman et al. (2023); Shao et al. (2024); OpenAI (2024; 2025); Wang et al. (2025b); Gou et al. (2023a); Liu et al. (2024); Qu et al. (2025); Song et al. (2025); Li et al. (2025d); Schick et al. (2023); Zhang et al. (2024b;c) pioneered delegating computational steps to external code interpreters, enhancing numerical accuracy. ToRA(Gou et al., 2023b) subsequently developed code-integrated reasoning frameworks tailored for mathematical problems, demonstrating the efficacy of specialized tools in complex computations. START(Li et al., 2025b) generates tool-augmented trajectories via prompt engineering, though random code insertion often yields inefficient utilization. STILL3(Chen et al., 2025b) relies on prompt-based data construction, and CoRT(Li et al., 2025a) employs high-quality human annotations but faces scalability constraints. These approaches predominantly depend on supervised fine-tuning, preventing models from learning debugging strategies from execution failures or adaptively mastering tool invocation timing and methods. While Retool(Feng et al., 2025a) combines data rewriting with reinforcement learning for optimization, improvements over existing LRMs (i.e, DeepSeek-R1-Distill-Qwen-32B(DeepSeek-AI et al., 2025)) remain marginal. Current tool-augmented methods thus face three critical challenges: scarcity of high-quality data, inadequate policy learning, and inefficient training on long sequences. AgentMath mitigates these limitations by automating tool-augmented data synthesis and employing reinforcement learning to enable autonomous exploration of optimal tool-use strategies, including tool invocation and code self-correction.

**Agentic Reinforcement Learning.** Reinforcement learning (RL) offers a powerful framework for cultivating autonomous, decision-making agents from LLMs (Dong et al., 2025; Zhang et al., 2025c; Xue et al., 2025; Li et al., 2025c; Singh et al., 2025; Shang et al., 2025; Nguyen et al., 2025; Wei et al., 2025; Luo et al., 2025b; Hao et al., 2025; Agarwal et al., 2025; Lu et al., 2025b; Zeng et al., 2025a; Liu et al., 2025d; Du et al., 2025b; Chang et al., 2025; Feng et al., 2025b; Li et al., 2025d; Song et al., 2025; Nakano et al., 2022; Mai et al., 2025; Wang et al., 2025a; Du et al., 2025a; Gao et al., 2025a; Mei et al., 2025; Wang et al., 2025c; Liu et al., 2025a; Li et al., 2025f; Lu et al., 2025a; Gao et al., 2025b; Liu et al., 2025e; Hu et al., 2024; Shen et al., 2024; Wang et al., 2025d; Zhu et al., 2025; Mei et al., 2024; Fan et al., 2025). In information retrieval, models like Search-R1 and R1-Searcher (Li et al., 2025d; Song et al., 2025; Nakano et al., 2022) have demonstrated how outcome-based rewards can successfully guide agents to query search engines. In mathematical reasoning, recent work has explored RL for emergent tool use. ToRL (Li et al., 2025e) utilizes RL to train an agent to operate a code interpreter without predefined patterns, while concurrent work on the scaling laws of agentic RL has revealed that simple, outcome-based rewards often foster greater exploration and policy innovation than complex process-based rewards(Lightman et al., 2023; Wang et al., 2023b). Similarly, ReTool(Feng et al., 2025a) leverages RL to teach models strategic tool call, significantly outperforming SFT baselines and uncovering cognitive patterns in code-invocation decisions. Nevertheless, existing RL methods face a critical bottleneck when applied to competition-level mathematics. These problems can generate exceptionally long reasoning chains (i.e., 64k tokens) with dense tool interactions (e.g., 64 calls), a scale that overwhelms conventional batch-synchronous training architectures. AgentMath alleviates this scalability challenge through a suite of technical innovations, including request-level asynchronous rollout scheduling, agentic partial rollouts, and prefix-aware weighted load balancing. These techniques enable efficient RL training on ultra-long sequences with massive tool usage, boosting training throughput by 4–5x and paving the way for developing more sophisticated and scalable mathematical reasoning agents.

## A.2 Problem Formulation and Interaction Protocol

### A.2.1 Problem Formulation

Tool-augmented mathematical reasoning is formalized as a Markov Decision Process (MDP), wherein the LLM-based policy agent iteratively interacts with a sandboxed execution environment. Given a problem statement $P$, the policy $\pi_\theta$ generates trajectories comprising interleaved reasoning segments and executable code blocks, while the environment $\mathcal{E}$ deterministically executes submitted code and returns corresponding outputs.

The objective is to construct an optimal trajectory $\tau^* = \{(z_1, o_1), \ldots, (z_T, o_T)\}$, where $(z_t, o_t)$ denotes the action-observation pair at timestep $t$. The state transition dynamics are characterized by:

$$\begin{aligned} z_t &\sim \pi_\theta(\cdot \mid s_t), \quad s_t = (P, \tau_{t-1}) \\ o_t &= \begin{cases} \mathcal{E}(c_t), & \text{if } z_t = c_t \in \mathcal{C} \\ \varnothing, & \text{if } z_t \in \mathcal{T} \end{cases} \\ \tau_t &= \tau_{t-1} \cup \{(z_t, o_t)\} \end{aligned} \tag{1}$$

where $s_t$ represents the current state comprising the problem and interaction history, $\mathcal{C}$ and $\mathcal{T}$ denote the code and thought action spaces respectively, and $\mathcal{E}(c_t)$ returns the execution result of code block $c_t$. The interaction terminates upon generation of a terminal token or exhaustion of the computational budget.

### A.2.2 Structured Interaction Protocol

The implementation employs a structured markup protocol to delineate reasoning and tool invocation boundaries. Natural language reasoning is encapsulated within <think> ...</think> tags, executable code is delimited by <code> ...</code> tags, and execution feedback is injected through <interpreter> ...</interpreter> tags.

The generation-execution cycle operates through bidirectional information exchange: upon completion of a <code> segment, generation is suspended while the extracted code undergoes execution in the sandboxed environment. The resulting output, whether successful execution, error message, or timeout notification, is subsequently incorporated into the context as an <interpreter> segment. This feedback mechanism enables adaptive strategy refinement, wherein the model conditions its subsequent generation on execution outcomes to perform error correction, strategy adjustment, or continued reasoning. Such fine-grained interaction traces provide rich supervision signals amenable to reinforcement learning optimization.

### A.2.3 Supervised Fine-Tuning with Selective Feedback Masking

During supervised fine-tuning on $\mathcal{D}_{\text{SFT}}$, the model must learn to generate reasoning and code while avoiding memorization of deterministic interpreter outputs. Consequently, tool outputs are masked during loss computation. For a training sample $\tau = (z_1, o_1, \ldots, z_T, o_T)$, where $z_t$ represents model-generated segments and $o_t$ denotes external feedback, the standard autoregressive loss is expressed

**Algorithm 1** Agentic Reinforcement Learning with Partial Rollouts

```
1: Initialize: Unfinished pool $\mathcal{U} \leftarrow \emptyset$; Experience buffer $\mathcal{B} \leftarrow \emptyset$; Global limits $L_{\text{global}}$, $T_{\text{global}}$;
   Segment limits $L_{\text{seg}}$, $T_{\text{seg}}$.
2: for each training iteration $k = 1, 2, \ldots$ do
3:     tasks_to_process $\leftarrow$ Sample($\mathcal{P} \cup \mathcal{U}$)
4:     new_segments $\leftarrow$ Rollout(tasks_to_process, $L_{\text{seg}}, T_{\text{seg}}$)        ▷ Asynchronous generation
5:     finished_trajectories $\leftarrow \emptyset$,    next_unfinished_pool $\leftarrow \emptyset$
6:     for each trajectory $\tau$ in new_segments do
7:         if $\tau$ ends with EOS or length($\tau$) $\geq L_{\text{global}}$ or tools($\tau$) $\geq T_{\text{global}}$ then
8:             Add $\tau$ to finished_trajectories
9:         else
10:            Add $\tau$ to next_unfinished_pool
11:    $\mathcal{U} \leftarrow$ next_unfinished_pool
12:    Add finished_trajectories to $\mathcal{B}$; UpdatePolicy($\mathcal{B}$)
```

as:

$$\mathcal{L}_{\text{SFT}}(\theta) = -\sum_{t=1}^{T} \log \pi_\theta(z_t \mid P, \tau_{<t}) .$$

A masking function $\mathbb{I}(\cdot)$ is introduced to identify tokens originating from <interpreter> segments, yielding the modified loss:

$$\mathcal{L}_{\text{SFT-masked}}(\theta) = -\sum_{t=1}^{T}\sum_{k=1}^{|z_t|} \big(1 - \mathbb{I}(z_{t,k})\big) \log \pi_\theta(z_{t,k} \mid P, \tau_{<t}, z_{t,<k}) ,$$

where $z_{t,k}$ denotes the $k$-th token of segment $z_t$, and $\mathbb{I}(z_{t,k}) = 1$ if and only if $z_{t,k}$ resides within <interpreter> tags. This selective masking ensures that gradient updates originate exclusively from model-generated reasoning and code, thereby shaping intrinsic reasoning capabilities and decision-making processes while treating external feedback as non-trainable contextual information.

## A.3 Group Relative Policy Optimization

We employs Group Relative Policy Optimization (GRPO) as the core optimization algorithm. GRPO eliminates the requirement for value function approximation, thereby reducing computational complexity through group-wise trajectory sampling and intra-group reward normalization. The optimization objective is formulated as:

$$\mathcal{J}_{\text{GRPO}}(\theta) = \mathbb{E}_{\substack{P\sim\mathcal{D},\\ \{T_i\}_{i=1}^{G}\sim\pi_{\theta_{\text{old}}}(\cdot|P)}} \left[ \frac{1}{G}\sum_{i=1}^{G} \frac{1}{|T_i|}\sum_{t=1}^{|T_i|} \min\Big(r_{i,t}(\theta)\,\hat{A}_i,\ \text{clip}(r_{i,t}(\theta),\ 1-\varepsilon,\ 1+\varepsilon)\,\hat{A}_i\Big) \right],$$

where $r_{i,t}(\theta)$ denotes the importance sampling ratio. The advantage estimate $\hat{A}_i$ is computed through within-group normalization:

$$\hat{A}_i = \frac{R(T_i) - \mu_{\mathcal{R}}}{\sigma_{\mathcal{R}} + \delta},$$

with $\mu_{\mathcal{R}}$ and $\sigma_{\mathcal{R}}$ representing the group mean and standard deviation, respectively, and $\delta$ serving as a numerical stability constant. Following recent advances in DAPO, the KL divergence penalty is omitted to facilitate exploration, while the Clip-Higher strategy is adopted to enhance learning of high-entropy, low-probability tokens critical for complex reasoning tasks.

## A.4 Agentic Partial Rollout Algorithm

## A.5 Experimental Details

This section describes the training data construction, model training, and evaluation settings.

### A.5.1 Supervised Fine-tuning (SFT) Data Construction

The supervised fine-tuning (SFT) data construction pipeline consists of three phases.

**Stage 1: Foundational Data Curation and Filtering.** We aggregate a raw corpus from multiple public math reasoning datasets (i.e., AM-Thinking, OpenThoughts, and AceReason). After problem-level deduplication, we apply N-gram $(N = 4)$ and MinHash LSH algorithms to eliminate overlaps with all evaluation sets, including AIME24, AIME25 and HMMT25 with 0.6 similarity threshold. To further prevent data leakage, we compute semantic similarities between training data and evaluation sets using gte-large model(Zhang et al., 2024a) , filtering out the top-5 most similar samples. We then annotate each problem with difficulty scores from 0 to 10 using Qwen3-30B, retaining data with scores above 5, which yields 392k samples. Finally, using DeepSeek-R1-0528 to generate solutions and removing instances with incorrect answers, we obtain 346k high-quality data.

**Stage 2: Tool-Augmented Data Synthesis.** We firstly decompose the problem-solving process into discrete reasoning segments and perform tool-augmented synthesis for each segment using the Prompt presented in Appendix A.6.2 via DeepSeek-V3-0324. During synthesis, we filter out samples with synthesis format error, tool execution failures, or incorrect final answer, yielding 302k high-fidelity, tool-augmented solution trajectories.

**Stage 3: Self-Correction Data Generation.** To incorporate self-correction mechanisms, we sample 30k instances from trajectories with unsuccessful code execution and leverage the Self-correction Prompt presented in Appendix A.6.1 to guide DeepSeek-V3-0324 in generating correction processes, producing 14k valid self-correction trajectories.

Through this comprehensive pipeline, we construct a 316k tool-augmented synthetic training set with an average of 8.3 tool calls and an average sequence length of 16.9K tokens per sample.

### A.5.2 Reinforcement Learning (RL) Data Construction

For RL, we collect problems from multiple public high-quality RL datasets (i.e., DeepScaler, Skywork-OR1, Retool, POLARIS). We apply the same deduplication strategy as for SFT data, ensuring no overlap with evaluation sets through N-gram (N=4), MinHash LSH, and semantic similarity computation with 0.6 similarity threshold. To identify challenging problems, we use AgentMath-8B-SFT to perform 8 inference attempts on all data, filtering out problems that are solved correctly 8 times, culminating in a final set of 42k high-difficulty RL training data. This focuses training on hard instances that push the model's strategic capabilities and maximize potential gains from RL.

### A.5.3 Training Settings

**Base Models.** Our experiments utilize four base models from the Qwen3 series: Qwen3-1.7B-Base and Qwen3-8B-Base are pre-trained models without post-training; Qwen3-30B-A3B-Instruct-2507 (Non-Thinking mode, 30B total parameters, 3B activated) and Qwen3-235B-A22B-Instruct-2507 (Non-Thinking mode, 235B total parameters, 22B activated) are instruction-tuned Mixture-of-Experts (MoE) models without long chain-of-thought training.

**SFT Training.** We employ the Llama-Factory framework, training for 6 epochs with learning rates of $6 \times 10^{-5}$ (1.7B, 8B, A3B models) and $2 \times 10^{-5}$ (A22B model), using cosine decay with 10% warmup, batch size of 512, and maximum sequence length of 32k tokens.

**RL Training.** Our RL training is built on the verl 0.5.0.dev0 framework(Sheng et al., 2024), initializing from the best SFT checkpoint and using VLLM(Kwon et al., 2023) as the inference engine, with a 128-node Sandbox cluster for large-scale code execution. We use a constant learning rate of $1 \times 10^{-6}$, a batch size of 64, and a temperature of 1.0, performing 8 rollouts per problem. Training progresses through three stages, dynamically adjusted to maintain length truncation and tool-call excess rates below 10%: maximum response length increases from 48k to 72k to 96k tokens, with corresponding tool invocation limits of 48, 72, and 96 calls, and partial rollout counts of 2, 3, and 4, ensuring each segment rollout remains within 24k tokens and 24 tool invocations. Due to computational constraints, AgentMath-235B-A22B is trained solely via supervised fine-tuning (SFT).

### A.5.4 Evaluation Settings

**Benchmarks.** We primarily evaluate on AIME24, AIME25, and HMMT25. These challenging U.S. high school math competitions feature problems in algebra, number theory, combinatorics, and geometry, providing a robust test of advanced mathematical modeling, multi-step logical reasoning, and strategic problem-solving.

**Evaluation Metrics.** To ensure robust evaluation, we perform 32 independent inference runs per test sample, using avg@32 as the pass@1 metric.

**Inference Parameters.** We use a consistent configuration: maximum sequence length = 96K tokens, maximum tool calls = 96, code interpreter output limit = 1024 tokens, temperature = 0.6, and top-p = 0.95.

**Answer Extraction and Validation.** We extract final answers from `\boxed{}` markers in model responses and employ Math-Verify library for exact comparison with ground truth answer, determining correctness only when verification returns True.

### A.5.5 Detail Results

Table 4: Performance comparison (avg@32 accuracy) of AgentMath against state-of-the-art models on AIME24, AIME25, and HMMT25 benchmarks. Evaluation follows DeepSeek-R1 framework (temperature=0.6, topp=0.95). AgentMath models (highlighted in blue) achieve superior results across all scales, with the 30B variant competitive against 671B models.

| Models | Base Model | Tool Use | AIME24 | AIME25 | HMMT25 |
|---|---|---|---|---|---|
| Proprietary models | | | | | |
| OpenAI-o4-mini-w/tools(OpenAI, 2025) | - | ✓ | 98.7 | 99.5 | - |
| Grok-4-w/tools(xAI, 2023) | - | ✓ | - | 98.8 | - |
| OpenAI-o3-w/tools(OpenAI, 2025) | - | ✓ | 95.2 | 98.4 | - |
| OpenAI-o4-mini(OpenAI, 2025) | - | ✗ | 93.4 | 92.7 | 83.0 |
| Gemini-2.5-Pro(Team et al., 2023) | - | ✗ | 92.0 | 88.0 | 82.5 |
| OpenAI-o3(OpenAI, 2025) | - | ✗ | 91.6 | 88.9 | 77.5 |
| Seed-1.6-thinking(Seed et al., 2025) | - | ✗ | 90.3 | 86.0 | - |
| OpenAI-o3-mini(OpenAI, 2025) | - | ✗ | 87.3 | 86.3 | 53.0 |
| Claude-Opus-4.0-Thinking(Claude, 2025) | - | ✗ | 83.0 | 72.0 | 58.3 |
| Grok-3-Beta Thining(xAI, 2023) | - | ✗ | 83.9 | 77.3 | - |
| Kimi-k1.5(Team et al., 2025) | - | ✗ | 77.5 | - | - |
| Frontier Models (1B $\sim$ 2B) | | | | | |
| ToRL-1.5B(Li et al., 2025e) | Qwen2.5-Math-1.5B-Base | ✓ | 26.7 | 26.7 | - |
| DeepSeek-R1-Distill-Qwen-1.5B(DeepSeek-AI et al., 2025) | Qwen2.5-Math-1.5B-Base | ✗ | 28.8 | 21.8 | 15.3 |
| DeepScaleR-1.5B-Preview(Luo et al., 2025a) | DeepSeek-R1-Distill-Qwen-1.5B | ✗ | 40.0 | 30.0 | - |
| CoRT-1.5B(Li et al., 2025a) | DeepSeek-R1-Distill-Qwen-1.5B | ✓ | 43.1 | 30.2 | 20.1 |
| Nemontron-Research-Reasoning-Qwen-1.5B(Liu et al., 2025c) | DeepSeek-R1-Distill-Qwen-1.5B | ✗ | 49.6 | 36.0 | 21.7 |
| Qwen3-1.7B Thinking(Team, 2025c) | Qwen3-1.7B-Base | ✗ | 52.0 | 35.3 | 23.3 |
| OpenThinker3-1.5B(Guha et al., 2025) | Qwen2.5-1.5B-Instruct | ✗ | 52.0 | 41.7 | 27.3 |
| OpenReasoning-Nemotron-1.5B(Ahmad et al., 2025) | Qwen2.5-1.5B-Instruct | ✗ | 55.5 | 45.6 | 31.5 |
| AgentMath-1.7B | Qwen3-1.7B-Base | ✓ | 59.6 | 48.1 | 40.2 |
| Frontier Models (7B $\sim$ 8B) | | | | | |
| Qwen2.5-7B-Math-Instruct-TIR(Yang et al., 2024b) | Qwen2.5-Math-7B-Base | ✓ | 20.0 | 26.7 | - |
| Eurus-2-PRIME-7B(Cui et al., 2025) | Qwen-2.5-Math-7B-Base | ✗ | 26.7 | 13.3 | - |
| SimpleRL-Zero-7B(Zeng et al., 2025b) | Qwen-2.5-Math-7B-Base | ✗ | 33.3 | 6.7 | - |
| ToRL-7B(Li et al., 2025e) | Qwen2.5-Math-7B-Base | ✓ | 43.3 | 30.0 | - |
| ZeroTIR-7B(Mai et al., 2025) | Qwen-2.5-7B-Base | ✓ | 46.7 | 30.0 | 22.5 |
| SimpleTIR-7B(Xue et al., 2025) | Qwen2.5-7B-Base | ✓ | 50.5 | 30.9 | 29.7 |
| AFM-7B(Li et al., 2025c) | Qwen2.5-7B-Instruct | ✓ | 51.9 | 37.8 | - |
| rStar-Math-Qwen-7B(Zhang et al., 2024b) | Qwen2.5-Math-7B-Base | ✓ | 53.3 | - | - |
| DeepSeek-R1-Distill-Qwen-7B(DeepSeek-AI et al., 2025) | Qwen2.5-Math-7B-Base | ✗ | 55.0 | 39.7 | - |
| OpenR1-Distill-7B(Face, 2025) | Qwen2.5-Math-7B-Base | ✗ | 57.7 | 39.7 | 25.7 |
| Light-R1-7B-DS(Wen et al., 2025) | DeepSeek-R1-Distill-Qwen-7B | ✗ | 59.1 | 44.3 | 27.6 |
| CIR-Qwen3-NT8-8B(Bai et al., 2025) | Qwen3-8B | ✓ | 61.5 | 46.3 | - |
| AReal-boba-7B(Fu et al., 2025) | DeepSeek-R1-Distill-Qwen-7B | ✗ | 61.9 | 48.3 | 29.4 |
| Skywork-OR1-7B(He et al., 2025a) | DeepSeek-R1-Distilled-Qwen-7B | ✗ | 70.2 | 54.6 | 35.7 |
| POLARIS-7B-Preview(An et al.) | DeepSeek-R1-Distill-Qwen-7B | ✗ | 72.6 | 52.6 | - |
| AceReason-Nemotron-1.1-7B(Chen et al., 2025a) | DeepSeek-R1-Distill-Qwen-7B | ✗ | 72.6 | 64.8 | 42.9 |
| OpenMath-Nemotron-7B(Moshkov et al., 2025) | Qwen2.5-Math-7B | ✗ | 74.8 | 61.2 | - |
| Qwen3-8B Thinking(Team, 2025c) | Qwen3-8B-Base | ✗ | 76.0 | 67.3 | 44.7 |
| MiMo-7B(Xiaomi, 2025) | MiMo-7B-Base | ✗ | 80.1 | 70.2 | 35.7 |
| OpenReasoning-Nemotron-7B(Ahmad et al., 2025) | Qwen2.5-7B-Instruct | ✗ | 84.7 | 78.2 | 63.5 |
| DeepSeek-R1-0528-Qwen3-8B(DeepSeek-AI et al., 2025) | Qwen3-8B-Base | ✗ | 86.0 | 76.3 | 61.5 |
| AgentMath-8B | Qwen3-8B-Base | ✓ | 89.8 | 84.7 | 71.3 |
| Frontier Models (30B $\sim$ 32B) | | | | | |
| Sky-T1-32B-Preview(Team, 2025b) | Qwen2.5-32B-Instruct | ✗ | 43.3 | - | - |
| Open-Reasoner-Zero-Qwen-32B(Hu et al., 2025) | Qwen2.5-32B-Base | ✗ | 48.1 | 36.0 | - |
| DAPO-Qwen-32B(Yu et al., 2025) | Qwen2.5-32B-Base | ✗ | 50.0 | 32.1 | - |
| s1-32B(Muennighoff et al., 2025) | Qwen2.5-32B-Instruct | ✗ | 56.7 | 50.0 | 37.0 |
| ZeroTIR-32B(Mai et al., 2025) | Qwen-2.5-32B-Base | ✓ | 56.7 | 33.3 | 20.0 |
| START-32B(Li et al., 2025b) | QwQ-32B | ✓ | 66.7 | 47.1 | - |
| AFM-32B(Li et al., 2025c) | Qwen2.5-32B-Instruct | ✓ | 66.7 | 59.8 | - |
| ReTool-32B(Feng et al., 2025a) | Qwen2.5-32B-Instruct | ✓ | 67.0 | 49.3 | - |
| rStar2-Agent-Qwen2.5-32B(Shang et al., 2025) | Qwen2.5-32B-instruct | ✓ | 69.4 | 57.3 | - |
| ReTool-R1-32B-distill(Feng et al., 2025a) | DeepSeek-R1-Distill-Qwen-32B | ✓ | 72.5 | 54.3 | - |
| DeepSeek-R1-Distill-Qwen-32B(DeepSeek-AI et al., 2025) | Qwen2.5-32B-Base | ✗ | 72.9 | 59.0 | 33.0 |
| Qwen3-30B-A3B-Instruct-2507(Team, 2025c) (Non-Thinking) | Qwen3-30B-A3B-Base | ✗ | 72.9 | 61.3 | 43.0 |
| Light-R1-32B(Wen et al., 2025) | Qwen2.5-32B-Instruct | ✗ | 76.6 | 64.6 | - |
| CoRT-32B(Li et al., 2025a) | DeepSeek-R1-Distill-Qwen-32B | ✓ | 76.7 | 67.1 | - |
| TinyR1-32B-Preview(Team, 2025e) | DeepSeek-R1-Distill-Qwen-32B | ✗ | 78.1 | 65.3 | - |
| QwQ-32B(Team, 2025d) | - | ✗ | 79.5 | 65.3 | 48.0 |
| Qwen3-30B-A3B-Thinking(Team, 2025c) | Qwen3-30B-A3B-Base | ✗ | 80.4 | 70.9 | 51.0 |
| Qwen3-32B-Thinking(Team, 2025c) | Qwen3-32B-Base | ✗ | 81.4 | 72.9 | - |
| STILL-3-TOOL-32B(Chen et al., 2025c) | DeepSeek-R1-Distill-Qwen-32B | ✓ | 81.7 | 64.2 | 45.4 |
| Skywork-OR1-32B(He et al., 2025a) | DeepSeek-R1-Distill-Qwen-32B | ✗ | 82.2 | 73.3 | - |
| AM-Thinking-v1-32B(Ji et al., 2025) | Qwen 2.5-32B-Base | ✗ | 85.3 | 74.4 | - |
| AM-DeepSeek-R1-0528-Distill-32B(a-m team, 2025) | Qwen 2.5-32B-Base | ✗ | 87.1 | - | - |
| Qwen3-30B-A3B-Thinking-2507(Team, 2025c) | Qwen3-30B-A3B-Base | ✗ | 87.7 | 85.0 | 71.4 |
| OpenReasoning-Nemotron-32B(Ahmad et al., 2025) | Qwen2.5-32B-Instruct | ✗ | 89.2 | 84.0 | 73.8 |
| AgentMath-30B-A3B | Qwen3-30B-A3B-Instruct-2507 | ✓ | 90.6 | 86.4 | 73.8 |
| Frontier Models (>32B) | | | | | |
| Qwen3-235B-A22B-Instruct-2507(Non-Thinking)(Team, 2025c) | Qwen3-235B-A22B-Base | ✗ | 79.2 | 70.3 | 55.4 |
| DeepSeek-R1-671B(DeepSeek-AI et al., 2025) | DeepSeek-V3-Base | ✗ | 79.8 | 70.0 | 44.4 |
| Qwen3-235B-A22B-Thinking(Team, 2025c) | Qwen3-235B-A22B-Base | ✗ | 85.7 | 81.5 | 62.5 |
| DeepSeek-R1-671B-0528(DeepSeek-AI et al., 2025) | DeepSeek-V3-Base | ✗ | 91.4 | 87.5 | 77.0 |
| Seed-Oss-36B-Instruct(Team, 2025a) | Seed-OSS-36B-Base | ✗ | 91.7 | 84.7 | - |
| Qwen3-235B-A22B-Thininking-2507(Team, 2025c) | Qwen3-235B-A22B-Base | ✗ | 94.2 | 92.3 | 83.9 |
| AgentMath-235B-A22B-SFT | Qwen3-235B-A22B-Instruct-2507 | ✓ | 93.4 | 90.8 | 81.7 |

## A.6 Prompt

### A.6.1 Data Synthesis For Code Self-correction Prompt

**Prompt 1: Data Synthesis For Code Self-correction Prompt**

The following is Your Response based on User Instruction. But there was a code interpreter execution error during the process. Please do the following:
Please:

1. Based on the interpreter's failed execution output, identify the exact code segment that caused the error and explain the reason for the failure.
2. Immediately after the interpreter's failed output, add a transition sentence , such as: "Oops, the code above appears to be throwing an error. I need to fix this to ensure it runs successfully."
3. Correct the erroneous code to ensure it runs successfully.
4. Continue the process from where you left off in your response, completing the remaining steps as planned.
5. Wrap the final output in <output></output>tags.

**User Instruction:** {Input}
**Your Response:** <revised_thinking_process>{output} </revised_thinking_process>

### A.6.2 Tool-Augmented Data Synthesis Prompt

**Prompt 2: Tool-Augmented Data Synthesis Prompt**

You are a professional assistant with expertise in mathematics and Python programming, and a multiple gold medalist in mathematics olympiads and programming competitions. You have the capability to write code and use a code interpreter for calculation. The code will be executed in a sandbox environment, and the results will enhance the reasoning process.

**Task Objective**

Enhance the provided mathematical problem-solving process by replacing complex manual calculations with Python code and their execution results, while preserving the original reasoning logic and structure.

**Instructions**

**1. Identify Computational Steps for Code Replacement**

Identify steps that would benefit from code execution, including:

- Complex symbolic algebra: polynomial expansion, factorization, solving equations
- Advanced calculus: differentiation, integration, evaluating definite integrals
- Probability and combinatorics: complex counting, probability distributions
- Linear algebra: matrix operations, inversion, eigenvalue decomposition
- Numerical computations: approximations, large number calculations, geometric calculations
- Any error-prone or computationally intensive calculations

**Important**: Simple calculations (basic arithmetic like $2 \times 3 = 6$) should remain as text. Only use code for complex computations that require at least 5 lines of implementation.

**2. Code Implementation Requirements**

Each code snippet must:

- Be complete and executable, including all necessary imports
- Use appropriate libraries (sympy, numpy, scipy, etc.)
- Include clear variable definitions and comments
- Explicitly use print() for all outputs
- Demonstrate the computation process, not just final results
- Contain at least 5 lines of code

**3. Integration Guidelines**

- Preserve the original reasoning flow: Keep all logical steps, explanations, and even failed attempts unchanged
- Seamless integration: Code and results should naturally fit within the surrounding text
- Context preservation: Maintain semantic coherence and logical consistency
- No unnecessary changes: Do not modify, delete, or polish unrelated content

**4. Formatting Requirements**

Wrap each code snippet as follows:

`<code>\n```python\n```\n</code>`

Follow immediately with execution results:

`<interpreter>\n</interpreter>`

**5. Input Format**

User Question:

`{question}\n<original_thinking_process>\n</original_thinking_process>`

**6. Output Format**

Provide the enhanced thinking process wrapped in:

`<revised_thinking_process>\n</revised_thinking_process>`

**7. Key Principles**

1. Code Necessity: Use code only for complex calculations that warrant automation.
2. Minimal Changes: Modify only the computational steps, preserving all other text.
3. Complete Scripts: Each code block must be self-contained and executable.
4. Accuracy: Execution results must match exactly what the code produces.

### A.6.3 CONSISTENCY JUDGMENT PROMPT

**Prompt 3: Consistency Judgment Prompt**

**Role and Objective**
You are a meticulous scientific analyst. Your mission is to determine if **Text A** and **Text B** are substantively equivalent in their core results.
Focus strictly on **numerical values, mathematical expressions, and final conclusions.** Ignore all differences in wording, formatting, and sentence structure.
**Core Principles**

1. **Content Over Form:** Prioritize the core message and data. Completely ignore stylistic choices like wording, formatting (bolding, spacing), and sentence construction.
2. **Standardize Before Comparing:** Before comparison, you must normalize all values to a common standard. Convert percentages to decimals (`50%` → `0.5`), unify units (`1m` → `100cm`), and resolve scientific notation.
3. **Compare Overlapping Information Only:** If one text contains data information absent in the other, ignore the missing parts. Base your comparison solely on the data and claims present in *both* texts. Asymmetry is not a basis for inequivalence.

**Evaluation Criteria**

1. **Numerical Equivalence**
   - **Rule:** Two numbers, `A` and `B`, are equivalent if their absolute difference is less than or equal to `1.0` after normalization.
   - **Formula:** $|A - B| \leq 1.0$
   - **Examples:**
     - **Equivalent**: $|1.453125 - 1.390625| = 0.0625$ ($\leq 1.0$)
     - **Equivalent**: $|-32.015744 - (-32.515744)| = 0.5$ ($\leq 1.0$)
     - **Inequivalent**: $|12.91829 - 11.78172| = 1.136$ ($> 1.0$)
   - **Clarifications:**
     - Differences in significant figures or decimal places are acceptable as long as the absolute difference rule is met.
     - Numerical signs must match (e.g., `5` and `-5` are not equivalent).
2. **Mathematical Expression Equivalence**
   - **Rule:** Assess if expressions are mathematically equivalent, not just if they are written identically.
   - **Examples of Equivalence:**
     - **Commutativity/Associativity:** `a + b` is equivalent to `b + a`
     - **Alternative Forms:** `x/2` is equivalent to `0.5x`
     - **Factoring/Expansion:** $x^2 - 1$ is equivalent to $(x - 1)(x + 1)$
     - **Variable Renaming:** $f(x) = x^2$ is equivalent to $g(y) = y^2$
   - **Important Caveat:** If a transformation alters the domain in a way that impacts the conclusion (e.g., introduces division by zero), the expressions are not equivalent.
3. **Conclusion Equivalence**
   - **Rule:** The final answers or main conclusions must align.
     - **Numerical Conclusions:** Must meet the numerical equivalence standard defined above.
     - **Categorical Conclusions:** Must be identical (e.g., ”Positive” vs. ”Positive”; ”Category A” vs. ”Category A”).

**Strict Output Format**

1. **Reasons:** Provide a concise, objective, bulleted list explaining your rationale.
2. **Verdict:** State the final decision: True (for equivalent) or False (for inequivalent).
3. **Boxed:** Wrap the final boolean value in \\boxed{}, for example \\boxed{True} or \\boxed{False}.

**Texts to Evaluate:**
**[Text A]** {Text_A}
**[Text B]** {Text_B}

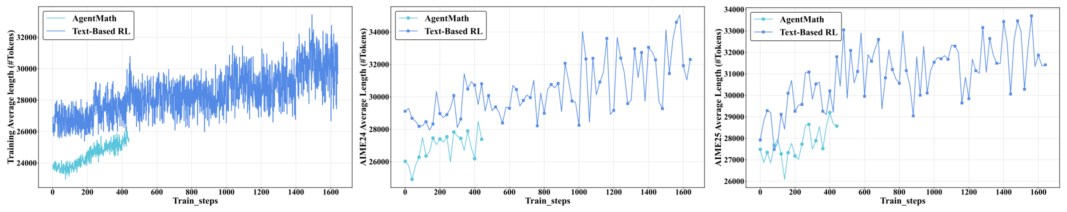

(a) Training response length (b) AIME24 response length (c) AIME25 response length

Figure 5: The evolution of sequence lengths for AgentMath and Text-Based model during RL training and on the AIME24 and AIME25. Both models started from their best SFT checkpoints trained on 20k data.

Table 5: Performance of different backbone models in SFT and RL stage on AIME24/25

| **Models** | **AIME24** | **AIME25** |
|---|---|---|
| Qwen3-1.7B-SFT-30w | 44.5% | 34.8% |
| Qwen3-1.7B-RL | 59.6% | 48.1% |
| Qwen3-8B-SFT-30w | 78.4% | 72.2% |
| Qwen3-8B-RL | 89.8% | 84.7% |
| Qwen3-30B-A3B-SFT-30w | 83.9% | 80.5% |
| Qwen3-30B-A3B-RL | 90.6% | 86.4% |

## A.7 Detailed analysis

### A.7.1 Tool-Augmented Synthetic Data vs. Text-Based Data

To assess the effectiveness of **AgentMath**, our proposed tool-augmented agent framework for complex mathematical reasoning, we conduct experiments addressing two key questions: (1) What performance advantages do tool-augmented synthetic data provide over text-only data in SFT phase? (2) Can tool augmentation enhance both model performance and training efficiency in RL phase? All experiments employ Qwen3-8B-Base as the backbone model with a maximum sequence length of 64k and a limit of 64 tool invocations in RL.

**Supervised Fine-Tuning Performance.** As shown in Table 2, when trained on an identical 20k SFT data, the tool-augmented model achieved accuracies of 60.5% on AIME24 and 53.3% on AIME25, surpassing the plain-text baseline (57.1% and 49.2%) by margins of 3.4% and 4.1%, respectively. This result confirms the effectiveness of our data synthesis method, which transforms computation-intensive reasoning steps into executable code.

**Agent RL Efficiency.** The benefits of tool augmentation are further amplified during RL. As detailed in Figure 4 and Table 2, the tool-augmented model required only approximately 400 training steps to improve from 60.5% to 76.2% on AIME24 and from 53.3% to 67.5% on AIME25. In contrast, the text-based model needed around 1,600 steps to reach 68.7% and 57.5%. This represents a 4.0$\times$ improvement in training efficiency. Notably, the tool-augmented model matched the final performance of the text-based model within just 100–200 steps, underscoring the advantage of dynamically interleaving natural language reasoning with code execution for accelerated policy optimization.

**Improved Inference Efficiency and Scalability.** As indicated in Figure 5, the tool-augmented model also demonstrated superior inference efficiency. During RL training and inference, its sequence length ranged from 24k to 29k tokens, compared to 28k–34k for the text-based model, with a reduction of roughly **4k tokens (**$\sim$**14%)**. Furthermore, the growth in sequence length was significantly slower for the tool-augmented model as training progressed. These efficiency gains stem from precise tool-based computations replacing verbose and error-prone manual calculation steps.

In conclusion, **AgentMath**, by seamlessly integrating natural language reasoning with precise computational tools, demonstrates substantial improvements across all critical metrics (accuracy, training efficiency, and inference cost). These findings validate the effectiveness of both our tool-augmented data synthesis method and the agent-based RL framework.

Table 6: Efficiency evaluation of AgentMath RL training framework

| **Method** | **Time per step (s)** | **Speedup** |
|---|---|---|
| Static Batch Synchronous Rollout | 3600–4000 | – |
| + Request-Level Asynchronous Rollout | 2100–2500 | 1.5–1.8× |
| + Agentic Partial Rollout | 1100–1300 | 3.0–3.3× |
| + Prefix-Aware Weighted Load Balancing | 750–900 | 4.0–5.0× |

Table 7: Impact of the number of partial rollout segments ($N$) on training efficiency and model performance.

| **Partial Rollout ($N$)** | **Time (100 steps)** | **AIME24** | **AIME25** |
|---|---|---|---|
| Partial Rollout N = 1 | 62h | 70.5% | 60.5% |
| Partial Rollout N = 2 | 28h | 70.1% | 60.7% |
| Partial Rollout N = 4 | 22h | 70.8% | 60.7% |
| Partial Rollout N = 6 | 22h | 69.8% | 60.1% |
| Partial Rollout N = 8 | 23h | 69.5% | 60.5% |

### A.7.2 Multi Stage RL Training

Following SFT, the model frequently produced responses exceeding 32k tokens on complex mathematical problems, with particularly challenging instances surpassing the 64k tokens. To balance training efficiency with model capacity, we developed an **adaptive, multi-stage reinforcement learning strategy**. This method progressively unlocks the model's potential by dynamically expanding the sequence length and tool-call budget. A truncation rate exceeding 10% for either response length or tool usage triggers an automatic budget increase: context length increases from 48k to 72k (step 120) and finally to 96k (step 280), while the tool-call limit expands from 48 to 72 (step 140) and then to 96 (step 320) as shown in Figure 3cand 3f.

As illustrated in Figure 3, the training progression reveals significant trends: As training progresses, generated trajectory lengths increase from 24k to 30k (Figure 3b), tool invocation frequency rises from 27 to 31 calls per problem (Figure 3e), and code utilization improved markedly from 70% to 95% (Figure 3d). These metrics indicate the model's growing proficiency in complex, multi-step reasoning and sophisticated tool use. Correspondingly, accuracy on the AIME24 benchmark rose from 78.4% to 89.8% (+11.4%), and on AIME25 from 72.2% to 84.7% (+12.5%), as shown in Figure 3a. Accuracy consistently improves following each capacity expansion. Crucially, the model exhibited emergent capabilities in self-correcting its generated code (Figure 9). These results confirm the efficacy of our multi-stage reinforcement learning strategy, which strikes an optimal balance between computational efficiency and model capability. Additionally, Table 5 details the performance of AgentMath with different backbones on AIME24 and AIME25. It shows that our approach brings significant enhancement in both SFT and RL stages, demonstrating the robustness and effectiveness of the data synthesis method and the multi-stage RL training strategy.

**Key Findings.** The experiments establish three critical insights: (1.) Expanded capacity is crucial: Increasing the sequence length and tool-call budget is essential for facilitating deeper reasoning chains. (2.) Effective reward shaping: The sustained growth in tool usage confirms that our composite reward function successfully guides the model's tool-call decisions. (3.) Framework robustness: Stable training under the extreme configuration of 96k tokens and 96 tool calls underscores the robustness of both the AgentMath framework and its asynchronous training infrastructure.

### A.7.3 Synthetic Data Refinement and Scaling Law

Table 3 presents a comprehensive evaluation of AgentMath's data synthesis pipeline. The initial, unrefined synthetic data yielded suboptimal results (AIME24: 35.3%; AIME25: 25.7%), primarily due to formatting inconsistencies and non-executable code. By progressively applying multi-dimensional quality refinement, including format consistency, code executability verification, and environment feedback alignment, model performance improved substantially, achieving accuracies of 58.6% on AIME24 and 50.8% on AIME25. The subsequent integration of self-correction ca-

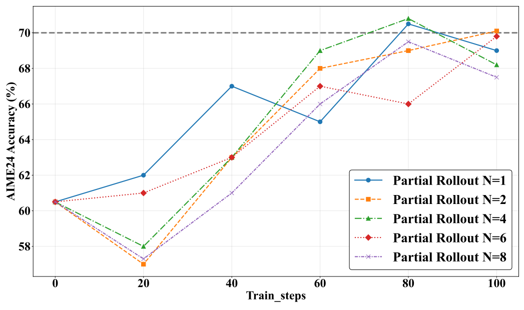

(a) AIME24 Acc

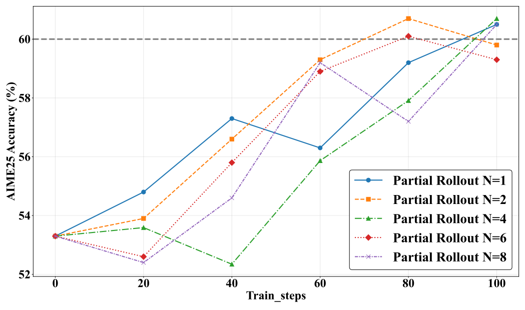

(b) AIME25 Acc

Figure 6: Exploring the performance impact of agent partial rollout segment count on AIME24/25, we adopt the Qwen3-8B-2w-SFT model as the RL initial point.

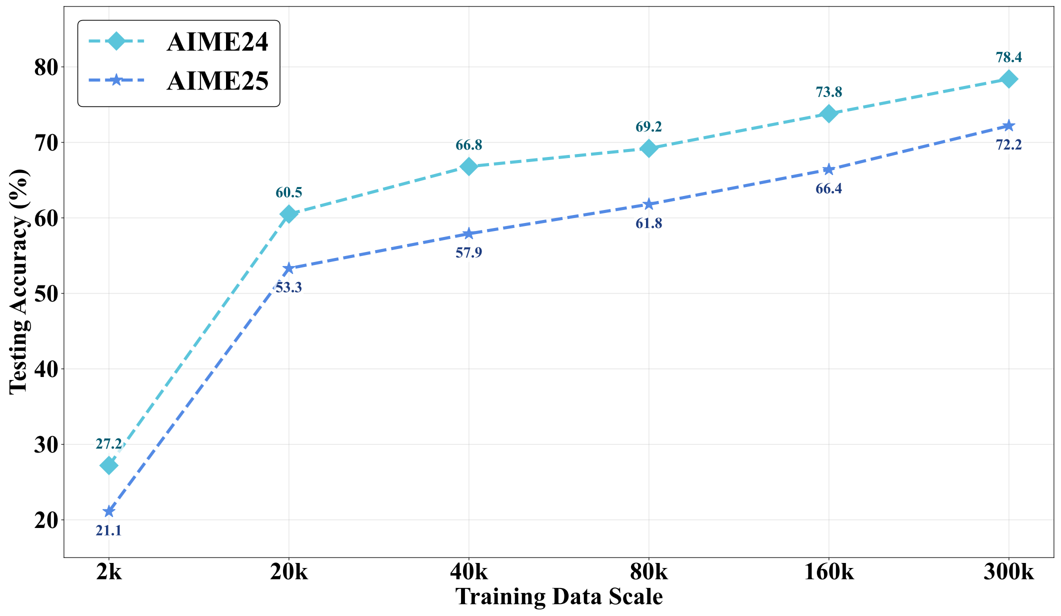

Figure 7: Exploring the scaling laws of tool-enhanced synthetic data, with performance evaluated on AIME24 and AIME25, using the Qwen3-8B-Base model as the backbone.

pabilities, combined with supervised fine-tuning using selective feedback masking based on code execution results, yielded final performance of 60.5% on AIME24 and 53.3% on AIME25. These results underscore the critical contribution of each refinement operation.

Building upon this validated data synthesis pipline, we further explored the impact of scaling the tool-augmented dataset, as shown in Figure 7. Scaling the dataset from 2k to 300k led to a performance increase from 27.2% to 78.4% on AIME24 and from 21.1% to 72.2% on AIME25, demonstrating the effective scalability of our approach. By combining rigorous quality control with effective scaling, AgentMath effectively alleviates the data scarcity in tool-augmented mathematical reasoning, laying a robust foundation for developing high-performance reasoning agents.

### A.7.4 Efficiency of AgentMath RL Training Framework

To alleviate the computational bottlenecks in agent reinforcement learning caused by ultra-long sequences and frequent tool use, we evaluated the efficiency of our AgentMath training framework. As shown in Table 6, a conventional static, batch-synchronous rollout approach required 3600–4000 s per training step. By introducing request-level asynchronous rollout scheduling, we cut this latency to 2100–2500 s (a 1.5–1.8$\times$ speedup), mitigating head-of-line blocking from tool invocations. Incorporating agentic partial rollouts further reduced latency to 1100–1300 s (a 3.0–3.3$\times$ speedup). Finally, adding prefix-aware weighted load balancing brought the per-step latency down to just 750–900 s, achieving a total 4.0–5.0$\times$ speedup and demonstrating AgentMath's advantages for long-sequence, tool-interactive tasks.

We also investigated how the number of partial rollout segments $(N)$ affects training efficiency. As shown in Table 7 and Figure 6, training 100 steps took 62 hours with $N = 1$, but this was reduced to 28 hours with $N = 2$ and 22 hours with $N = 4$. However, the benefits plateaued for $N \geq 6$ due to the scheduling overhead from excessive segmentation. Critically, these optimizations did not harm performance; the model maintained consistent accuracy of approximately 70% on AIME24 and 60% on AIME25 across all segmentation strategies. These results confirm that AgentMath effectively resolves the efficiency challenges of long-sequence agent RL, offering a scalable solution for scenarios that require extended sequences and intensive tool use.

## A.8 Case study

The following example illustrates the dynamic interaction between text reasoning and tool use in AgentMath's problem-solving process. Notably, the model also exhibits an emergent capability for code self-correction. Code blocks highlighted in red indicate an execution error.

### A.8.1 AgentMath Case 1

### A.8.2 AgentMath Case 2

## A.9 LLM Usage Statement:

LLM is employed solely for grammar checking and expression polishing to enhance the readability of the text.

**(AIME24-22) Question:** Let $ABC$ be a triangle inscribed in circle $\\omega$. Let the tangents to $\\omega$ at $B$ and $C$ intersect at point $D$, and let $\\overline{AD}$ intersect $\\omega$ at $P$. If $AB=5$, $BC=9$, and $AC=10$, $AP$ can be written as the form $\\frac{m}{n}$, where $m$ and $n$ are relatively prime integers. Find $m + n$. **Ground Truth Answer: 113**

**AgentMath Response: I need to solve this geometry problem. We have a triangle ABC inscribed in a circle ω. Tangents to ω at points B and C intersect at point D. Line AD intersects the circle again at point P. Given the sides AB = 5, BC = 9, AC = 10, I need to find AP as a fraction m/n in simplest terms and then find m + n.\n\nFirst, ... So equations:\n\n1) 252x + 33 s y = 0\n\n2) 252x - 33 s y = 2268\n\nNow, add them together: (252x + 33s y) + (252x - 33s y) = 0 + 2268 => 504x = 2268 => x = 2268 / 504. Let\'s use code to simplify this fraction.\n \n <code> \n```python\nfrom fractions import Fraction\n\n# We need to solve for x from the equation: 504x = 2268\n # The initial fraction for x is 2268/504.\n x_fraction = Fraction(2268, 504)\n \n print(f"The simplified value for x is: {x_fraction}")\n ```\n </code> \n \n <interpreter> \n The simplified value for x is: 9/2 \n\ n </interpreter>n \n So x = 9/2 = 4.5. Now from equation 1: 252x + 33 s y =0, so 33 s y = -252 x, y = -252 x / (33 s). Let\'s calculate this with code.\n \n <code> \n ```python \n from fractions import Fraction \n \n# We substitute x = 9/2 into the equation y = -252x / (33*s)\n# where s = sqrt(14).\n# We calculate the coefficient of 1/s. \n coefficient = Fraction(-252) * Fraction(9, 2) / 33 \n \n print(f"The coefficient for 1/s is: {coefficient}")\n```\n</code>\n\n<interpreter>\nThe coefficient for 1/s is: -378/11\n\n</interpreter>\\n\nSo y = -378 / (11 sqrt(14)). Rationalize: multiply numerator and denominator by sqrt(14): [-378 sqrt(14)] / (11 * 14) = -378 sqrt(14) / 154. Let\'s use code to simplify this fraction.\n\n <code> \n ```python \n from fractions import Fraction \n \n # We need to simplify the fraction -378/154. \n # The full expression for y is -378 * sqrt(14) / 154. \n simplified_fraction = Fraction(-378, 154) \n \n print(f"The simplified fraction is: {simplified_fraction}") \n ``` \n </code> \n \n \n <interpreter> \n The simplified fraction is: -27/11\n\n</interpreter>\n …Now, we can compute the squares and the denominator.\n\n<code>\n```python\nimport math\n\n# Numerator parts\nval1 = 264**2\nval2 = 225**2\n\n# Denominator parts\nval3 = 22**2\nval4 = 157\nval5 = 107\n\n# Calculate the full numerator and denominator\nnumerator = val1 * val2\ndenominator = val3 * val4 * val5\n\nprint(f"264^2 = {val1}")\nprint(f"225^2 = {val2}")\nprint(f"22^2 = {val3}")\nprint(f"Numerator (264^2 * 225^2) = {numerator}")\nprint(f"Denominator (22^2 * 157 * 107) = {denominator}")\n```\n</code>\n\n<interpreter>\n264^2 = 69696\n225^2 = 50625\n22^2 = 484\nNumerator (264^2 * 225^2) = 3528360000\nDenominator (22^2 * 157 * 107) = 8130716\n\n</interpreter>.... 100 and 13 coprime, yes.\n\nSo m/n = 100/13, m+n=113.\n\nBut let me confirm.\n\nIn the problem, sides are 5,9,10, which is almost isosceles, but not, and AP=100/13≈7.692, which is plausible.\n\nNow, to box the answer.\n\nSo m+n=100+13=113.\n\nBut let me make sure.\n\nSince we have AP, and it\'s rational, and matches.\n\nAnother way to confirm: using the formula.\n\nI recall that in some geometries, the length can be found using formulas, but I think it\'s correct.\n\nSo the answer is 113.**

Figure 8: AgentMath Case study

**(AIME24-29) Question:** Let $\\omega\ \n eq 1$ be a 13th root of unity. Find the remainder when \\[\\prod_{k=0}^{12}(2-2\\omega^k+\\omega^{2k})\\] is divided by 1000.
**Ground Truth Answer: 321**

**AgentMath Response: The problem states: Let ω ≠ 1 be a 13th root of unity. I need to find the remainder when the product from k=0 to 12 of (2 - 2ω^k + ω^{2k}) is divided by 1000. Since it\'s a product over all 13th roots of unity except 1, but k goes from 0 to 12, which includes all roots. ω is a primitive 13th root of unity, I assume, since it\'s specified ≠1, but k=0 gives ω^0=1, so it includes k=0. \n \n Let me denote the expression inside as f(k) = 2 - 2ω^k + ω^{2k}. ...... \n Now, let me compute the product numerically to check. \n \n <code> \n ```python \n import cmath \n import math \n \n # Let omega be the primitive 5th root of unity, omega = exp(2*pi*i / 5) \n omega = cmath.exp(2 * cmath.pi * 1j / 5) \n \n # Calculate the five terms g(omega^k) \n g_0 = (omega**0)**2 - 2 * (omega**0) + 2 \n g_1 = omega**2 - 2 * omega + 2 \n g_2 = omega**4 - 2 * omega**2 + 2 \n g_3 = omega**6 - 2 * omega**3 + 2 \n g_4 = omega**8 - 2 * omega**4 + 2 \n \n # Calculate the product of the five terms \n total_product = g_0 * g_1 * g_2 * g_3 * g_4 \n \n # Print the individual terms and the final product \n # Using round to get cleaner numbers as the imaginary parts might be very small \n print(f"g(1) = {round(g_0, 5)}") \n print(f"g(omega) = {round(g_1, 5)}") \n print(f"g(omega^2) = {round(g_2, 5)}") \n print(f"g(omega^3) = {round(g_3, 5)}") \n print(f"g(omega^4) = {round(g_4, 5)}") \n print(f"Total product = {round(total_product, 5)}") \n ``` \n </code>** \n\n <interpreter> \n Traceback (most recent call last): \n File "/tmp/tmpwjpzt94l/tmp2mcwv09t.py", line 19, in <module> \n print(f"g(1) = {round(g_0, 5)}") \n ^^^^^^^^^^^^^ \n **TypeError: type complex doesn\'t define __round__ method** \n \n </interpreter> \n \n Oops, the code above appears to be throwing an error. I need to fix this to ensure it runs successfully.< The error occurs because the `round()` function cannot handle complex numbers directly. I will modify the code to handle complex numbers correctly. \n \n <code> \n ```python \n import cmath \n import math \n \n # Let omega be the primitive 5th root of unity, omega = exp(2*pi*i / 5) \n omega = cmath.exp(2 * cmath.pi * 1j / 5) \n \n # Calculate the five terms g(omega^k) \n g_0 = (omega**0)**2 - 2 * (omega**0) + 2 \n g_1 = omega**2 - 2 * omega + 2 \n g_2 = omega**4 - 2 * omega**2 + 2 \n g_3 = omega**6 - 2 * omega**3 + 2 \n g_4 = omega**8 - 2 * omega**4 + 2 \n \n # Calculate the product of the five terms \n total_product = g_0 * g_1 * g_2 * g_3 * g_4 \n \n # Print the individual terms and the final product \n print(f"g(1) = {g_0.real:.5f}{g_0.imag:+.5f}j") \n print(f"g(omega) = {g_1.real:.5f}{g_1.imag:+.5f}j") \n print(f"g(omega^2) = {g_2.real:.5f}{g_2.imag:+.5f}j") \n print(f"g(omega^3) = {g_3.real:.5f}{g_3.imag:+.5f}j") \n print(f"g(omega^4) = {g_4.real:.5f} {g_4.imag:+.5f}j") \n print(f"Total product = {total_product.real:.5f} {total_product.imag:+.5f}j") \n ``` \n </code> \n <interpreter>\ng(1) = 1.00000+0.00000j \n g(omega) = 0.57295 - 1.31433j \n g(omega^2) = 3.92705 - 2.12663j \n g(omega^3) = 3.92705+2.12663j \n g(omega^4) = 0.57295+1.31433j \n Total product = 41.00000-0.00000j \n \n </interpreter> **\n\n The numerical calculation shows the total product is 41. The small imaginary part is due to floating-point inaccuracies… So here f=g(x), so f2=1, f1=-2, f0=2 \n\n g=r(x), so g1=-64, g0=-1 \n\n ......Thus P=8321. \n\n Now, 8321 mod 1000 is 321. \n\n So the remainder is 321.**

Figure 9: AgentMath Case study For code self-correction

### A.10 The paper's contribution is mostly on the development of the entire pipeline from my perspective. As many technical innovations claimed in the paper are either standard or mostly from engineering aspects, as agentic RL training is not a fresh concept nowadays (including coding-assisted math reasoning). I value a lot of the paper's efforts on developing such a comprehensive pipeline (SFT data collection and large-scale RL system building), which I understand is very challenging and helpful for the open-source community; however, the lack of technical contribution is the major factor preventing me providing a higher score.

We agree that agentic RL training is not a fresh concept nowadays (including coding-assisted math reasoning), as prior works such as Retool and ToRL tried to explore this direction. However, we believe the field currently faces two critical challenges that remain inadequately addressed:

**1. Lack of efficient tool-augmented data synthesis methods and scaling law studies for long-chain reasoning scenarios**

Existing approaches face substantial limitations when synthesizing tool-augmented data in long-chain reasoning scenarios. For instance, CoRT relies on manual annotation, making it costly and difficult to scale. While Retool employs LLM-based synthesis, it produces only 2k samples and provides insufficient details about the synthesis process. Moreover, existing research lacks systematic investigation of scaling laws for agent synthesized data. In code-assisted mathematical reasoning, what is the relationship between data scale and performance? Can superior performance be achieved through data scaling law? These fundamental questions have rarely been systematically studied in the open-source community.

**2. Agent RL training encounters severe efficiency bottlenecks in ultra-long sequence and large-scale tool invocation scenarios**

When models perform well on code-assisted mathematical reasoning, can performance be continuously improved through large-scale Agent RL to achieve adaptive tool invocation? However, under conditions involving ultra-long reasoning chains and large-scale tool invocations (e.g., 96k token length, 96 tool calls), training efficiency becomes a critical bottleneck. Frequent environment interactions and ultra-long trajectory generation cause traditional batch synchronous rollout training on Qwen3-8B to require 3600-4000 seconds per training step, with rollout generation accounting for 70%-80% of total training time. This inefficiency severely constrains researchers' exploration of Agent RL training in long-horizon and large-scale tool-calling scenarios.

We note that training efficiency is crucial for RL training. The ability to train for thousands of steps and break through performance plateaus directly impacts final results. For instance, DeepSeek-R1-Zero requires 4000-8000 training steps to observe the model's "Aha moment" phenomenon and continuous performance improvements. To address this core bottleneck, our work introduces innovative optimization that reduce per-step training time from 3600-4000 seconds to 700-900 seconds, achieving a 4–5$\times$ speedup. This provides critical support for advancing large-scale Agent RL in LLMs.

Furthermore, while leading proprietary models (GPT-5, Gemini 3.0, Claude 4.5, etc.) demonstrate exceptional performance on agent tasks such as code-assisted mathematical reasoning, the lack of technical details and training methods hinders the open-source community's ability to reproduce and advance this research. By providing a clear, transparent, and complete pipeline for data synthesis and large-scale agent RL training that achieve competitive performance with proprietary models (e.g., Gemini 2.5-Pro, OpenAI-o3), our work aims to offer the open-source community a reproducible technical roadmap, thereby advancing the development of the Agent LLM field.

Therefore, we highlight our core technical contributions across four key dimensions: (1) an efficient tool-augmented data synthesis method, (2) exploration of scaling laws for tool-augmented synthetic data, (3) efficient agent RL training techniques for ultra-long sequences and large-scale tool invocation scenarios, and (4) state-of-the-art performance.

**1. Efficient Tool-Augmented Data Synthesis Method**

1.1. Compared to existing work (e.g., Retool), AgentMath achieves significant improvements in data synthesis. We observe that previous methods (e.g., Retool) suffer from tool overuse issues, including invoking tools for simple calculations and performing redundant verification of already-verified correct results, which leads to an increase in ineffective tokens. To address this issue, AgentMath focuses on applying tool invocations to genuinely necessary complex computational scenarios (e.g., solving complex equations, performing complex large-number arithmetic, and handling advanced linear algebra and calculus operations). We propose a segmented synthesis strategy that partitions DeepSeek-R1's long chain-of-thought process into fixed-length segments (e.g., 3K tokens) and transforms them into tool-augmented chains-of-thought, and incorporates automated multi-dimensional quality refinement to ensure high data quality.

Under identical training settings, we use the same 2k synthetic data problems from Retool's official open-source release, the same DeepSeek-R1 teacher model responses, the same base model (Qwen2.5-32B-Instruct), and the same number of RL training steps (400 steps). The only difference lies in the data synthesis strategy: AgentMath employs our paper's proposed tool-augmented synthesis method (Appendix A.6.2, lines 1404–1456), while Retool uses its original synthesis prompts. As shown in the table 8, AgentMath-32B-SFT-2k achieves 44.1% on AIME24 and 37.3% on AIME25, outperforming Retool-32B-SFT-2k (40.9%, 34.5%); meanwhile, AgentMath-32B-RL achieves 74.8% on AIME24 and 56.6% on AIME25, similarly outperforming Retool-32B-RL (67.0%, 49.3%). These experimental results demonstrate that AgentMath significantly outperforms Retool in both SFT and RL performance on AIME24 and AIME25, validating the effectiveness of our data synthesis method and the superior quality of the synthesized data.

Table 8: Performance comparison between AgentMath and Retool on AIME24 and AIME25 benchmarks under identical training configurations, demonstrating the superiority of AgentMath's tool-augmented data synthesis method over Retool's approach in both SFT and RL stages.

| Model | AIME24 Acc | AIME25 Acc |
|---|---|---|
| Retool-32B-SFT-2k | 40.9% | 34.5% |
| AgentMath-32B-SFT-2k | 44.1% | 37.3% |
| Retool-32B-RL | 67.0% | 49.3% |
| AgentMath-32B-RL | 74.8% | 56.6% |

1.2. Furthermore, we emphasize the multi-dimensional quality refinement pipeline in our data synthesis process, which includes correcting format inconsistencies, excluding samples with failed code execution, performing Environmental Feedback Alignment, filtering low-complexity code (e.g., $\leq 5$ lines of code), and injecting self-correction capabilities. As shown in the table 9, through our multi-dimensional quality refinement pipeline, accuracy on AIME24 improves from 35.3% with initially unrefined synthetic data to 60.5%, and on AIME25 from 25.7% to 53.3%, substantially demonstrating the critical role and effectiveness of each refinement module in optimizing data quality. We therefore consider the multi-dimensional quality refinement pipeline in data synthesis to be of paramount importance, which constitutes one of our key contributions. We are committed to maintaining transparency and clarity in our synthesis and refinement procedures, whereas some recent works provide limited details on this crucial aspect, thereby posing challenges for research reproducibility.

**2. Scaling Laws for Tool-Augmented Synthetic Data**

We systematically validate the scaling laws associated with tool-augmented synthetic data. Through AgentMath's segmented data synthesis strategy and multi-dimensional quality refinement, we progressively scale the dataset from 2k to 300k samples, as shown in the table 10. Fine-tuning the Qwen3-8B-Base model, we observe consistent performance improvements: accuracy on AIME24 increases from 27.2% to 78.4%, and on AIME25 from 21.1% to 72.2%. Performance continues to improve with data scale, ultimately achieving excellent results. These findings robustly demonstrate that scaling laws remain effective for tool-augmented synthetic data. In contrast, some recent studies (e.g., Retool) utilize only limited data (e.g., 2k samples) and do not sufficiently explore the potential benefits of data scaling.

Table 9: Progressive improvement in model accuracy on AIME24 and AIME25 benchmarks through multi-dimensional quality refinement pipeline. Each refinement step is applied cumulatively, demonstrating substantial accuracy gains from 35.3% to 60.5% on AIME24 and from 25.7% to 53.3% on AIME25.

| Models / Refinement Steps | AIME24 | AIME25 |
|---|---|---|
| Initial Unrefined CI-Synthetic Data (20k) | 35.3% | 25.7% |
| + Format consistency correction | 47.4% | 40.1% |
| + Code executability verification | 52.8% | 44.8% |
| + Environmental feedback alignment | 56.3% | 48.3% |
| + Tool-usage rationality assessment | 57.2% | 48.9% |
| + Self-correction capability injection | 58.6% | 50.8% |
| + SFT with selective feedback masking | 60.5% | 53.3% |

Table 10: Performance data scaling law of AgentMath-8B models across different benchmarks as a function of supervised fine-tuning (SFT) training data volume, demonstrating consistent improvements from 2k to 300k samples on AIME24, AIME25, and Google-IMO-AnswerBench datasets.

| SFT Training Data Volume | AIME24 | AIME25 | Google-IMO-AnswerBench | Avg Score |
|---|---|---|---|---|
| AgentMath-8B-SFT-2k | 27.2 | 21.1 | 5.3 | 17.9 |
| AgentMath-8B-SFT-20k | 60.5 | 53.3 | 12.8 | 42.2 |
| AgentMath-8B-SFT-40k | 66.8 | 57.9 | 17.6 | 47.4 |
| AgentMath-8B-SFT-80k | 69.2 | 61.8 | 21.4 | 50.8 |
| AgentMath-8B-SFT-160k | 73.8 | 66.4 | 25.6 | 55.3 |
| AgentMath-8B-SFT-300k | 78.4 | 72.2 | 28.8 | 59.8 |

**3. Efficient Agent RL Training for Ultra-Long Sequences and Large-Scale Tool Calling Scenarios**

In Agent RL, the combination of long-context generation and frequent external tool interactions creates heterogeneous computational workloads, posing significant challenges to training efficiency. To address this, we have designed targeted optimization strategies comprising three core improvements:

1. **Request-Level Asynchronous Rollout Scheduling:** We replace the conventional static batch synchronous processing with a coroutine-driven, request-level asynchronous scheduler. Each trajectory rollout is treated as an independent long-running request, where the inference engine (server) and the agent (client) are fully decoupled through asynchronous communication. This effectively mitigates the efficiency bottleneck caused by synchronous waiting.
2. **Agentic Partial Rollout:** To alleviate the long-tail latency issues arising from ultra-long sequences and large-scale tool calls, we propose an agentic partial rollout mechanism, including Length Partial Rollout and Tool Partial Rollout. This mechanism decomposes each trajectory $\tau$ into budget-constrained segments, where each segment is limited to a fixed maximum sequence length (e.g., 32k tokens) and a fixed maximum number of tool calls (e.g., 32). Incomplete sequences or tool calls are carried over to subsequent batches for continued execution, while completed trajectories immediately participate in training, thereby significantly improving training efficiency.
3. **Prefix-Aware Weighted Load Balancing:** Since Partial Rollout introduces ultra-long sequences, leading to a substantial increase in KV cache memory consumption and prefill computational overhead, we design a prefix-aware weighted load balancing strategy. This strategy dynamically assigns weights based on the prefix length of requests and intelligently routes them to the least-loaded inference engine instances, effectively alleviating memory and computational pressure.

We systematically evaluate the efficiency improvements of the AgentMath training framework. As shown in Table 11, the traditional static batch synchronous rollout method requires 3600–4000 seconds per training step. With the introduction of request-level asynchronous rollout scheduling, latency is reduced to 2100–2500 seconds (a 1.5–1.8$\times$ speedup), effectively mitigating head-of-line blocking caused by tool calls. Further incorporating the Agentic Partial Rollout mechanism reduces latency to 1100–1300 seconds (a 3.0–3.3× speedup). Finally, with the incorporation of prefix-aware weighted load balancing, the per-step latency is only 750–900 seconds, achieving an overall training speedup of 4.0–5.0×.

This framework enables efficient Agent RL training in extreme scenarios (e.g., 96k sequence length, 96 tool calls), for which training with such ultra-long sequences and large-scale tool calls has few precedents in the open-source community. We believe this work provides an important technical reference for training complex agent systems.

Table 11: Progressive training efficiency improvements in the AgentMath framework through cumulative optimization strategies, demonstrating up to 5.0× speedup over baseline static batch synchronous rollout.

| **Method** | **Time per step (s)** | **Speedup** |
|---|---|---|
| Static Batch Synchronous Rollout | 3600–4000 | — |
| + Request-Level Asynchronous Rollout | 2100–2500 | 1.5–1.8× |
| + Agentic Partial Rollout | 1100–1300 | 3.0–3.3× |
| + Prefix-Aware Weighted Load Balancing | 750–900 | 4.0–5.0× |

**4. Large-Scale Agent RL Training Achieving State-of-the-Art Performance**

AgentMath undergoes a three-stage curriculum learning process, with sequence lengths progressively increasing from 48k to 72k to 96k tokens and tool invocations scaling from 48 to 72 to 96. Across diverse model backbones spanning 1.5B to 32B parameters, we successfully conduct stable Agent RL training on ultra-long sequences with large-scale tool invocations, achieving consistent performance improvements. As detailed in Table 12, we achieve state-of-the-art performance on challenging mathematical competition benchmarks including AIME24, AIME25, and HMMT25, significantly outperforming leading open-source models of comparable size. Specifically, AgentMath-30B-A3B achieves accuracies of 90.6%, 86.4%, and 73.8% on AIME24, AIME25, and HMMT25 respectively, surpassing OpenAI-o3-mini and Claude-Opus-4.0-Thinking while remaining competitive with OpenAI-o3, Gemini-2.5-Pro, and DeepSeek-R1-671B-0528. These results validate the effectiveness and scalability of our data synthesis method and Agent RL training strategy, paving the way for building more sophisticated and scalable mathematical reasoning agents.

In summary, we highlight our core contributions as follows:

1. We propose an efficient tool-augmented data synthesis method that focuses on applying tool invocation to genuinely demanding complex computational scenarios (e.g., solving complex equations, large-number arithmetic, advanced linear algebra, and calculus). By combining a segmented synthesis strategy with a multi-dimensional quality refinement mechanism, AgentMath significantly outperforms Retool in both SFT and RL stages on AIME24 and AIME25 under identical training configurations.
2. We systematically validate the scaling laws associated with tool-augmented synthetic data, scaling the dataset from 2K to 300K samples. Building on the Qwen3-8B-Base model, accuracy on AIME24 improves from 27.2% to 78.4%, and on AIME25 from 21.1% to 72.2%, demonstrating consistent performance gains with increased data scale.
3. To alleviate the training efficiency bottleneck in Agent RL under ultra-long sequences and large-scale tool invocation scenarios, we introduce request-level asynchronous rollout scheduling, propose Agent Partial Rollout, and design prefix-aware weighted load balancing. Through these technical innovations, our overall framework achieves a 4-5× speedup in training efficiency, reducing the time per training step from 3600-4000 seconds to 750-900 seconds, thereby enabling efficient agent RL training in extreme scenarios (e.g., 96K sequence length with 96 tool invocations). To the best of our knowledge, such exploration of large-scale Agent RL training with extremely long sequences and massive tool invocations is rarely conducted in the open-source community.
4. Through three-stage curriculum Agent RL training, AgentMath achieves state-of-the-art performance on challenging mathematical competition benchmarks including AIME24,

Table 12: Performance comparison of AgentMath against proprietary and frontier open-source models on AIME24, AIME25, and HMMT25 benchmarks. Our model AgentMath is highlighted in blue.

| **Models** | **AIME24** | **AIME25** | **HMMT25** |
|---|---|---|---|
| **Proprietary models** | | | |
| OpenAI-o4-mini-w/tools | 98.7 | 99.5 | - |
| Gemini-2.5-Pro | 92.0 | 88.0 | 82.5 |
| OpenAI-o3 | 91.6 | 88.9 | 77.5 |
| OpenAI-o3-mini | 87.3 | 86.3 | 53.0 |
| Claude-Opus-4.0-Thinking | 83.0 | 72.0 | 58.3 |
| **Frontier Models (1B $\sim$ 2B)** | | | |
| DeepSeek-R1-Distill-Qwen-1.5B | 28.8 | 21.8 | 15.3 |
| Qwen3-1.7B Thinking | 52.0 | 35.3 | 23.3 |
| OpenReasoning-Nemotron-1.5B | 55.5 | 45.6 | 31.5 |
| AgentMath-1.7B | 59.6 | 48.1 | 40.2 |
| **Frontier Models (7B $\sim$ 8B)** | | | |
| DeepSeek-R1-Distill-Qwen-7B | 55.0 | 39.7 | - |
| Qwen3-8B Thinking | 76.0 | 67.3 | 44.7 |
| OpenReasoning-Nemotron-7B | 84.7 | 78.2 | 63.5 |
| DeepSeek-R1-0528-Qwen3-8B | 86.0 | 76.3 | 61.5 |
| AgentMath-8B | 89.8 | 84.7 | 71.3 |
| **Frontier Models (30B $\sim$ 32B)** | | | |
| ReTool-32B | 67.0 | 49.3 | - |
| DeepSeek-R1-Distill-Qwen-32B | 72.9 | 59.0 | 33.0 |
| Qwen3-30B-A3B-Thinking-2507 | 87.7 | 85.0 | 71.4 |
| OpenReasoning-Nemotron-32B | 89.2 | 84.0 | 73.8 |
| AgentMath-30B-A3B | 90.6 | 86.4 | 73.8 |
| **Frontier Models (>32B)** | | | |
| DeepSeek-R1-671B-0528 | 91.4 | 87.5 | 77.0 |
| Qwen3-235B-A22B-Thinking-2507 | 94.2 | 92.3 | 83.9 |
| AgentMath-235B-A22B-SFT | 93.4 | 90.8 | 81.7 |

AIME25, and HMMT25 across various model backbones ranging from 1.5B to 32B parameters, significantly outperforming leading open-source models of comparable size. Notably, AgentMath-30B-A3B surpasses OpenAI-o3-mini while remaining competitive with Gemini-2.5-Pro and DeepSeek-R1-671B-0528. We are committed to open-sourcing our code, data synthesis pipeline, and model training workflow to advance the LLM reasoning community.

### A.11 Concern about benchmark: The math benchmarks (AIME24, AIME25, HMMT) each contain only about 30 questions. Prior work has shown that these datasets may have leaked into open-source model training corpora. Thus, it is unclear whether the reported results are entirely reliable. The authors are encouraged to provide more evidence on the independent contribution of the proposed approach.

To systematically validate the reliability of our results and mitigate potential evaluation benchmark leakage concerns, we conducted supplementary experiments and analyses from three complementary perspectives.

**(1) IMO-AnswerBench: A latest High-Difficulty Benchmark**

Considering that datasets such as AIME24, AIME25, and HMMT25 may have partially appeared in the pre-training corpora of open-source models, we evaluate AgentMath on IMO-AnswerBench, a recent mathematics olympiad benchmark released by Google DeepMind in November 2025. This benchmark comprises 400 carefully curated problems spanning four domains about algebra, combinatorics, geometry, and number theory, with 100 problems per category, all sourced from national, regional, and international olympiad competitions.

To mitigate data memorization and leakage, IMO-AnswerBench systematically rewrites original competition problems through several strategies: renaming points or lines in geometry problems, rephrasing problem statements, modifying numerical values and or introducing distractors, and reformulating problems using entirely different yet semantically equivalent expressions. This design substantially reduces the probability of verbatim matches in pre-training corpora and minimizes the potential for memorization-based advantages, thereby enhancing evaluation robustness and fairness.

The performance of current frontier models on this benchmark: DeepSeek-V3 at 37.0%, Qwen3-235B at 53.8%, and DeepSeek-R1 at 60.8%, indicates that the benchmark possesses sufficient discriminative power and challenge. Moreover, the benchmark's release date (November 2025) is notably later than the public release of Qwen3-series models (May 2025), further minimizing the likelihood of contamination in their training corpora.

Following the experimental setup specified in the IMO-AnswerBench paper, we report results averaged over 8 independent runs. At comparable parameter scales, AgentMath achieves the following performance across the four categories (as detailed in the table 13):

**At the 1.5B–1.7B scale:** AgentMath-Qwen3-1.7B achieves 20.3%, outperforming OpenReasoning-Nemotron-1.5B (17.8%);

**At the 7B–8B scale:** AgentMath-Qwen2.5-7B achieves 35.1% and AgentMath-Qwen3-8B achieves 37.9%, both substantially outperforming OpenReasoning-Nemotron-7B (33.0%);

**At the 30B–32B scale:** AgentMath-30B-A3B achieves 51.2%, surpassing Qwen3-30B-A3B-Thinking-2507 (41.4%), Claude Sonnet 4, DeepSeek-V3, and Kimi-K2-Instruct, while approaching the performance of Qwen3-235B;

**At scales larger than 32B:** AgentMath-235B-A22B-SFT achieves 55.4%, surpassing Qwen3-235B and approaching DeepSeek-R1.

These results demonstrate that AgentMath maintains strong performance and robustness across different parameter scales on a challenging evaluation set that is demonstrably free from data leakage concerns.

**(2) Validation Using Base Models Released Prior to Evaluation Benchmark Publication**

To further mitigate concerns regarding potential evaluation data leakage into the pretraining corpus, we employ open-source base models released before the publication of evaluation benchmarks for our SFT and RL training. The timeline is as follows:

- Qwen2.5-7B-Base release: September 2024
- Llama3.1-8B-Base release: July 2024
- AIME25 publication: February 2025
- HMMT25 publication: February 2025
- Google-IMO-AnswerBench publication: November 2025

All benchmarks were thus published after model pretraining was completed, thereby precluding any possibility of data contamination.

As shown in the table 14 and table 15, AgentMath trained on these earlier base models achieves superior performance across multiple benchmarks:

- Building on Llama3.1-8B-Base, AgentMath-Llama-8B achieves 66.2% and 53.1% on AIME25 and HMMT25, respectively, significantly outperforming Llama3.1-Nemotron-Nano-8B-v1 (48.0% and 26.7%);
- Building on Qwen2.5-7B-Base, AgentMath-Qwen2.5-7B attains 79.8% and 65.9% on AIME25 and HMMT25, respectively, surpassing OpenReasoning-Nemotron-7B (78.2% and 63.5%);

Table 13: Performance of AgentMath on Google-IMO-AnswerBench, a recent mathematics olympiad benchmark released by Google DeepMind in November 2025. Our model (highlighted in blue) is compared against other leading models, with accuracy (avg@8) as the evaluation metric according to the IMO-AnswerBench.

| Model (Google-IMO-AnswerBench) | Algebra | Combinatorics | Geometry | Number Theory | Avg score |
|---|---|---|---|---|---|
| Proprietary models | | | | | |
| Gemini Deep Think (IMO Gold) | 85.0% | 69.0% | 88.0% | 78.0% | 80.0% |
| Grok 4 | 75.5% | 55.9% | 80.1% | 80.9% | 73.1% |
| Gemini 2.5 Deep Think | 78.0% | 49.0% | 83.0% | 77.0% | 71.8% |
| Gemini 2.5 Pro | 73.4% | 48.0% | 74.3% | 77.1% | 68.2% |
| o4-mini (high reasoning) | 71.3% | 46.6% | 78.4% | 75.3% | 67.9% |
| GPT-5 | 69.9% | 46.4% | 74.8% | 71.2% | 65.6% |
| o3 | 62.8% | 43.0% | 70.6% | 68.0% | 61.1% |
| Claude Sonnet 4 | 20.6% | 17.8% | 26.0% | 27.6% | 23.0% |
| Claude Opus4 | 19.4% | 20.0% | 23.3% | 26.6% | 22.3% |
| Frontier Models (1B–2B) | | | | | |
| DeepSeek-R1-Distill-Qwen-1.5B | 5.5% | 9.9% | 14.5% | 8.7% | 9.7% |
| Qwen3-1.7B Thinking | 11.4% | 12.5% | 21.5% | 17.5% | 15.7% |
| OpenReasoning-Nemotron-1.5B | 16.3% | 14.0% | 22.6% | 18.4% | 17.8% |
| AgentMath-Qwen3-1.7B | 18.6% | 16.2% | 24.4% | 21.8% | 20.3% |
| Frontier Models (7B–8B) | | | | | |
| DeepSeek-R1-Distill-Llama3.1-8B | 10.2% | 17.4% | 21.6% | 17.0% | 16.6% |
| DeepSeek-R1-Distill-Qwen-7B | 12.8% | 20.6% | 22.8% | 18.0% | 18.5% |
| Qwen3-8B-Thining | 17.0% | 26.8% | 38.0% | 25.8% | 26.9% |
| DeepSeek-R1-0528-Distill-Qwen3-8B | 21.2% | 31.7% | 43.3% | 27.3% | 30.9% |
| OpenReasoning-Nemotron-7B | 23.6% | 35.2% | 43.2% | 29.9% | 33.0% |
| AgentMath-Qwen2.5-7B | 24.9% | 37.4% | 45.6% | 32.5% | 35.1% |
| AgentMath-Qwen3-8B | 28.3% | 39.8% | 49.5% | 33.8% | 37.9% |
| Frontier Models (30B–32B) | | | | | |
| DeepSeek-R1-Distill-Qwen-32B | 17.2% | 25.1% | 33.0% | 22.5% | 24.4% |
| Qwen3-30B-A3B-Instruct-2507 | 27.8% | 29.9% | 36.2% | 27.4% | 30.3% |
| AM-Thinking-v1-32B | 27.9% | 36.2% | 50.1% | 29.2% | 35.8% |
| Qwen3-30B-A3B-Thinking-2507 | 34.7% | 44.3% | 53.2% | 33.3% | 41.4% |
| AgentMath-30B-A3B | 43.4% | 40.0% | 69.6% | 51.9% | 51.2% |
| Frontier Models (¿32B) | | | | | |
| DeepSeek V3 | 39.0% | 26.0% | 35.0% | 48.0% | 37.0% |
| Kimi-K2-Instruct | 45.6% | 31.1% | 49.3% | 56.9% | 45.8% |
| Qwen3-235B | 57.6% | 37.5% | 57.6% | 62.3% | 53.8% |
| AgentMath-235B-A22B-SFT | 49.4% | 43.2% | 73.5% | 55.3% | 55.4% |
| DeepSeek R1 | 65.0% | 40.0% | 73.0% | 65.0% | 60.8% |

- On the more challenging Google-IMO-AnswerBench, AgentMath-Llama-8B achieves 25.2%, outperforming DeepSeek-R1-Distill-Llama3.1-8B (16.6%), while AgentMath-Qwen2.5-7B (35.1%) also exceeds OpenReasoning-Nemotron-7B (33.0%).

Therefore, by leveraging base models released in 2024 (Qwen2.5-7B-Base and Llama3.1-8B-Base), AgentMath demonstrates consistent and leading performance across multiple mathematical reasoning benchmarks released in 2025 (AIME25, HMMT25, and IMO-AnswerBench). These results not only eliminate data contamination risks but also establish the robustness and reliability of our model.

**(3) Systematic Comparison of SFT and RL Improvements on Non-Contaminated Evaluation Benchmarks**

To rigorously evaluate the independent contributions of SFT and RL in AgentMath while mitigating potential data contamination, we conduct systematic comparisons exclusively on benchmarks confirmed to be released after the pre-training cutoff date of their corresponding backbone models, as shown in the table 16 and table 17:

- For Llama3.1-8B-Base and Qwen2.5-7B-Base, we report results on AIME25, HMMT25, and Google-IMO-AnswerBench;
- For Qwen3-1.7B-Base, Qwen3-8B-Base, and Qwen3-30B-A3B-Instruct-2507, we report results on Google-IMO-AnswerBench only.

The results reveal consistent improvements across all base models. Based on Llama3.1-8B-Base, AgentMath-Llama-8b-SFT achieves an average score of 39.2% across the three benchmarks (AIME25, HMMT25, and Google-IMO-AnswerBench), while AgentMath-Llama-8b-RL reaches 48.2%. Based on Qwen2.5-7B-Base, AgentMath-Qwen2.5-7B-SFT attains 49.6%, with AgentMath-Qwen2.5-7B-RL achieving 60.3%.

Table 14: Performance of AgentMath on AIME24/25, and HMMT25 based on Llama3.1-8B-Base and Qwen2.5-7B-Base. Our model (highlighted in blue) is compared against other leading models, with accuracy (avg@32) as the evaluation metric.

| Models | Base Model | Tool Use | AIME25 | HMMT25 |
|---|---|---|---|---|
| Based on Llama3.1-8B-Base/Instruct | | | | |
| DeepSeek-R1-Distill-Llama-8B | Llama-3.1-8B-Base | ✗ | 28.7 | 13.8 |
| Llama3.1-Nemotron-Nano-8B-v1 | Llama-3.1-8B-Instruct | ✗ | 48.0 | 26.7 |
| AgentMath-Llama-8B | Llama-3.1-8B-Base | ✓ | 66.2 | 53.1 |
| Based on Qwen2.5-7B-Base/Instruct | | | | |
| ZeroTIR-7B | Qwen-2.5-7B-Base | ✓ | 30.0 | 22.5 |
| SimpleTIR-7B | Qwen2.5-7B-Base | ✓ | 30.9 | 29.7 |
| DeepSeek-R1-Distill-Qwen-7B | Qwen2.5-Math-7B-Base | ✗ | 39.7 | 16.3 |
| OpenR1-Distill-7B | Qwen2.5-Math-7B-Base | ✗ | 39.7 | 25.7 |
| Light-R1-7B-DS | DeepSeek-R1-Distill-Qwen-7B | ✗ | 44.3 | 27.6 |
| AReal-boba-7B | DeepSeek-R1-Distill-Qwen-7B | ✗ | 48.3 | 29.4 |
| Skywork-OR1-7B | DeepSeek-R1-Distilled-Qwen-7B | ✗ | 54.6 | 35.7 |
| AceReason-Nemotron-1.1-7B | DeepSeek-R1-Distill-Qwen-7B | ✗ | 64.8 | 42.9 |
| OpenReasoning-Nemotron-7B | Qwen2.5-7B-Instruct | ✗ | 78.2 | 63.5 |
| AgentMath-Qwen2.5-7B | Qwen2.5-7B-Base | ✓ | 79.8 | 65.9 |

Table 15: Performance of AgentMath on Google-IMO-AnswerBench based on Llama3.1-8B-Base and Qwen2.5-7B-Base. Our model (highlighted in blue) is compared against other leading models, with accuracy (avg@8) as the evaluation metric.

| Model (Google-IMO-AnswerBench) | Base Model | Algebra | Combinatorics | Geometry | Number Theory | Avg Score |
|---|---|---|---|---|---|---|
| Based on Llama3.1-8B-Base | | | | | | |
| DeepSeek-R1-Distill-Llama3.1-8B | Llama3.1-8B-Base | 10.2% | 17.4% | 21.6% | 17.0% | 16.6% |
| AgentMath-Llama-8b | Llama3.1-8B-Base | 18.8% | 24.6% | 33.7% | 23.7% | 25.2% |
| Based on Qwen2.5-7B Base/Instruct | | | | | | |
| OpenReasoning-Nemotron-7B | Qwen2.5-7B -Instruct | 23.6% | 35.2% | 43.2% | 29.9% | 33.0% |
| AgentMath-Qwen2.5-7B | Qwen2.5-7B -Base | 24.9% | 37.4% | 45.6% | 32.5% | 35.1% |

Based on Qwen3-series, we observe similar trends on Google-IMO-AnswerBench: Based on Qwen3-1.7B-Base, AgentMath-Qwen3-1.7B-SFT scores 11.7% while AgentMath-Qwen3-1.7B-RL scores 20.3%; Based on Qwen3-8B-Base, AgentMath-Qwen3-8B-SFT scores 28.8% while AgentMath-Qwen3-8B-RL scores 37.9%; Based on Qwen3-30B-A3B-Instruct-2507, AgentMath-Qwen3-30B-A3B-SFT scores 43.5% while AgentMath-Qwen3-30B-A3B-RL scores 51.2%.

These results demonstrate that tool-augmented SFT substantially enhances mathematical reasoning capabilities across all base models, while RL consistently delivers an additional 7%–10% performance gain over SFT.

Table 16: The SFT and RL performance of AgentMath on AIME25, HMMT25, Google-IMO-AnswerBench based on Llama3.1-8B-Base and Qwen2.5-7B-Base.

| Model | Base Model | AIME25 | HMMT25 | Google-IMO-AnswerBench | Avg Score |
|---|---|---|---|---|---|
| Based on Llama3.1-8B-Base | | | | | |
| AgentMath-Llama-8b-SFT | Llama3.1-8B-Base | 53.5% | 45.8% | 18.3% | 39.2% |
| AgentMath-Llama-8b-RL | AgentMath-Llama-8b-SFT | 66.2% | 53.1% | 25.2% | 48.2% |
| Based on Qwen2.5-7B Base | | | | | |
| AgentMath-Qwen2.5-7B-SFT | Qwen2.5-7B -Base | 66.4% | 55.1% | 27.3% | 49.6% |
| AgentMath-Qwen2.5-7B-RL | AgentMath-Qwen2.5-7B-SFT | 79.8% | 65.9% | 35.1% | 60.3% |

In summary, we mitigate potential benchmark contamination through both temporal controls, utilizing a latest high-difficulty benchmark (Google IMO-AnswerBench, November 2025) with earlier pre-trained base models (Llama3.1-8B-Base and Qwen2.5-7B-Base, 2024) and model diversity, validating across architectures spanning 1.7B to 30B parameters. The consistent and substantial performance improvements across all configurations validate the effectiveness of our tool-augmented data synthesis method and large-scale reinforcement learning on ultra-long sequences with massive tool-calls, while confirming the reliability and robustness of our model.

Table 17: The SFT and RL performance of AgentMath on AIME25, HMMT25, Google-IMO-AnswerBench based on Qwen3-series base model (1.7B, 8B, 30B).

| Model | Base Model | Google-IMO-AnswerBench |
|---|---|---|
| | Based on Qwen3-1.7B-Base | |
| AgentMath-Qwen3-1.7B-SFT | Qwen3-1.7B-Base | 11.7% |
| AgentMath-Qwen3-1.7B-RL | AgentMath-Qwen3-1.7B-SFT | 20.3% |
| | Based on Qwen3-8B-Base | |
| AgentMath-Qwen3-8B-SFT | Qwen3-8B-Base | 28.8% |
| AgentMath-Qwen3-8B-RL | AgentMath-Qwen3-8B-SFT | 37.9% |
| | Based on Qwen3-30B-A3B-Instruct-2507 | |
| Qwen3-30B-A3B-Instruct-2507 | Qwen3-30B-A3B-Base | 30.3% |
| AgentMath-Qwen3-30B-A3B-SFT | Qwen3-30B-A3B-Instruct-2507 | 43.5% |
| AgentMath-Qwen3-30B-A3B-RL | AgentMath-Qwen3-30B-A3B-SFT | 51.2% |

## A.12 Training-testing overlap: The authors report 346k training questions for SFT and 42k for RL, while the total number of testing questions is under 100. It is questionable whether the training data already contains components or similar structures to the test questions. Although an n-gram filtering algorithm is mentioned, the specific implementation details are missing. Have the authors performed ablation studies to evaluate the effect of training data volume on test performance?

Q1: It is questionable whether the training data already contains components or similar structures to the test questions. Although an n-gram filtering algorithm is mentioned, the specific implementation details are missing.

To rigorously prevent data contamination, we employed a three-stage progressive deduplication pipeline as follows:

**Stage 1: Problem-level Exact Deduplication**

We remove all training samples whose problem statements are exact matches with those in the test sets by string matching.

**Stage 2: 4-gram + MinHash LSH Similarity-based Deduplication**

To further eliminate problems with highly similar surface forms, we employ a combination of 4-gram analysis and MinHash LSH:

- **4-gram construction:** For each problem, we construct a n-gram (n=4) set by first tokenizing the text (word-level tokenization for English; Jieba tokenizer for Chinese) and then extracting all consecutive 4-token sequences.
- **Similarity measurement:** For any test problem $A$ and training problem $B$, we compute the Jaccard similarity of their 4-gram sets:
$$J(A, B) = \frac{|A \cap B|}{|A \cup B|}$$
where $J(A, B) \in [0, 1]$, with higher values indicating greater n-gram-level similarity.
- **Filtering criterion:** We set the Jaccard similarity threshold at **0.6**. Training samples with Jaccard similarity exceeding 0.6 relative to any test problem are removed from the training set.
- **Computational optimization:** To efficiently handle large-scale deduplication, we employ MinHash LSH, which uses hash functions to map MinHash signatures into buckets. This enables similar texts to be clustered together, transforming the problem from global pairwise comparisons into localized bucket-wise searches and substantially reducing computational complexity.
- **Implementation:** This procedure is implemented using NLTK and the MinHashLSH module from the datasketch library.

**Stage 3: Semantic Embedding-based Deduplication**

To account for problems that exhibit substantial lexical differences yet remain semantically similar, we perform an additional semantic deduplication step:

- We generate embeddings for all problem texts in both training and test sets using the gte-large model.
- We compute semantic similarity (cosine similarity) between each test problem and all training problems using the sentence_transformers library.
- For each test problem, we rank all training problems by descending similarity and remove the **top 5** most semantically similar training samples.

Through this comprehensive three-stage pipeline (exact matching + n-gram/LSH-based filtering + semantic embedding-based filtering), we removed approximately **8.3K** samples from the training set. This rigorous deduplication ensures that AgentMath's SFT and RL training data contain no overlapping or highly similar samples with respect to any evaluation benchmark (AIME24, AIME25, HMMT25), thereby effectively preventing data contamination and guaranteeing the reliability and integrity of our evaluation results.

Q2: Have the authors performed ablation studies to evaluate the effect of training data volume on test performance?

Regarding the scaling law of SFT training data, we conducted systematic scalability experiments using the Qwen3-8B-Base model. As shown in the table 18, when the training data scales from 2k to 300k, the model exhibits significant and consistent performance gains across all benchmarks:

- **AIME24**: Accuracy increases from 27.2% to 78.4%
- **AIME25**: Accuracy increases from 21.1% to 72.2%
- **Google-IMO-AnswerBench**: Accuracy increases from 5.3% to 28.8%
- **Overall Average**: Performance improves from 17.9% to 59.8% (+41.9%)

These results demonstrate that our proposed tool-augmented data synthesis approach exhibits strong scalability and effectiveness.

Table 18: Performance across benchmarks about the scaling law of SFT training data.

| SFT Training Data Volume | AIME24 | AIME25 | Google-IMO-AnswerBench | Avg Score |
|---|---|---|---|---|
| AgentMath-8B-SFT-2k | 27.2 | 21.1 | 5.3 | 17.9 |
| AgentMath-8B-SFT-20k | 60.5 | 53.3 | 12.8 | 42.2 |
| AgentMath-8B-SFT-40k | 66.8 | 57.9 | 17.6 | 47.4 |
| AgentMath-8B-SFT-80k | 69.2 | 61.8 | 21.4 | 50.8 |
| AgentMath-8B-SFT-160k | 73.8 | 66.4 | 25.6 | 55.3 |
| AgentMath-8B-SFT-300k | 78.4 | 72.2 | 28.8 | 59.8 |

(2) Regarding the scaling law of RL training data, we conducted systematic scalability experiments based on the best-performing AgentMath-8B-SFT-300k model. To ensure fair comparison, all experiments were conducted using the same number of training steps (200 steps) and hyperparameter configurations, varying only the RL training data size (10k, 20k, 30k, 42k).

As shown in the table 19, when the RL training data scales from 10k to 42k, the model demonstrates consistent improvements across all benchmarks:

- **AIME24**: Accuracy increases from 80.8% to 85.3%
- **AIME25**: Accuracy increases from 75.5% to 80.4%
- **Google-IMO-AnswerBench**: Accuracy increases from 30.9% to 34.7%
- **Overall Average**: Performance improves from 62.4% to 66.8%

These results demonstrate the effectiveness and scalability of our RL training data.

Table 19: Performance across benchmarks about the scaling law of RL training data.

| RL Training Data Volume | AIME24 | AIME25 | Google-IMO-AnswerBench | Avg Score |
|---|---|---|---|---|
| AgentMath-8B-SFT-300k | 78.4 | 72.2 | 28.8 | 59.8 |
| AgentMath-8B-RL-10k | 80.8 | 75.5 | 30.9 | 62.4 |
| AgentMath-8B-RL-20k | 82.7 | 77.8 | 32.4 | 64.3 |
| AgentMath-8B-RL-30k | 84.2 | 79.0 | 33.7 | 65.6 |
| AgentMath-8B-RL-42k | 85.3 | 80.4 | 34.7 | 66.8 |

In summary, combining the scaling law experiments from both the SFT and RL stages, we demonstrate that as the tool-augmented training data size increases, AgentMath exhibits sustained and consistent performance improvements across all evaluation benchmarks, further validating the strong scalability of AgentMath.

## A.13 Unclear heuristic data synthesis: The data synthesis process involves multiple human heuristics (e.g., computational component segmentation, code complexity filtering), and several components appear to require iterative manual adjustment. These steps may limit scalability to new benchmarks or domains. Moreover, the data synthesis and cleaning costs seem high given the repeated use of LLMs.

Q1: Unclear heuristic data synthesis: The data synthesis process involves multiple human heuristics (e.g., computational component segmentation, code complexity filtering), and several components appear to require iterative manual adjustment.

**1. Computational Component Segmentation.** This strategy segments each long chain-of-thought response generated by DeepSeek-R1 into fixed-length chunks (e.g., 3k tokens), yielding $N$ segments $(S_1, S_2, S_3, \ldots, S_N)$. We then use DeepSeek-V3-0324 to independently perform tool-augmented rewriting on each segment. In our 346k-example synthetic SFT dataset, responses have an average length of 18.3k tokens; thus, each response is on average split into 6 segments.

**Motivation.** In early experiments, we attempted to rewrite the full DeepSeek-R1 response without segmentation. This led to several issues:

- DeepSeek-R1 responses are excessively long.
- The instruction-following ability of DeepSeek-V3-0324 degrades markedly under ultra-long inputs, and the model becomes more prone to hallucinations.
- Consequently, the rewritten data exhibits a low frequency of tool usage, a high code execution failure rate, and extensive abbreviation or omission of intermediate natural language reasoning steps (which we refer to as the "textual reasoning omission rate").

To quantitatively assess the effect of segment length on data quality and downstream performance, we conducted controlled experiments on 20k synthetic examples and performed SFT on Qwen3-8B-Base. As shown in the table 20, the results are summarized below:

- **No segmentation (AgentMath-SFT-20k-No-Segment):** The average number of tool calls is 1.6; the code execution failure rate is 31.8%; the textual reasoning omission rate (the proportion of intermediate reasoning steps omitted) is 78.5%; and AIME24/AIME25 accuracies are 40.3%/35.6%.
- **Segmentation with 9k tokens (AgentMath-SFT-Segment-with-9k-token):** This setting improves over no segmentation, but segments remain relatively long, so tool usage and evaluation performance are still limited.
- **Segmentation with 3k tokens (AgentMath-SFT-Segment-with-3k-token):** The average number of tool calls increases to 7.8; the code execution failure rate drops to 6.2%; the textual reasoning omission rate decreases to 2.3%; and AIME24/AIME25 accuracies reach 60.5%/53.3%.

- **Segmentation with 2k tokens (AgentMath-SFT-Segment-with-2k-token):** Although the number of tool calls further increases, downstream performance does not improve significantly and appears to saturate.

Based on this analysis, we adopt a 3k-token segment length as the default configuration for computational component segmentation, as it strikes a favorable balance: it effectively controls data-quality metrics while maximizing downstream task performance.

Table 20: Results on 20k AgentMath synthetic data about Computational Component Segmentation.

| 20k AgentMath synthetic data | Mean Tool Calls | Code Execution Failure Rate | Textual Reasoning Omission Rate | AIME24 Acc | AIME25 Acc |
|---|---|---|---|---|---|
| AgentMath-SFT-20k-No-Segment | 1.6 | 31.8% | 78.5% | 40.3% | 35.6% |
| AgentMath-SFT-Segment-with-9k-token | 2.1 | 28.4% | 67.9% | 44.8% | 38.7% |
| AgentMath-SFT-Segment-with-6k-token | 3.2 | 23.3% | 38.6% | 49.2% | 44.3% |
| AgentMath-SFT-Segment-with-4k-token | 5.7 | 12.5% | 8.8% | 57.3% | 51.6% |
| AgentMath-SFT-Segment-with-3k-token | 8.3 | 6.2% | 2.3% | 60.5% | 53.3% |
| AgentMath-SFT-Segment-with-2k-token | 10.1 | 5.9% | 2.1% | 59.4% | 51.9% |

**2. Code Complexity Filtering:** At an early stage, we conducted a statistical analysis of code-length distributions over 20k synthetic instances. The results showed that samples with fewer than 5 lines of code constituted 5% of the dataset, with exactly 5 lines representing 7%, 6 lines 13%, 7 lines 24%, 8 lines 29%, 9 lines 13%, and 10 or more lines comprising 10%. To investigate the relationship between code complexity and line count, we performed stratified uniform sampling, drawing 40 samples from each line-count category (280 samples total). Three authors independently annotated each sample's complexity as "Easy," "Medium," or "Hard" based on whether it involved computationally demanding operations (e.g., large-number arithmetic, complex equation solving, advanced linear algebra, combinatorial computations, or calculus). The annotation statistics are presented in the table 21.

Our analysis shows that among samples with $\leq 5$ lines of code, over 65% were labeled "Easy" while fewer than 10% were labeled "Hard." To prevent the model from learning to overuse tool invocations during training, we conservatively filtered out all samples containing 5 or fewer lines of code. In future work, we plan to employ LLMs such as Qwen3-30B for automated complexity assessment, replacing manual annotation to improve both objectivity and scalability of our filtering pipeline.

Table 21: the statistics of code complexity by lines of code.

| Lines of Code | Easy (%) | Medium (%) | Hard (%) |
|---|---|---|---|
| $<5$ lines | 87% | 9% | 4% |
| $=5$ lines | 66% | 27% | 7% |
| $=6$ lines | 43% | 38% | 19% |
| $=7$ lines | 24% | 49% | 27% |
| $=8$ lines | 13% | 56% | 31% |
| $=9$ lines | 7% | 51% | 42% |
| $\geq 10$ lines | 4% | 43% | 53% |

Q2: These steps may limit scalability to new benchmarks or domains.

In response, we have extended AgentMath's automated data synthesis and cleaning pipeline to non-mathematical domains, including physics, chemistry, and biology, and evaluated the resulting model on the GPQA Diamond benchmark. GPQA Diamond assesses large language models' ability to solve graduate-level problems across biology, physics, and chemistry—a highly challenging benchmark where even PhD-level domain experts achieve only 65% accuracy.

We randomly sampled 40K examples from the open-source Science 220K dataset released by AM-Thinking and applied AgentMath's data synthesis method. Specifically, we segmented DeepSeek-R1's reasoning response into 3K-token chunks and transformed them into tool-augmented reasoning chains by replacing complex, error-prone computational steps with executable code. We then applied our automated cleaning pipeline, which includes: (1) filtering examples with $\leq 5$ lines of code, (2) correcting formatting errors, (3) removing samples with failed code execution, and (4) performing environmental feedback alignment to ensure consistency.

Using Qwen3-8B-Base as the foundation model, we conducted SFT and evaluated performance on GPQA across 8 independent runs, reporting the average accuracy (Avg@8). As shown in the table 22, AgentMath-8B-SFT-40k achieves 58.9% accuracy on GPQA, substantially outperforming DeepSeek-R1-Distill-Qwen-7B (49.1%). These results demonstrate that AgentMath's tool-augmented synthesis approach and automated cleaning pipeline generalize effectively beyond mathematics to scientific domains (physics, chemistry, and biology), highlighting the scalability and broad applicability of our method.

Table 22: The GPQA accuracy of different models and AgentMath-8B models at the 7B-8B scale.

| Model | Base Model | GPQA Acc |
|---|---|---|
| OpenThinker-7B | Qwen2.5-7B-Instruct | 42.4% |
| AReaL-boba-RL-7B | DeepSeek-R1-Distill-Qwen-7B | 47.6% |
| DeepSeek-R1-Distill-Qwen-7B | Qwen2.5-Math-7B | 49.1% |
| Light-R1-7B | DeepSeek-R1-Distill-Qwen-7B | 49.4% |
| AgentMath-8B-SFT-40k | Qwen3-8B-Base | 58.9% |

Q3: Moreover, the data synthesis and cleaning costs seem high given the repeated use of LLMs.

We build upon the open-source AM-Thinking dataset, leveraging their existing responses generated by DeepSeek-R1-0528 to obtain 346K data samples. We employ DeepSeek-V3 for data synthesis, completing this process on 128 GPUs (each with 96GB memory) in approximately 62 hours. We then utilize Qwen3-30B as a judge model to verify consistency between actual code execution results and model-simulated outputs, requiring approximately 3 hours.

Subsequently, we perform SFT on the 316K synthetic samples using Qwen3-8B-Base as the base model, which takes approximately 44 hours. In total, the complete pipeline—encompassing data synthesis, cleaning, verification, and SFT training, requires approximately $62 + 3 + 44 = 109$ hours.

Notably, we also explore a more cost-effective alternative to address computational overhead. As illustrated in Figure 4, we apply SFT to only 20K samples starting from Qwen3-8B-Base, followed by 400 steps of large-scale reinforcement learning. This streamlined approach enables our AgentMath model to achieve the leading performance: 76.2% on AIME24 and 67.5% on AIME25, surpassing both OpenMath-Nemotron-7B (74.8% and 61.2%, respectively) and Qwen3-8B-Thinking (76.0% and 67.3%, respectively). This entire workflow, including data synthesis, cleaning, SFT, and RL training, requires only 76 hours total, providing a substantially more efficient solution.

### A.14 The paper does not clarify how textual answers are segmented into computational parts or how the model determines when code usage is beneficial. Different models may prefer distinct code-usage patterns even for the same question.

Q1: The paper does not clarify how textual answers are segmented into computational parts

We utilized the long chain-of-thought responses generated by DeepSeek-R1 from the open-source AM-Thinking dataset. Each response is segmented into fixed-length 3k-token chunks, yielding $N$ segments $(S_1, S_2, S_3, \ldots, S_n)$. Across the 316k SFT synthetic data, the responses have an average length of 16.9k tokens, corresponding to roughly six segments per response.

Subsequently, for each segment, we applied the Tool-Augmented Data Synthesis Prompt detailed in Appendix A.6.2. We employed DeepSeek-V3-0324 to independently transform each segment by replacing complex and error-prone computational processes with executable code.

To accelerate the synthesis process, we initially instructed DeepSeek-V3-0324 to simulate code execution results based on the textual reasoning context. During post-processing, we replaced these simulated results with actual code execution outputs and employed Qwen3-30B as a judge model to assess their consistency. Samples exhibiting inconsistencies were filtered out to ensure data quality.

Q2: how the model determines when code usage is beneficial.

We present the design of the Tool-Augmented Data Synthesis Prompt in Appendix A.6.2. This prompt guides DeepSeek-V3-0324 to first identify complex and error-prone computational processes, and then replace these manual calculations with code. Specifically, it covers the following types of computational tasks:

- **Complex Symbolic Algebra**: polynomial expansion, factorization, equation solving
- **Advanced Calculus**: differentiation, integration, definite integral computation
- **Probability and Combinatorics**: complex counting problems, probability distribution calculations
- **Linear Algebra**: matrix operations, matrix inversion, eigenvalue decomposition
- **Numerical Computation**: approximation calculations, large number arithmetic, geometric calculations
- **Other Error-Prone or Computation-Intensive Problems**

To control code complexity and ensure the reliability of the synthesized data, we further filter out low-complexity samples with $\leq 5$ lines of code. Furthermore, we randomly sampled 100 instances from the synthesized data and manually annotated whether DeepSeek-V3 effectively replaced complex textual computational processes with code. Results show that code replacement is beneficial and reasonable in 84% of the samples, thereby confirming the reliability of our proposed tool-augmented data synthesis approach.

Q2: What criteria or metrics determine whether using code is more effective for a given part of the reasoning chain?

Below, we demonstrate the effectiveness of code-augmented methods in replacing manual complex computations from two perspectives.

We randomly sampled 100 instances from the synthetic data and annotated whether DeepSeek-V3 effectively employs code to replace manual complex computations based on the following criteria. The evaluation reveals that code-based computation proves more effective in 84% of cases. The evaluation criteria encompass the following mathematical domains:

- Complex symbolic algebra: polynomial expansion, factorization, equation solving
- Advanced calculus: differentiation, integration, definite integral computation
- Complex probability and combinatorics: complex counting, probability distributions
- Complex linear algebra: matrix operations, matrix inversion, eigenvalue decomposition
- Complex numerical computation: approximation, large number arithmetic, geometric calculations
- Any error-prone or computationally intensive operations

As shown in the table 23, we systematically compare code-based and pure text-based reasoning along two dimensions: inference efficiency (measured by average token count) and performance metricx.

- **Token Analysis on Synthetic Data**: The SFT training dataset comprises 316k instances in total. Pure text-based reasoning averages 18.3k tokens per sample, while tool augmentation reduces this to 16.9k tokens. This demonstrates that substituting code for lengthy computational processes effectively reduces overall token consumption.
- **SFT stage**: We comprehensively compare the efficiency and performance of code augmentation against pure text-based reasoning. Specifically, when trained on identical 20k SFT data, AgentMath-SFT-20k achieves accuracies of 60.5% and 53.3% on AIME24 and AIME25, respectively, significantly outperforming Text-based-SFT-20k (57.1% and 49.2%). Additionally, AgentMath-SFT-20k reduces the average token count by approximately 1.3k–3k compared to Text-based-SFT-20k.
- **RL stage**: In tool-augmented RL training, using only 440 steps, AgentMath-RL-440-steps improves accuracy from 60.5% to 76.2% on AIME24 and from 53.3% to 67.5% on AIME25. In contrast, pure text-based RL training requires 1600 steps (Text-based-RL-1600-steps) to achieve improvements from 57.1% to 68.7% on AIME24 and from 49.2% to

57.5% on AIME25. These results demonstrate that the code-augmented approach achieves approximately $4\times$ higher training efficiency while reducing the overall token count by 2.5k–5k compared to Text-based-RL-1600-steps.

In summary, introducing code augmentation in both SFT and RL stages yields substantial improvements in performance and efficiency over pure text-based reasoning, thereby validating that using code is more effective for a given part of the reasoning chain.

Table 23: Accuracy and average inference token usage on AIME24 and AIME25 for pure text-based models and code-augmented AgentMath at both SFT and RL stages.

| Model | Base Model | AIME24 Acc | AIME24 Avg Tokens | AIME25 Acc | AIME25 Avg Tokens |
|---|---|---|---|---|---|
| Text-based-SFT-20k | Qwen3-8B-Base | 57.1% | 29k | 49.2% | 28k |
| AgentMath-SFT-20k | Qwen3-8B-Base | 60.5% | 26k | 53.3% | 26.7k |
| Text-based-RL-1600-steps | Text-based-SFT-20k | 68.7% | 32.3k | 57.5% | 31.2k |
| AgentMath-RL-440-steps | AgentMath-SFT-20k | 76.2% | 27.2k | 67.5% | 28.6k |

Q3: Different models may prefer distinct code-usage patterns even for the same question.

We agree that different models can prefer different code usage patterns for the same question, including variations in code injection positions, line counts, and code implementation details.

In our early experiments, we conducted a comparative study between two candidate teacher models: DeepSeek-V3-0324 and Qwen3-235B-Instruct-2507. Specifically, we synthesized training data using each model on the 20k training set and performed supervised fine-tuning on Qwen3-8B-Base. As shown in Table 24, the experimental results are as follows:

- Data synthesized by DeepSeek-V3-0324 averaged 6.5 tool calls per sample, compared to 5.3 tool calls per sample for Qwen3-235B-Instruct-2507.
- On the AIME24 and AIME25 benchmarks, the model trained on DeepSeek-V3-0324-synthesized data (AgentMath-20k-SFT-DeepSeek-V3) achieved accuracies of 60.5% and 53.3%, respectively, marginally outperforming the model trained on Qwen3-235B-Instruct-2507-synthesized data (59.3% and 51.7%). Notably, the former also demonstrated a higher average tool call frequency.

Based on these comprehensive performance results, we selected DeepSeek-V3-0324 as the teacher model for our data synthesis pipeline.

## A.15 The dataset synthesis employs larger teacher models (DeepSeek R1 and V3, Qwen-30B). This may imply knowledge distillation from more powerful teacher models. Comparing such distilled models with those trained without teacher guidance may be unfair.

Q1: The dataset synthesis employs larger teacher models (DeepSeek R1 and V3, Qwen-30B). This may imply knowledge distillation from more powerful teacher models. Comparing such distilled models with those trained without teacher guidance may be unfair.

To ensure a rigorous and fair comparison, we strictly followed the experimental setup of Retool, controlling for all key factors: the same 2k synthetic dataset, identical teacher model responses from DeepSeek-R1, the same base model (Qwen2.5-32B-Instruct), and 400 training steps during the RL phase. The sole difference lies in the data synthesis strategy: AgentMath leverages our proposed tool-augmented data synthesis method in Appendix A.6.2, whereas Retool employs its original synthesis prompt. Both approaches undergo identical two-stage training comprising SFT and RL. As shown in the table 25, the experimental results are summarized as follows:

- AgentMath-32B-SFT-2k achieves 44.1% on AIME24 and 37.3% on AIME25, surpassing Retool-32B-SFT-2k (40.9% and 34.5%, respectively), thereby demonstrating the effectiveness of our tool-augmented data synthesis approach;
- AgentMath-32B-RL attains 74.8% on AIME24 and 56.6% on AIME25, consistently outperforming Retool-32B-RL (67.0% and 49.3%, respectively), further validating the superiority of our reinforcement learning training strategy.

Table 24: Comparison of Qwen3-8B-Base models fine-tuned on the 20k AgentMath SFT dataset synthesized by DeepSeek-V3-0324 and Qwen3-235B-Instruct-2507. We report AIME24 and AIME25 accuracies (%) and the average number of tool calls per problem on each benchmark.

| Model | AIME24 | AIME24 Tool Calls Avg | AIME25 | AIME25 Tool Calls Avg |
|---|---|---|---|---|
| AgentMath-20k-SFT-DeepSeek-V3 | 60.5% | 5.1 | 53.3% | 5.7 |
| AgentMath-20k-SFT-Qwen3-235B-Instruct-2507 | 59.3% | 4.4 | 51.7% | 5.0 |

In summary, AgentMath exhibits consistent and substantial performance gains across both training stages, confirming the efficacy and robustness of our proposed method.

Table 25: Comparison of AgentMath and Retool performance under the same experimental setup in both the SFT and RL stages.

| Model | AIME24 Acc | AIME25 Acc |
|---|---|---|
| Retool-32B-SFT-2k | 40.9% | 34.5% |
| AgentMath-32B-SFT-2k | 44.1% | 37.3% |
| Retool-32B-RL | 67.0% | 49.3% |
| AgentMath-32B-RL | 74.8% | 56.6% |

Q2: Would the performance gap shrink if competing models were also allowed to distill from comparable teacher models?

We adopted the open-source dataset from AM-Thinking, using the same 316k prompts and responses generated by DeepSeek-R1. We conducted supervised fine-tuning (SFT) on the Qwen3-8B-Base model for 6 epochs with a learning rate of 6e-5. To ensure experimental rigor, all configurations were kept identical except for the core difference in reasoning chain types: AM-Thinking uses pure textual reasoning chains, while AgentMath employs tool-augmented reasoning chains. We conducted 8 independent training runs and report pass@1 results from the checkpoint with the best validation performance.

As shown in Table 26, AgentMath-8B-SFT achieves 78.4% accuracy on AIME24 and 72.2% accuracy on AIME25, outperforming AM-Thinking-8B-SFT (74.9% and 67.4%, respectively), with an overall average performance gap of 4.1%. These results confirm that the performance gap will shrink if competing models were also allowed to distill from comparable teacher models.

Table 26: Comparison of pass@1 accuracy on AIME24 and AIME25 for AM-Thinking-8B-SFT and AgentMath-8B-SFT under the same training settings.

| Model | AIME24 Acc | AIME25 Acc | Avg Score |
|---|---|---|---|
| AM-Thinking-8B-SFT | 74.9% | 67.4% | 71.2% |
| AgentMath-8B-SFT | 78.4% | 72.2% | 75.3% |

## A.16 Reward Design in RL

Our reward function consists of two components: an answer correctness reward $R_{\text{acc}}$ and a tool usage efficiency reward $R_{\text{tool}}$. The correctness reward $R_{\text{acc}}$ provides binary (0,1) feedback based on mathematical equivalence (verified using the math_verify library):

$$R_{\text{acc}} = \begin{cases} 1, & \text{if is\_equivalent}(\hat{a}, a), \\ 0, & \text{otherwise,} \end{cases}$$

where $\hat{a}$ denotes the predicted answer and $a$ the ground truth answer. Conditioned on answer correctness, the tool usage reward $R_{\text{tool}}$ incentivizes efficient utilization of computational resources:

$$R_{\text{tool}} = \min\bigl(R_{\max},\, \alpha + \beta \cdot N_{\text{code}}\bigr) \quad \text{if } N_{\text{code}} > 0,$$

where $\alpha$ is the base tool usage reward, $\beta$ is the scaling factor for the number of invocations, and $R_{\text{max}}$ is the reward upper bound. The total reward function is defined as:

$$R_{\text{total}} = R_{\text{acc}} + \mathbb{I}(R_{\text{acc}} = 1) \cdot R_{\text{tool}}.$$

In our work, we set $\alpha = 0.1$ and $\beta = 0.01$, and constrain the maximum tool reward to $R_{\text{max}} = 1$, which encourages tool usage while preventing over-reliance. This design is motivated by the following considerations: applying $R_{\text{tool}}$ only to correct answers encourages the model to use tools appropriately to arrive at accurate solutions, avoiding rewarding erroneous tool invocations; $\alpha = 0.1$ differentiates between cases with and without tool usage, while the smaller $\beta = 0.01$ accommodates high-frequency tool calls during RL training (some exceeding 64 invocations), preventing reward inflation.

In early experiments, to validate the effectiveness of the reward design, we conducted controlled experiments using the SFT model trained on 20k synthetic data (AgentMath-SFT-20k), with a fixed 100 training steps, as shown in the table 27. Our experiments demonstrate:

- **Effectiveness of tool rewards:** Introducing tool rewards (all answers) outperforms the no-tool-reward baseline in both average accuracy (61.4% vs. 60.2%) and average tool calls (6.2 vs. 5.7), indicating that tool rewards effectively incentivize the model to leverage computational tools and improve performance.
- **Advantage of tool rewards (correct answers only):** Furthermore, compared to tool rewards (all answers), applying tool rewards exclusively to correct answers ($\alpha = 0.1, \beta = 0.01$) achieves the best performance in both average accuracy (62.6% vs. 61.4%) and average tool calls (6.3 vs. 6.2).
- **Optimal hyperparameter configuration:** In a grid search over $\alpha \in \{0.1, 0.2\}$ and $\beta \in \{0.01, 0.02\}$, $\alpha = 0.1, \beta = 0.01$ achieves the best accuracy-efficiency trade-off (62.6% average accuracy, 6.3 average tool calls).

Therefore, based on performance and tool call metrics, we ultimately adopt the correctness-conditioned tool reward design with parameters $\alpha = 0.1$ and $\beta = 0.01$ for RL training.

Table 27: Ablation study results on reinforcement learning reward design.

| **Reward Configuration** | **AIME24 Accuracy** | **AIME24 Tool Calls** | **AIME25 Accuracy** | **AIME25 Tool Calls** | **Avg. Accuracy** | **Avg. Tool Calls** |
|---|---|---|---|---|---|---|
| AgentMath-SFT-20k (Baseline) | 60.5% | 5.1 | 53.3% | 5.7 | 56.9% | 5.4 |
| RL with No tool reward | 65.2% | 5.5 | 55.1% | 5.9 | 60.2% | 5.7 |
| RL with Tool reward (all answers), $\alpha = 0.1$, $\beta = 0.01$ | 66.4% | 6.1 | 56.3% | 6.3 | 61.4% | 6.2 |
| **RL with Tool reward (correct answers only),** $\alpha = 0.1$**,** $\beta = 0.01$ | **67.4%** | **6.0** | **57.7%** | **6.5** | **62.6%** | **6.3** |
| RL with Tool reward (correct answers only), $\alpha = 0.1$, $\beta = 0.02$ | 66.7% | 6.4 | 56.8% | 6.7 | 61.8% | 6.6 |
| RL with Tool reward (correct answers only), $\alpha = 0.2$, $\beta = 0.01$ | 66.9% | 5.9 | 56.5% | 6.2 | 61.7% | 6.1 |